2013

Designing a cost effective microalgae harvesting strategy for biodiesel production with electrocoagulation and dissolved air flotation

Adam James Dassey
Louisiana State University and Agricultural and Mechanical College

DESIGNING A COST EFFECTIVE MICROALGAE HARVESTING STRATEGY FOR BIODIESEL PRODUCTION WITH ELECTROCOAGULATION AND DISSOLVED AIR FLOTATION

A Dissertation

Submitted to the Graduate Faculty of the
Louisiana State University and
Agricultural and Mechanical College
in partial fulfillment of the
requirements for the degree of
Doctor of Philosophy

in

The Department of Engineering Sciences

by
Adam James Dassey
B.S., Louisiana State University, 2007
M.S., Louisiana State University, 2010
August 2013

Acknowledgments

Upon receiving my doctorate in the summer of 2013, I will have spent nearly a decade on LSU's campus furthering my education. During that time, I made great and longtime friends, was inspired by dedicated professors, strove to make my parents proud and found the love of my life. These years have treated me well, and I owe that honor to the people who have journeyed with me and the support they have provided.

I would like to thank Dr. Chandra Theegala for seeing the potential in me as an academic and advising me through both my master's and doctorate work. You introduced me to a subject matter and skillset that I look forward to utilizing to its fullest potential. It was truly a pleasure working with you these past five and half years. Special thanks to my committee members: Dr. Ron Malone, Dr. Steven Hall, Dr. Robin McCarley, and Dr. James Oard. You all challenged me to put forth a product I could be proud of and inspired me to be an effective researcher.

To my friends who have spent countless weekends coming back for football games and spending the night at my house; good luck! I have many great memories of the times we have had, but I do not see how you will survive without me.

To my parents; Lani, Amy, and I owe you both everything. I cannot imagine anyone having a better family and support structure. You have made me the man I am today and I will continue to strive to always make you proud. One day, but not too soon, I hope to be lucky enough to be the kind of parent that you have been to me. I love you both. Lani and Amy, I am proud to be your big brother and continue to support you in your ventures as you have supported me.

And to my love; Val, you have been my best friend for over 8 years now. You patiently waited for me to finish my work as I continuously pushed my timeline back. You are an amazing woman and I am lucky to have you in my life. I look forward to our future where we finally get to spend our lives together. I love you. Yo te quiero. Yo te amo.

Table of Contents

List of Tables

List of Figures

Abstract

Microalgal harvesting strategies for biodiesel production have been a major setback in the industry with high energy estimates of $3400/ton biomass by centrifugation. The present study utilized effective mass and energy balances to reduce these large operating costs. The energy for Stage 1 centrifugation was reduced by 82% when harvesting 28.5% of biomass at 18 L/min as opposed to 95% harvesting at 1 L/min. This strategy was further confirmed using electrocoagulation (EC) with *Nannochloris* and *Dunaliella* algae with perforated aluminum and iron electrodes at low (< 6 mg/L) metal ion concentrations. Despite 20% lower harvesting efficiencies, the iron electrodes were more energy and cost efficient with operating costs less than $0.03/L oil when flocculating and settling *Nannochloris* and *Dunaliella* cultures. Furthermore, a continuous multistage algae harvester using EC and dissolved air flotation (DAF) for Stage 1 harvesting and centrifugation for Stage 2 dewatering was designed. It was determined throughout the testing that greater EC costs for improved harvesting efficiencies were necessary to offset the large energy requirements of the DAF. The multistage system dewatered a low density (100 mg/L) *Nannochloris* to 20% solids for a final energy requirement of 1.536 kWh/kg algae ($138/ton). Using the data collected from this research and existing literature, a life cycle analysis was assembled to judge the sustainability of microalgal biofuels in Louisiana. High and low energy estimates for culturing (mixing, CO_2, nutrients), harvesting, lipid extraction and energy conversion were compared with the current research. Scaling the EC/DAF system for a full size facility was expected to reduce the harvesting costs to 1.133 kWh/kg algae, resulting as $0.44/L oil for a culture with 20% lipids. Despite this improvement in harvesting costs, the production of algae for the sole purpose of biodiesel was not economically viable. Considering a system with a growth rate of 15 g/m^2/day and lipid content of 20%, the energy inputs exceeded the outputs from biodiesel production by 36% under the most ideal conditions. However, incorporating additional revenue through wastewater treatment and biogas production from residual biomass could improve sustainability and profitability of algal biodiesel to an 18.5% energy surplus at its current state.

Chapter 1: Introduction

1.1 The Potential of Microalgae as a Biodiesel Feedstock

Increases in U.S. energy prices and national mandates to reduce the dependence on foreign oil have brought renewed interests in research of alternative energy. One challenge for alternative energy has been the development of a liquid alternative to petroleum, which dominates the country's transportation sector (EIA, 2010). The Energy Independence and Security Act of 2007 established a mandatory Renewable Fuel Standard requiring transportation fuel sold in the U.S. to contain a minimum of 36 billion gallons of renewable fuels, including advanced and cellulosic biofuels and biomass-based diesel, by 2022 (DOE, 2010). Of these 36 billion gallons, only 15 billion gallons are permitted to be produced from corn based ethanol. The remaining 21 billion gallons must be derived from other biomass sources.

Biodiesel from used vegetable oil has shown potential as a viable option as a liquid alternative, but is not an ideal feedstock to make biodiesel competitive with petroleum. The most significant concern is the inefficiency and sustainability of 1st generation crops such as corn, sugarcane, and soybean as biofuel feedstocks (Patil et al., 2008). Utilizing the proper feedstock is imperative for sustainable biofuel production, since 70-80% of the total costs are in the raw materials (Gui et al., 2008; Ahmad et al., 2011).

One feedstock that has shown potential in biodiesel production is microalgae, eukaryotic oxygenic photosynthetic microorganisms. Algae can be a competitive fuel crop for reasons such as: i) high per-acre productivity, ii) algal-feedstock based on non-food resource, iii) use of otherwise non-productive, non-arable land, iv) utilization of a wide variety of water sources (fresh, brackish, saline, and wastewater), v) mitigation of greenhouse gases released, and vi) production of both biofuels and valuable co-products (Pienkos and Darzins, 2009).

High per-acre productivity

With some species containing lipid contents as high as 70% of the cell's biomass, microalgae could potentially produce over 140,000 L/ha (15,000 gal/acre) of biodiesel per year in a raceway system as compared to soybean which is capable of only 446 L/ha (47 gal/acre) per year (Chisti, 2007). Algae would require 300 times less land than soybean to supply the entire nation's transportation fuel needs with biodiesel; 4 million hectares of land area (2.2% of existing cropping area) for mass cultivation (Chisti, 2007). These estimated production numbers from algal oil arise due to a combination of high lipid percentages and accelerated growth rate for the aquatic species. Algae can double their biomass within 24 hours with exponential growth phase reaching doubling times of 3.5 hours (Vijayaraghavan and Hemanathan, 2009). Using conservative growth rates, the potential oil production from microalgae with various lipid content and culture densities was estimated (Table 1.1).

Table 1.1: Predicted yearly oil production from an acre of algal culture based on its culture density and lipid percentage

L of Oil/Acre/Year											
		Culture Density (mg-dry/L)									
		50	**100**	**150**	**200**	**250**	**300**	**350**	**400**	**450**	**500**
Percent Lipids (%)	**10**	1,142	2,285	3,427	4,569	5,712	6,854	7,997	9,139	10,281	11,424
	15	1,714	3,427	5,141	6,854	8,568	10,281	11,995	13,708	15,422	17,135
	20	2,285	4,569	6,854	9,139	11,424	13,708	15,993	18,278	20,563	22,847
	25	2,856	5,712	8,568	11,424	14,280	17,135	19,991	22,847	25,703	28,559
	30	3,427	6,854	10,281	13,708	17,135	20,563	23,990	27,417	30,844	34,271
	35	3,998	7,997	11,995	15,993	19,991	23,990	27,988	31,986	35,984	39,983
	40	4,569	9,139	13,708	18,278	22,847	27,417	31,986	36,556	41,125	45,694
	45	5,141	10,281	15,422	20,563	25,703	30,844	35,984	41,125	46,266	51,406
	50	5,712	11,424	17,135	22,847	28,559	34,271	39,983	45,694	51,406	57,118
	55	6,283	12,566	18,849	25,132	31,415	37,698	43,981	50,264	56,547	62,830
	60	6,854	13,708	20,563	27,417	34,271	41,125	47,979	54,833	61,688	68,542
	65	7,425	14,851	22,276	29,701	37,127	44,552	51,977	59,403	66,828	74,253

These numbers are representative of an algae species reaching the displayed culture density every three days before being harvested from a 1,645 m^3 pond (1 acre x 40.6 cm). As seen in Table 1.1, achieving a modest algal density (50 mg/L) and lipid percentage (10%) is enough to surpass terrestrial crops such as soybean in yearly oil production.

Non-food resource

Crops such as corn, soybean and palm oil were explored as biofuel feedstocks because the techniques for cultivation, harvesting, and oil extraction have previously been implemented. The use of these first generation biofuels, however, has generated a lot of controversy, mainly due to their impact on global food markets and on food security, especially with regards to the most vulnerable regions of the world economy (Brennan and Owende, 2010). It is believed that large-scale production of biodiesel from edible oils may bring global imbalance to the food supply and demand market (Gui et al., 2008). Since microalgae is not a major competitor on the current global food market, it does not attract the controversy seen with most 1st generation feedstocks. Biodiesel production from edible oil also has a negative environmental impact because a significant quantity of available arable land is required to contribute to the world's fuel demand (Ahmad et al., 2011).

Resources needed

Unlike other terrestrial crops, algae do not require arable land for development. Raceway systems used for algae cultivation mainly require an impervious foundation to prevent water loss. However, the most suitable location for algae production on the basis of land area is typically least suitable on the basis of water consumption (Clarens et al., 2010). Utilizing freshwater resources for the production of algae fuel in areas with limited water resources due to location or population is a concern (Li et al., 2008). Despite their growth in aqueous media, microalgae require lower rates of water renewal than terrestrial crops need as irrigation water, so the load on freshwater sources is strongly reduced (Amaro et al., 2011). If freshwater use is not an economical option, salt or brackish water algae species are also available for biofuel production.

An alternative to natural water sources is wastewater effluent from various treatment facilities. Microalgae ponds used for secondary or tertiary treatment of domestic wastewater would bring advantages such as cost effectiveness, low energy requirements, reductions in sludge formation and

pollutants discharged into the environment, greenhouse gas mitigation, and the production of useful microalgal biomass (Kumar et al., 2010; Pittman et al., 2011; Sydney et al., 2011). Small-scale decentralized wastewater treatment could also allow water reuse onsite and reduce the need for transportation of hazardous wastes (Munoz and Guieysse 2006). Thus, this algae phycoremediation comprises of nutrient removal from municipal wastewater rich in organic matter, removal and degradation of xenobiotic compounds, treatment of acidic and metal wastewaters, and CO_2 sequestration (Olguin, 2003).

Mitigation of greenhouse gases

Algae, like any other photosynthetic plant, utilize atmospheric carbon dioxide to synthesize carbohydrates. If 63.6 million acres of land were used to cultivate algae at a conservative rate of 10 g/m^2day, then 2 billion tons of carbon dioxide could be captured in the biomass in one year (Pienkos and Darzins, 2009). Atmospheric CO_2 levels (~0.0387% v/v), however, are not sufficient to support the high microalgal growth rates and productivities needed for full-scale biofuel production (Kumar et al., 2010). Higher CO_2 concentrations are needed since every unit of microalgae grown, requires 1.83 times their mass in carbon dioxide (Pate et al., 2011). Therefore, many reports on the potential and bio-economics of algal biomass to generated fuels are based on the premise that CO_2 would be utilized from fossil fuelled power stations or other industrial sources of CO_2 (Singh and Olsen, 2011). Additionally, combustion products such as NO_x or SO_x can be effectively used as nutrients for microalgae, simplifying flue gas scrubbing for combustions systems (Um and Kim, 2009).

Valuable co-products

While only a fraction of the algal biomass is used for lipid extraction for biodiesel production, all species contain varying proportions of carbohydrates, proteins, and nucleic acids that can be used for valuable co-products (Demirbas, 2009). The carbohydrate fraction can be further converted to simple sugars and fermented into ethanol, replacing 16.25 kg of corn for every 1,000 MJ of algal

biodiesel (Sander and Murthy, 2009). The residual protein can add market value as an animal feed producing a supplemental $500 per tonne (Dismukes, et al., 2008; Williams and Laurens, 2010). Depending on the species, additional high-value chemical compounds such as pigments, antioxidants, B-carotenes, fatty acids and vitamins can be extracted for use in pharmaceuticals, cosmetics, nutraceuticals and foods (Mata et al., 2010). Obtaining the most value out of the algae biomass is crucial for sustainable biodiesel production in an industrial setting.

1.2 Culturing and Harvesting Challenges with Algal Biomass

Recirculating raceway ponds are the most common facilities used for culturing microalgae in the commercial sector (Beilen, 2010; Chen et al., 2011). These oval-shaped ponds are cheap to operate and are designed such that photosynthetic efficiency (PE) is the limiting factor affecting the growth rate of the microalgae. Photosynthetic efficiency is the fraction of light energy that can be fixed as chemical energy for biomass production of an algal cell. The maximum photosynthetic efficiency that can be achieved is only 10% due to photoinhibition (Beilen, 2010), because the light capturing antennae of algae harvest one photon every 0.5 ms, but the dark phase reaction centers can only process one photon every 5 ms.

This value however, is the theoretical ‘‘upper limit’’ of PE, as it does not account for other factors that could decrease efficiency and conversion (e.g. photosaturation, photorespiration, and poor light absorption) and significantly reduce PE (Brennan and Owende, 2010). Due to such impacting factors, most autotrophic organisms attain PE levels typically between 1% and 3% (Vasudevan and Briggs, 2008; Beilen, 2010). Therefore, assuming a PE of 2%, algal production can realistically be expected to produce approximately 12,771 L/ha/a from 4.6 kWh/m^2/d of solar radiation. From the theoretical data in Table 1.1, this production rate is equivalent to harvesting a 100 mg/L algae culture (0.01% dry weight) from a 1,645 m^3 pond every 3 days.

However, the harvested algal biomass must be increased to at least 20% dry weight for effective lipid extraction (Putt, 2007). This requires dewatering the culture nearly 2000 times before further use. Large harvesting expenses arise because bringing the algal biomass to a paste consistency from relatively dilute cultures requires processing large volumes of water (Alabi et al., 2009; Amaro et al., 2011). Therefore, discovering a proper harvesting technique is crucial for affordable algal biodiesel. An efficient algal harvesting process should be applicable for all kinds of algal species, yield a product with a high dry weight percentage and require minimum investment, energy, and maintenance (Poelman, 1997).

1.3 Harvesting Techniques

1.3.1 Sedimentation

Sedimentation is defined by Stokes' law, which predicts that the sedimentation velocity is proportional to the difference in density between the cell and medium and on the square of the radius of the cells (Schenk et al., 2008). This method of particle separation is popular in wastewater treatment because sedimentation basins require little energy input, are relatively inexpensive to install and operate, require no specialized operational skills, and can be easily incorporated into new and existing facilities (Timmons et al., 2002). Due to algal size and density, however, settling is a difficult and time consuming process.

Cell mass densities range from 1.02 to 1.25 g/m^3 for algal cultures, making the density difference with the fluid medium minimal (Reynolds, 1984). These densities result in slow settling velocities of 0.1-2.6 cm/h where smaller algae such as *Stephanodiscs*, *Scenedesmus*, and *Ankistrodesmus* consistently settle below 1.0 cm/h (Choi et al., 2006). Even to achieve these settling rates, biomass concentrations of 3 g/L were reported, whereas typical pond concentrations of 0.3-0.5 g/L could not be separated spontaneously by sedimentation (Janelt et al., 1997). Therefore, the small

size of the microalgae and their low specific gravity results in a settling rate that is too low for routine algal harvesting (Pittman et al., 2011).

1.3.2 Centrifugation

Continuous flow centrifuge systems allow sediment bearing water to be pumped continuously through the bowl assembly, forcing particles to the wall while clarified water passes through the overflow (Rees et al., 1991). Quick dewatering of algae is evident with 84% removal efficiency of 0.2 g/l algal culture at a flow of 100 gpm under a rotational velocity of 3000 rpm (Kothandaraman and Evans, 1972). Unfortunately, the use of centrifuges for algal separation is very energy intensive. The use of centrifugation for harvesting algae cultures on average costs 1.3 kWh/m^3 of pond water (Sim et al., 1988). Therefore, centrifugation may be feasible for high-value products, but is far too costly in an integrated system producing lower-value products, such as algal oils for biofuel production (Pienkos and Darzins, 2009).

1.3.3 Filtration

1.3.3.1 Membrane Filtration

The use of low-pressure membrane filtration—microfiltration (MF) and ultrafiltration (UF)—has rapidly increased in the last decade due to stricter regulations for finished water quality, decreased cost, improved membrane materials and modules, relative simplicity of installation, and improved reliability when compared with conventional treatment processes such as sedimentation and rapid filtration (Choi and Dempsey, 2004). However, a major obstacle in incorporating membrane filtration for algae harvesting is the flux reduction due to membrane fouling by the microscopic algae (Babel et al., 2002). Once imbedded in the filter membrane, the algae form a cake which reduces flow rates and increases head loss unless the membrane is cleaned. One report indicated that conventional coagulation produced larger particles which reduced fouling during membrane filtration by reducing

adsorption in membrane pores, increasing cake porosity, and increasing transport of foulants away from the membrane surface (Hwang and Liu, 2002).

1.3.3.2 Granular Media Filtration

Granular media filtration involves the passage of water either downward or upward through a bed of granular material which entraps the solids on the media. The media may consist of a variety of substances such as sand, gravel, or synthetic beads. At a filtration velocity of 120 m/h, a flexible nylon media filter was able to remove 85% of the algae from solution with 1 mg/l coagulant (Cha et al., 2009). A 0.2 mm diameter sand with a depth of 3.175 mm had an average algal removal of 96% at a flow rate of 246 m/d (Naghavi, 1982). The glaring difference between these two systems is the rate of filtration where better removal was achieved at a much slower velocity. In practice, the effectiveness of granular filters is limited by backwashing requirements, head loss through the filter media, and biofouling (Chen and Malone, 1991).

1.3.4 Coagulation/Flocculation

Coagulation is the process of chemically changing colloids so that they are able to form bigger particles by coming close to one another (Jarvis et al., 2005). It involves the formation of chemical flocs that absorb, entrap, or otherwise bring together suspended matter that are colloidal (Nemerow, 1978). The aggregation process of these particles to form flocs is described as colloidal destabilization. Chemical flocculants like alum and ferric chloride are used to harvest microalgae, but it is often too expensive for large operations (Hung et al., 2010).

Other options, such as autoflocculation, rely on increased pH either by CO_2 consumption through photosynthesis or the addition of alkali resulting in excess calcium and phosphate ions. In the presence of excess calcium ions, the calcium phosphate precipitate is positively charged and therefore adsorbed on the negatively charged algal cells agglomerating them and promoting algal flocculation (Lavoie and Noue, 1987). Calcium and phosphate are limiting reagents in autoflocculation and

generally become coagulant additions to induce floc formation. To attain flocs within the pH range of 8.5-9.0, the culture should contain 0.1-0.2 mM orthophosphate and between 1.0-2.5 mM calcium (Sukenik and Shelef, 1984).

1.3.5 Flotation

Flotation techniques, in which finely suspended particles are separated by adhering to the surface of rising bubbles, have proven efficient, practical and reliable separation methods for the removal of oils, as well as dissolved ions, fats, biomolecules and suspended solids from water (Zouboulis et al., 2000). The idea is to develop agglomerates with lower density than water, causing the particulates to rise through the water and accumulate at the surface where they can be removed as sludge (Lundh et al., 2000). Two common flotation techniques that are used in water treatment applications are dissolved air flotation and induced air flotation.

1.3.5.1 Dissolved Air Flotation

Dissolved air flotation uses pressure saturation to increase the solubility of air in water to produce fine microbubbles for solids removal. Typical pressures used to ensure small bubble production range from 345-621 kPa (Edzwald, 1995). At these pressures, the air solubility in water increases drastically, causing the water to become supersaturated with air. When the pressurized water is released to atmospheric conditions, the dissolved air is released from saturation and forms tiny microbubbles with diameters ranging from 10 to 100 um with typical diameters of 40 um (Edzwald, 1995). Dissolved air flotation is an effective method of particle separation because the high concentration of microbubbles and their slow rise rates allow for more collision opportunities with the particulate matter (Al-Shamrani et al., 2002). However, aluminum and iron coagulants are frequently used to augment the flotation process (Aulenbach et al., 2010). Using alum and polyaluminum chloride (PAC) as coagulants, Craenenbroeck et al., (1993) demonstrated that over 80% of 18 types of

algae can be removed from water by DAF. The use of small amounts of chemical coagulants to aid in flotation could be cost effective, depending on the amount used (Pienkos and Darzins, 2009).

1.3.5.2 Induced (Dispersed) Air Flotation

In this method of flotation, bubbles 700-1500 μm in diameters are mechanically formed by a combination of a high-speed mechanical agitator and an air injection system (Rubio et al., 2001). The advantage of the larger bubbles is a quicker flotation time, but they rely on adhesive surface interactions through chemical pretreatment. Holtman (1982) indicated 90% removal efficiency with a surfactant dose between 5 and 7 mg/l at pH 8. However, it has been found that IAF suffers from floc shearing due to weak hydrophilic bonds associated with metal hydroxides (Jameson, 1999).

1.4 Problem Statement

Biomass harvesting poses to be one of the greater challenges that is preventing practical production of algal biodiesel. Given the relatively low biomass concentration obtainable in microalgal cultivation systems (<500 mg/L), marginal density difference with culture water (average ~ 1,020 kg/m^3), and the small size of microalgal cells (5 to 50 μm in diameter), costs and energy consumption for biomass harvesting are significant concerns that need to be addressed properly (Pieterse and Cloot, 1997; Li et al., 2008; Kumar et al., 2010). Depending on species, cell density, and culture conditions, harvesting algal biomass has been estimated to contribute 20–30% to the production cost (Gudin and Thepenier, 1986; Grima et al., 2003). To remove large quantities of water and process large algal biomass volumes, a suitable harvesting strategy may involve one or more stages and be achieved in several physical, chemical, or biological ways, in order to perform the desired solid–liquid separation (Mata et al., 2010).

1.5 Objectives

The ultimate objective of this study was to develop a cost effective microalgae harvesting strategy for biodiesel production. To accomplish this objective, four sub-goals were set in place:

1. Develop a harvesting strategy with final costs being the primary concern using centrifugation. Most harvesting strategies focus on 100% biomass capture under optimal conditions. This was believed to be a flawed strategy and that costs can be reduced if the harvesting efficiency was not the primary focus.
2. Prove that electrocoagulation was a viable option as a pre-concentration step using small scale batch reactors. The pre-concentration stage of algae harvesting was critical for cost effective biomass capture since it required treating the algae at its most dilute concentration (100 mg/L).
3. Create a continuous multistage harvesting system (4 L/min) for a low density algae culture that combined electrocoagulation and dissolved air flotation for the Stage 1 pre-concentration step followed by centrifugation for the Stage 2 final dewatering. The complete dewatering (final concentration ~20% dry weight) costs were aimed to be less than $0.80/L of oil if the algal culture contained 20% lipids for oil extraction.
4. Conduct a complete life cycle analysis on microalgae as a potential biomass feedstock for biodiesel in Louisiana and determine how the current harvesting system compared with other analyses.

Chapter 2: Harvesting Economics and Strategies Using Centrifugation for Cost Effective Separation of Microalgae Cells for Biodiesel Applications[1]

2.1 Introduction

When implementing an effective algae harvesting strategy, mass and energy balances are necessary to maintain equilibrium between the influent substrate, growth rates, and harvested biomass. Microalgal growth is affected by reactor operating conditions such as hydraulic residence time and harvesting rates because they affect CO_2 availability and light exposure (Kumar et al., 2010). If the algae culture is too dense, the light-saturated surface layer cells might prevent penetration of light deeper into the culture resulting in a reduced growth rate (Stephenson et al., 2011). Therefore microalgae are grown to steady state concentrations and are continuously harvested at a rate equal to the growth rate (Davis et al., 2011). Typically between 20 and 40% of the algae biomass within the pond is harvested per day (Beilen, 2010). The remaining biomass is returned as inoculum for continued algal production.

In a continuous culture system, dilution rates and influent substrates are the two parameters controlled to optimize algal growth (Maier et al., 2009). Dilution rates (D, time^{-1}) directly affect growth rates (μ, time^{-1}) while substrate concentration (S, mg/L) affects the pond biomass concentration (X, mg/L). This change in biomass over time is effectively described through Monod's equation:

$$\frac{dX}{dt} = \mu X - DX = \frac{\mu_{max} S X}{K_s + S} - D_{ss} X \qquad Eq\ 2.1$$

Where: μ_{max}= maximum specific growth rate

K_s = the substrate concentration at which growth occurs at 0.5 the value of μ_{max}

The substrate concentration is not considered a growth rate limiting factor; therefore $S >> K_s$.

[1] Parts of this chapter previously appeared as Dassey and Theegala (2013) Harvesting Economics and Strategies Using Centrifugation for Cost Effective Separation of Microalgae Cells for Biodiesel Applications. Bioresource Technology, 128, 241-245. It is reprinted by permission of Elsevier – see the permission letter for proper acknowledgement phrase.

After steady state conditions are achieved and operation efficiencies are optimized, μ_{max} equals the steady state dilution rate (D_{ss}, time^{-1}). The steady state dilution rate affects the rate such that if the pond operates at $D < D_{ss}$, operation efficiency is not optimized, whereas if $D > D_{ss}$, washout of cells occurs (Maier et al., 2009). From the mass balance model in Figure 2.1, the steady state dilution rate is a factor of flowrate (Q, L/min) and system volume (V, L):

$$\mu_{max}X = D_{ss}X = \frac{QX}{V} \qquad Eq\ 2.2$$

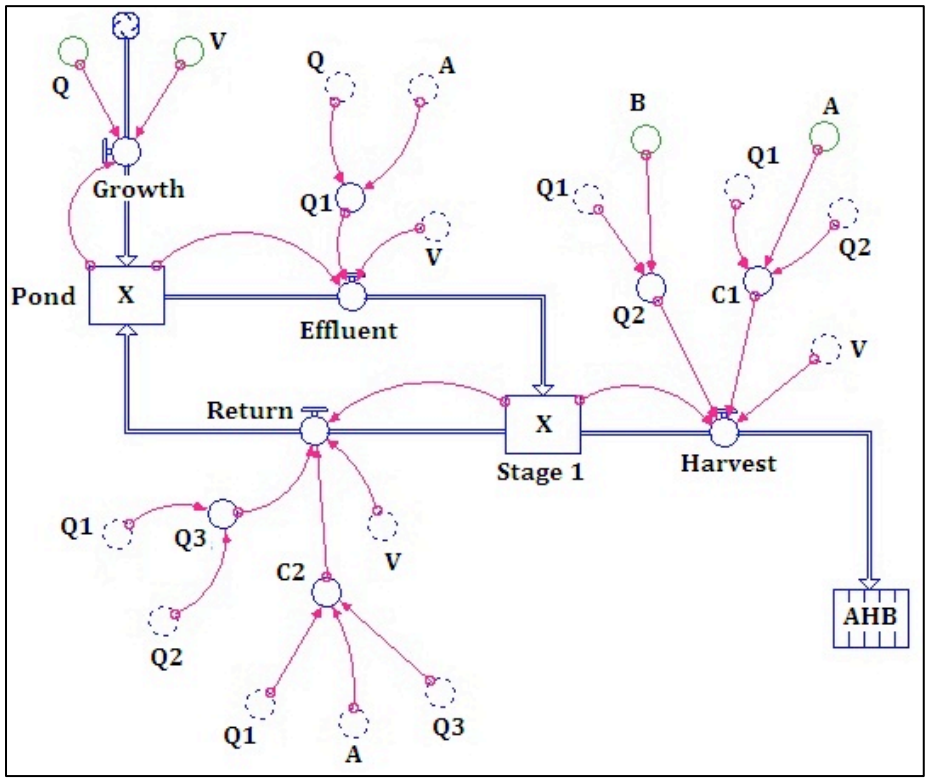

Figure 2.1: Stella model representing the mass balance between growth rate and biomass harvesting

With the maximum growth rate of a specific algal species predetermined, an effective harvesting strategy can be implemented such that μ_{max} equals the rate of harvest (mgL^{-1}min^{-1}) as determined by $D_{ss}X$.

Two factors of importance for planning a harvesting strategy are harvest efficiency (A, % as decimal) and dewatering efficiency (B, % as decimal) in Figure 2.1. The harvest efficiency is the percent of biomass harvested from the effluent, and therefore, influences the flowrate (Q1, L/min) that

is processed for harvesting the biomass. If the harvest efficiency is less than 100% at Stage 1, then Q1 increases by a factor of (1/A) so that the harvested biomass equals μ_{max} of the pond.

The dewatering efficiency is the percent of water that is removed from the effluent, and therefore, influences the harvested flowrate (Q2, L/min) and the flowrate (Q3, L/min) that is returned to the pond after harvesting. Both A and B influence the concentration factors of the harvested biomass (C1, unitless) and the biomass returning to the pond (C2, unitless). For most harvesting applications, the desired harvested biomass concentration (C1*X, mg/L) is approximately 200,000 mg/L (20% biomass). Depending on the final requirements of the system, any combination of A and B can be applied to the mass balance and the Accumulated Harvested Biomass (AHB, $mgL^{-1}min^{-1}$) will increase at a rate equal to that of the growth rate.

The objective, therefore, is to determine which combination of A and B is most affordable to harvest the algae biomass for biodiesel production. Most harvesting strategies aim for the most cost effective approach to achieve 100% algal harvest efficiency. However, achieving 100% harvest efficiencies may not always be conducive to the most affordable product.

For example, harvesting by centrifugation is generally characterized by high capture efficiency (>90%) under low flow rates and high energy consumption. The use of centrifugation for harvesting algae cultures from 0.04% to 4% dry weight on average costs 1.3 kWh/m^3 of pond water (Sim et al., 1988). Increasing the concentration to 22% dry algal biomass can utilize 8 kWh/m^3 (Mohn, 1980). However, if the flow rates passed through a centrifuge were increased, the energy applied per volume of culture would decrease. A decrease in harvest efficiency would also be expected, but could potentially be offset by the greater volume of culture effluent treated. To further defend this hypothesis, harvesting algae by centrifugation was used to develop a strategy based on harvest efficiency and energy consumption.

2.2 Materials and Methods

Nannochloris sp., a unicellular green alga, was cultivated outdoors in a 161 cm D x 84 cm H fiberglass tank filled with approximately 1700 L of F/2 medium. The culture was circulated using 2 submerged air lifts made out of 5 cm PVC pipe that stood 109 cm tall with a tee coupling 30.5 cm from the top. Extending from the tee was 61 cm of PVC with an elbow at the end. The bottom of the tee and PVC arm marked the water height of the tank. The air flow was supplied 2.5 cm from the bottom of the vertical PVC pipe by a Sweetwater air blower (K55JXEPT-395) through 1.3 cm hose barb. This arrangement facilitated gas transfer (CO_2, O_2, and degassing) and brought lower-dwelling cells to the surface for sunlight exposure while providing rotational movement. The algae was cultured until it reached a density of approximately 100 mg-dry/L. When testing began, a portion of the culture was continuously transferred to a 55-L secondary sump for easier access before being pumped to the nearby centrifuge.

The 1.5-HP (1.12 kW) continuous-flow centrifuge from US Filter-Maxx (3000G Centrifuge) was powered through a 220V outlet and allowed to run non-stop throughout the testing. The culture from the secondary sump was drawn by a rotary vane pump (Procon 115B330F31XX) connected to the 0.635-cm National Pipe Thread (NPT) stem on top of the centrifuge bowl. Flow rates were varied from 0.94 to 23.2 L/min using a flow regulator attached on the suction side of the pump. The effluent leaving the 3.81-cm NPT outlet was expelled to a nearby drainage system, but would be returned for further algal culturing in a real life scenario (Figure 2.2).

The centrifuge was switched on and allowed to reach its maximum speed before the algae inflow was initiated. The start-up normally took between 5 and 10 sec. When the inflow was initially applied, the centrifuge was operated for 10 min before the first effluent sample was collected in a 100 mL glass bottle. After collecting the first sample, additional samples were collected at 1-min intervals. When the flow rate was varied, an additional 10 min was allowed before sampling to return the system

to new steady-state conditions. The effluent samples were compared to the initial culture density which was randomly sampled from the 55-L secondary sump throughout the entire testing. Samples were compared by absorbance measurements with a spectrophotometer operating at 680 nm. The absorbance values were correlated to the total suspended solids (TSS determined in triplicate for each data point.

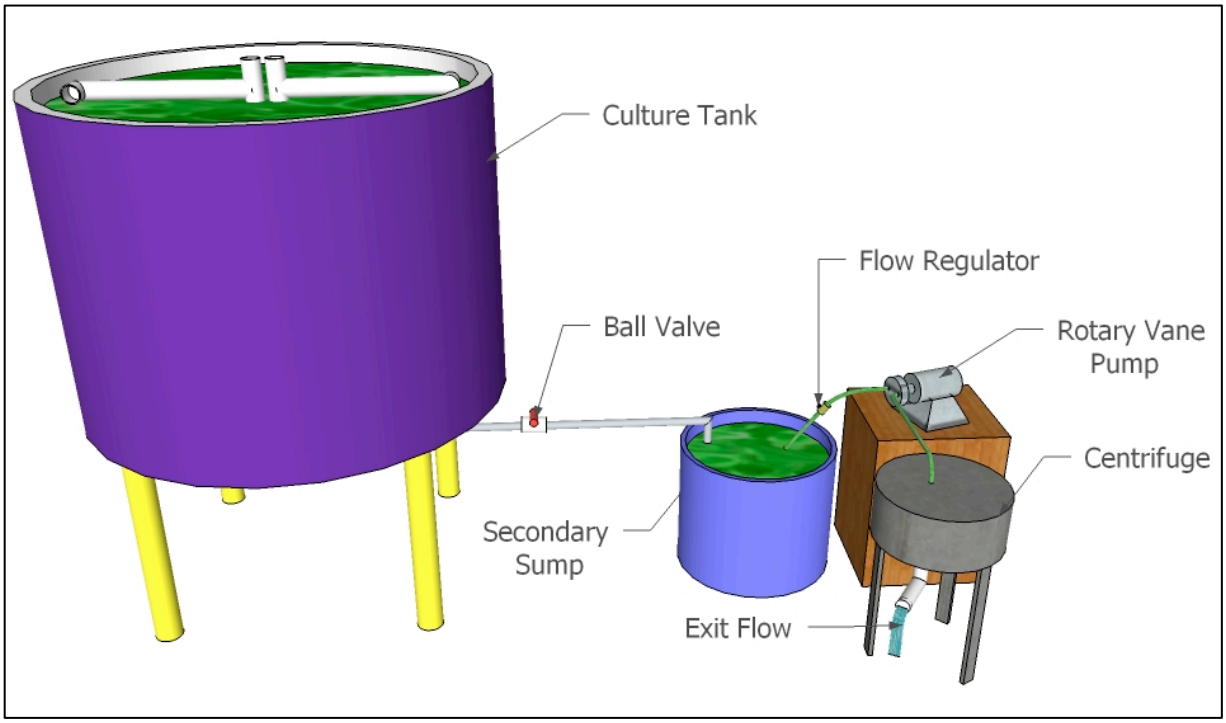

Figure 2.2: Experimental setup for centrifugation testing. The primary culture was diverted to a secondary sump, from where it was pumped through the centrifuge (one-pass). The cell capture efficiency was computed based on algal densities in the influent and the water exiting from the centrifuge.

2.3 Results and Discussion

Generally, centrifuges are considered to be too energy intensive to be suitable for microalgae harvesting for biodiesel production. For most applications, centrifuges are adjusted primarily to maximize capture efficiency. However, cost-effective harvesting of algal cells may or may not coincide with the highest capture efficiency. At higher flow rates (>1 L/min), the lower capture efficiencies will be offset by the larger volumes of culture processed through the centrifuge. Due to the microscopic size of the cells, longer retention times within the centrifuge bowl are required for their

sedimentation. As anticipated, results indicated that longer retention times (slower flow rates) correlated with more energy being directed to a smaller volume of culture per min (Figure 2.3).

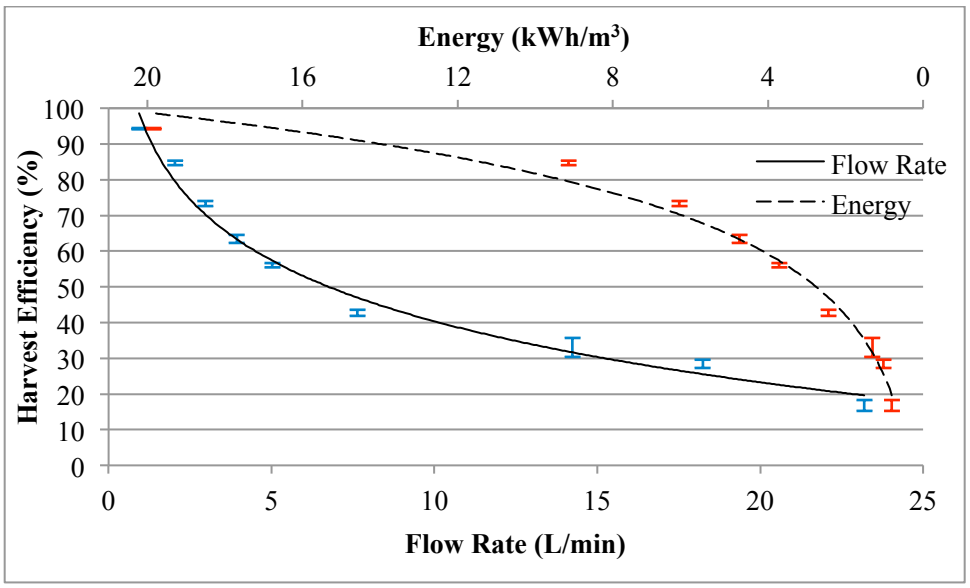

Figure 2.3: Capture efficiency of microalgal cells by centrifugation as a product of various flow rates and the concurrent energy consumed. The dashed trendline corresponds to the energy consumed and solid trendline corresponds to the flow rate.

The harvesting efficiency was determined by calculating the percentage of biomass removed from the influent culture solution. The harvest efficiency for the centrifuge reached 94% (± 0.24%) when an incoming flow rate of 0.94 L/min was applied. However, to collect biomass at these high capture efficiencies, an energy input of nearly 20 kWh/m^3 (of culture water) was required to harvest the cells. As the incoming flow increased, the amount of energy per cubic meter decreased, but the harvested mass also decreased. Only 17% (± 1.57%) of the incoming biomass was harvested when the flow rate was increased to 23 L/min; however, at this rate only 0.80 kWh/m^3 was required to harvest the biomass. The full effect of the harvesting efficiency in relation to energy consumption and flow rate cannot be realized unless a final cost on algal oil is plotted (Figure 2.4).

The algal oil density was assumed to be 864 g/L, which falls within the range determined by Kumar et al. (2011) for various species (857-892 g/L). At 100 mg/L culture density, 20% lipid concentration, and $0.09 per kWh electricity cost, the cost of harvesting algal cells for an equivalent 1

L of algal oil was determined from the energy (x, kWh/m^3) consumed at various flow rates and the corresponding capture efficiencies (y, % as decimal).

$$\frac{Energy\ \$}{L_{\ oil}} = x * \frac{\$0.09}{kWh} * \frac{m^3{}_{culture}}{g_{algae}} * \frac{1}{y} * \frac{1}{\%_{lipids}} * \frac{864\ g_{oil}}{L_{oil}} \qquad Eq\ 2.3$$

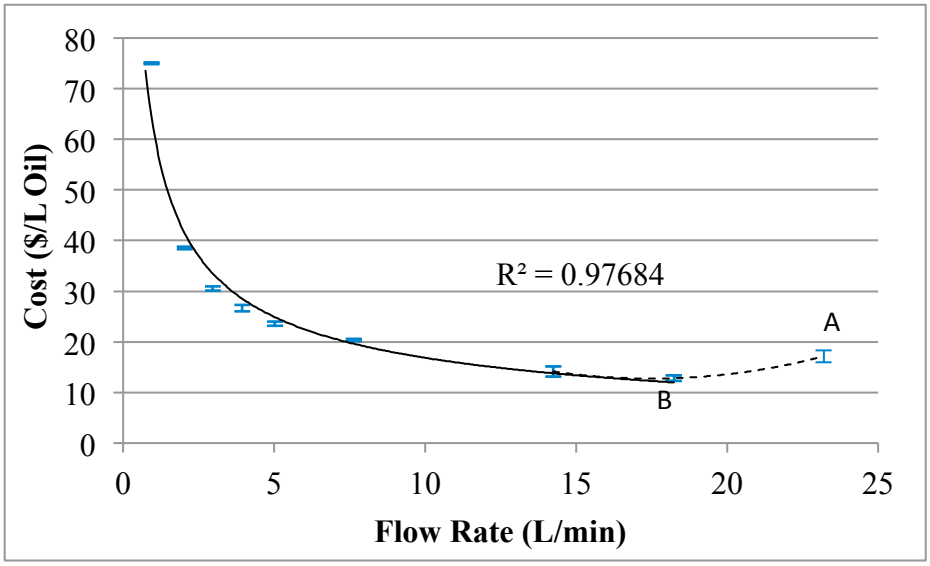

Figure 2.4: Harvesting cost per L of oil as a result of various flow rates. The final cost reached a minimum at 18 L/min (Point B). Costs increased again with greater flow rates (point A).

As anticipated, the decrease in capture efficiency was more than offset by increasing culture volumes processed through the centrifuge. The combined effect of higher process volumes treated under lower energy conditions was reflected by the decrease in the overall cost per L of oil. In simplified terms, despite lower harvesting efficiencies, greater process volumes with lower energy consumptions were more economical than greater harvesting efficiencies of smaller process volumes which required more energy; however, the increased volume processed at 23 L/min was negated by the poor harvesting efficiency. At that point (Point A in Figure 2.4), costs increased again. The costs of pumping were not accounted for in the final harvesting costs, primarily due to the fact that this was a very low-head application and the pumping costs were anticipated to be insignificant when compared to the centrifuge operational costs. For example, assuming a 1-h operational time for the centrifuge for each case, a small test pump operating at 1 L/min consumed 24 W for an energy usage of 0.4 kWh/m^3. The large pump operating at 23 L/min consumed 375 W for an energy usage of 0.27 kWh/m^3.

2.4 Economics

For the present study, the algal culture density was approximately 100 mg/L with 20% oil content and these values were used for all economic projections in the present chapter. As seen in Table 2.1, that density and oil content would require approximately 43.2 m^3 of culture to be completely harvested (100% capture) to produce 1 L of algal oil.

Assuming the cell residence time dictates cell capture efficiency and, applying the same correlation between flow rates and capture efficiencies (Figure 2.3) at all culture densities, it can be concluded that a capture efficiency of 28.5% (Point B in Figure 2.4) yields the most cost-effective harvesting strategy. Therefore, the volume of culture processed through the centrifuge at each point will be 3.5 L times the values stated in Table 2.1. For the purpose of this chapter and for the proposed economic projections, several assumptions were made:

1) the field-deployed centrifuge will have capture efficiencies that are similar to the efficiencies achieved by the lab scale experiments (Figure 2.3).
2) the field centrifuge will have continuous removal of harvested biomass by a solids scrapper to prevent declining performance due to algal buildup on the centrifuge walls.
3) the economics and harvesting estimates from a larger centrifuge, such as a 15-HP (11.2 kW) centrifuge, will be equal to ten 1.5-HP (1.12 kW) centrifuges).
4) the suppression of specific growth rates at high algal densities and culture related economics/difficulties are considered to be outside the scope of this paper
5) harvesting economics are only based on the cells that are captured by the centrifuge. No negative value was assigned to cells that are missed by the centrifuge. In a field setting, the non-harvested or returned cells are not discarded, but serve as new biomass or inoculum for the next growth cycle.

Table 2.1: Theoretical volume (m^3) of pond culture to be processed to produce 1 L of algal oil as function of culture density and lipid concentration.

m^3 of Culture/L of Oil											
		Culture Density in mg-dry/L									
		50	**100**	**150**	**200**	**250**	**300**	**350**	**400**	**450**	**500**
Percent Lipids	**10**	172.8	86.4	57.6	43.2	34.6	28.8	24.7	21.6	19.2	17.3
	15	115.2	57.6	38.4	28.8	23.0	19.2	16.5	14.4	12.8	11.5
	20	86.4	43.2	28.8	21.6	17.3	14.4	12.3	10.8	9.6	8.6
	25	69.1	34.6	23.0	17.3	13.8	11.5	9.9	8.6	7.7	6.9
	30	57.6	28.8	19.2	14.4	11.5	9.6	8.2	7.2	6.4	5.8
	35	49.4	24.7	16.5	12.3	9.9	8.2	7.1	6.2	5.5	4.9
	40	43.2	21.6	14.4	10.8	8.6	7.2	6.2	5.4	4.8	4.3
	45	38.4	19.2	12.8	9.6	7.7	6.4	5.5	4.8	4.3	3.8
	50	34.6	17.3	11.5	8.6	6.9	5.8	4.9	4.3	3.8	3.5
	55	31.4	15.7	10.5	7.9	6.3	5.2	4.5	3.9	3.5	3.1
	60	28.8	14.4	9.6	7.2	5.8	4.8	4.1	3.6	3.2	2.9
	65	26.6	13.3	8.9	6.6	5.3	4.4	3.8	3.3	3.0	2.7

From these assumptions and the data previously gathered, the total kW required by one or several combined centrifuge systems needed to harvest enough biomass for 1 L of oil was determined (Table 2.2). It has to be noted that these assumptions may or may not be completely valid for a field-scale harvesting system as the performance of a specific centrifuge will be as unique as a pumping curve developed for a specific pump head.

Table 2.2: Theoretical kW required to produce 1 L of oil if a centrifuge operates at 28.5% capture efficiency and harvesting is to be completed within 12 h.

kW/L Oil											
		Culture Density in mg/l									
		50	**100**	**150**	**200**	**250**	**300**	**350**	**400**	**450**	**500**
Percent Lipids	**10**	51.78	25.89	17.26	12.94	10.36	8.63	7.40	6.47	5.75	5.18
	15	34.52	17.26	11.51	8.63	6.90	5.75	4.93	4.31	3.84	3.45
	20	25.89	12.94	8.63	6.47	5.18	4.31	3.70	3.24	2.88	2.59
	25	20.71	10.36	6.90	5.18	4.14	3.45	2.96	2.59	2.30	2.07
	30	17.26	8.63	5.75	4.31	3.45	2.88	2.47	2.16	1.92	1.73
	35	14.79	7.40	4.93	3.70	2.96	2.47	2.11	1.85	1.64	1.48
	40	12.94	6.47	4.31	3.24	2.59	2.16	1.85	1.62	1.44	1.29
	45	11.51	5.75	3.84	2.88	2.30	1.92	1.64	1.44	1.28	1.15
	50	10.36	5.18	3.45	2.59	2.07	1.73	1.48	1.29	1.15	1.04
	55	9.41	4.71	3.14	2.35	1.88	1.57	1.34	1.18	1.05	0.94
	60	8.63	4.31	2.88	2.16	1.73	1.44	1.23	1.08	0.96	0.86
	65	7.97	3.98	2.66	1.99	1.59	1.33	1.14	1.00	0.89	0.80

At optimum capture efficiency and flow rates, the kW for all culture densities and lipid concentrations was reduced by 82% in comparison to the 100% efficient harvesting process. With the kW known for each case, 12 h allotted for harvesting and assuming $0.09/kWh, a final harvesting cost can be determined by the following equation:

$$\frac{\$}{L_{oil}} = \frac{kW}{L_{oil}} * \frac{\$0.09}{kWh} * 12\ h \qquad Eq\ 2.4$$

The output from the above equation is plotted as a 3-D plot (Figure 2.5). With increasing culture density and lipid concentration, the harvesting costs decreased; but even under the best conditions, the cost of harvesting algae ($0.864/L oil) is still too high for biodiesel production. Economic models (Figure 2.5) indicated that centrifugation has the potential to be the primary harvesting process if proper harvest strategies as determined by Figures 2.3 and 2.4 are selected and the algal culture can achieve high growth densities (500 mg/L) and lipid contents (65% by mass). However, such culture densities and lipid contents are not anticipated to be sustainable for a large scale facility at this time.

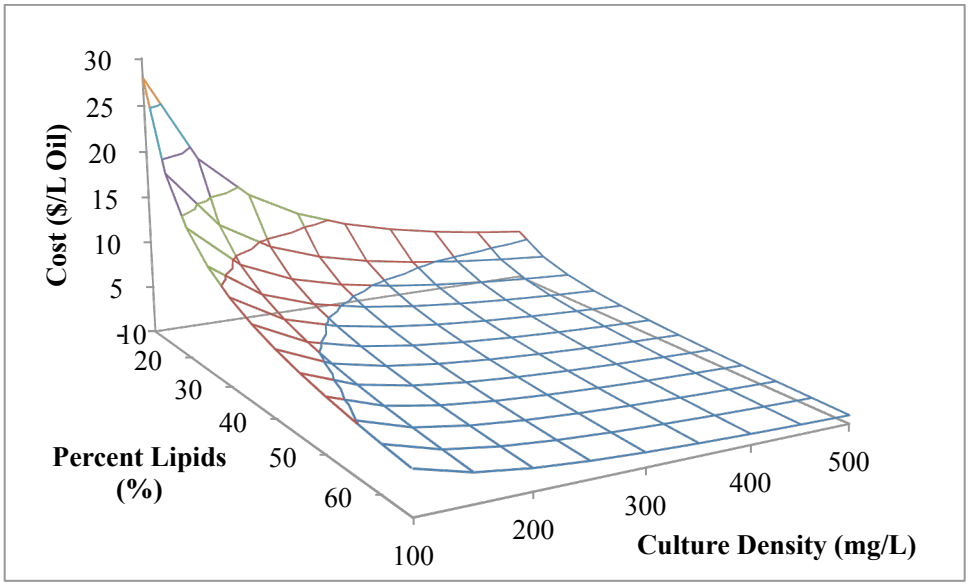

Figure 2.5: Final theoretical cost of harvesting microalgae by centrifugation as a function of culture density and lipid concentration

2.5 Conclusion

Algal harvesting by centrifugation can be achieved with significant variations to the flow rates passing the centrifuge. In general, faster flow rates lead to reduced capture efficiency and vice-versa. However, the faster flow rates will also see reduced energy consumption with respect to the volume processed. For the tested algal species at the tested densities, it was determined that a capture efficiency of approximately 28% produced the most cost-effective strategy for operating the centrifuge, resulting in an 82% decrease in harvesting costs. The theoretical harvesting costs could be lowered significantly (to $0.864/L oil) with increasing culture densities and lipid contents. By sacrificing biomass harvesting efficiencies for greater process volumes with lower energy consumptions, commercial scale algal plants can develop a cost effective harvesting strategy.

Chapter 3: Reducing Electrocoagulation Harvesting Costs for Practical Microalgae Biodiesel Production

3.1 Introduction

While the strategy discussed in Chapter 2 improved the economics of centrifugal harvesting as a primary harvesting technique, the results were not significant enough for practical algal biodiesel applications. However, a 1-stage algae harvesting system is not likely to be incorporated into a facility regardless of the process or technique that is used. Most harvesting systems will employ a 2-stage dewatering process, where Stage 1 increases the algae concentration from 0.01% biomass to 1-2% biomass and Stage 2 increases the final concentration to ~20% biomass (Figure 3.1).

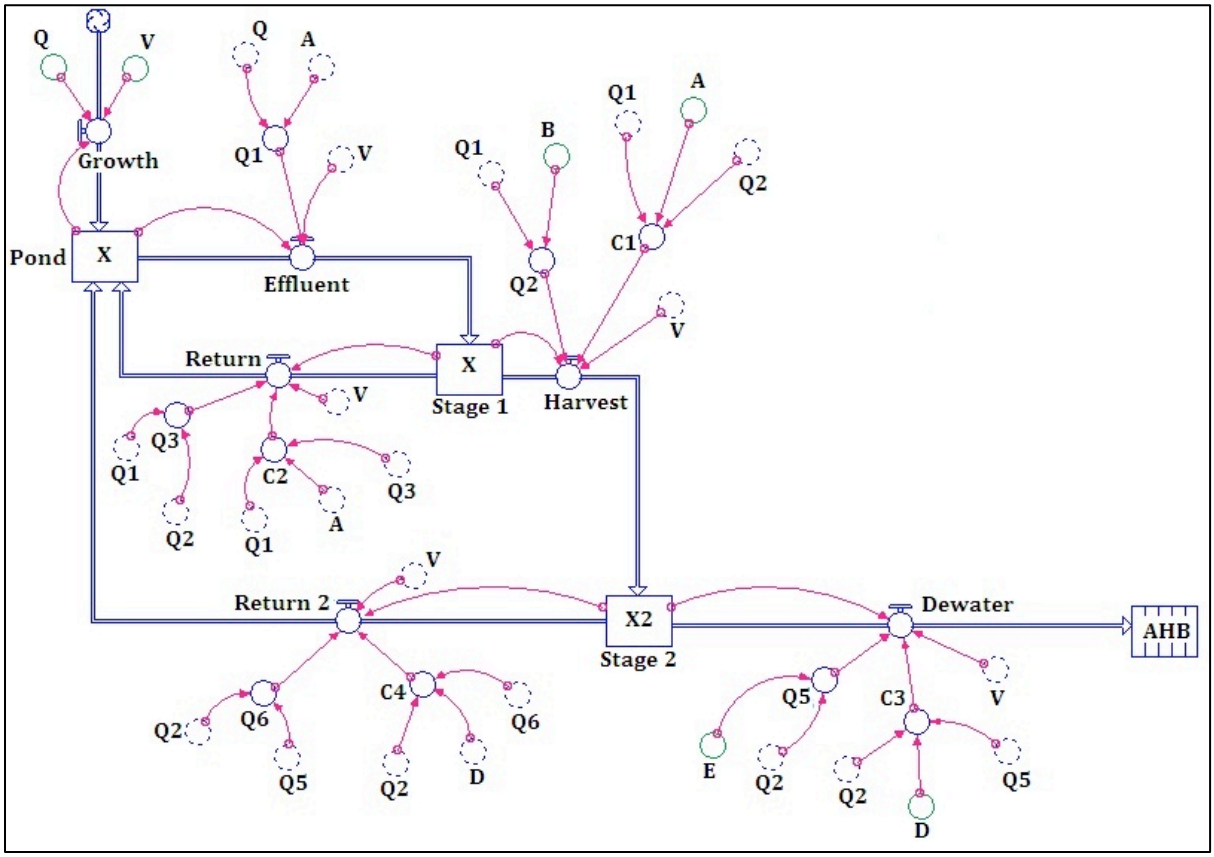

Figure 3.1: Stella model representing the mass balance between growth rate and a 2-stage biomass harvesting system

The 2-stage harvesting scenario follows the same guidelines as the 1-stage harvesting scenario with the understanding that mass balance is key to a successful operation. In this case, the strategy for Stage 1 previously discussed in Chapter 2 remains the same, where harvesting efficiency is sacrificed

for lower energy consumption. The difference is that a more cost effective alternative to centrifugation such as filtration, flotation, sedimentation, or coagulation/flocculation is incorporated in Stage 1. The harvest flow (Q2, L/min) which has an increased biomass concentration (X2, mg/L) in comparison to the initial biomass concentration (X, mg/L) is then processed in Stage 2 for final dewatering. Here the harvest efficiency (D, % as a decimal) is typically 100% and the dewatering efficiency (E, % as a decimal) should produce a concentration factor (C3, unitless) that will bring the final biomass concentration (X2*C3, mg/L) to 20% biomass or greater. The Return 2 flow (Q6, L/min) brings the remaining culture volume back to the pond with a concentration factor (C4, unitless) of 0, which is absent of algal biomass. As a result of the mass balance, the Accumulated Harvested Biomass (AHB, $mgL^{-1}min^{-1}$) will increase at a rate equal to that of the growth rate.

Because of the pre-concentration of Stage 1, the maximum energy used by centrifugation will have minimal impact on the final cost of algal oil. For example, to harvest nearly 100% of the algal biomass at 100 mg/L (0.01% m/m) required 19.8 kWh/m^3 for the centrifuge used in Chapter 2, which would have cost $57.72/L oil for an algal culture with 20% lipids. However, using centrifugation to harvest 100% of the biomass after the culture was increased to 10 g/L (1%) would only cost $0.57/L oil. The main objective, therefore, becomes discovering an effective Stage 1 harvesting option that can increase the algal concentration from 0.01% to $\leq$ 1% biomass.

3.1.1 Electrocoagulation as a Stage 1 Harvesting Option

Electrochemical techniques such as electroflotation and electrocoagulation offer the possibility to be an innovative, cheap, and effective method of algae harvesting that requires minimum amounts of chemicals (Mollah et al., 2004). Electrocoagulation (EC) is an electrochemical water treatment technique designed to disperse coagulating metal ions from oxidizing metal electrodes (typically aluminum or iron). Compared to coagulation with metal salts, EC has the advantage of no anions such as chlorine or sulphate being introduced to the process water (Vandamme et al., 2011). These anions

from traditional metal salts tend to generate large volumes of sludge with high bound-water content that can be difficult to dewater (Barkley et al., 1993). Releasing coagulating ions electrochemically requires an electric potential between the anode and cathode to drive the forward reaction. This electrode potential is linked to the concentration of oxidants (C_O) and reactants (C_R) by the Nernst Equation:

$$E = E' + \frac{RT}{nF} ln \frac{C_O}{C_R} \qquad Eq\ 3.1$$

Where: E = the electrode potential (V)

E' = is the standard potential (V)

R = the universal gas constant (8.314 J K^{-1} mol^{-1})

T = the absolute temperature (K)

F = Faradays Constant (96485 C)

n = the number of moles of electrons transferred

The chemical reactions that take place are made up of two independent half-reactions at each electrode. As seen using aluminum electrodes, oxidation occurs at the anode, producing aluminum ion and free electrons:

$$Al \leftrightarrow Al^{3+} + 3e^- \qquad Eq\ 3.2$$

When using iron electrodes, however, it is not entirely clear whether ferrous or ferric irons are formed:

$$Fe \leftrightarrow Fe^{2+} + 2e^- \quad or \quad Fe \leftrightarrow Fe^{3+} + 3e^- \qquad Eq\ 3.3/3.4$$

Simultaneously, reduction occurs at the cathode, receiving water molecules and free electrons to produce hydroxide ions and hydrogen gas. The final pH is always higher than the initial pH due to hydroxyl formation at the cathode (Harif, and Adin, 2007).

$$2H_2O + 2e^- \rightarrow 2OH^- + H_2 \qquad Eq\ 3.5$$

The number of electrons released from the electrodes is stoichiometrically related to the amount of reactants consumed or products generated. These electrons are measured as the charge

placed across the electrodes. The relationship between charge and the mass of product generated is expressed by Faraday's law:

$$m = \frac{i * t * MW}{96485 * e} \qquad Eq\ 3.6$$

Where: m = the mass of the product generated (g)

i = the current applied between electrodes (A)

t = the time the current was applied (s)

MW = the molecular weight of the element in question

e = the number of electrons produced from the half reaction

The opinions on the accuracy of Faraday's Law, however, vary greatly amongst researchers. Some have indicated that only 50% of the predicted mass is produced (Pouet and Grasmick, 1995) while others indicated that 200% is actually produced (Donini et al., 1994). Sasson et al. (2009) recently showed that regardless of pH values and electric currents, at least 80% of the iron in solution complied with Faraday's laws of oxidation.

The metal ions then combine with the hydroxyl ions, creating a metal-hydroxide complex which is a standard coagulating mechanism (Koren and Syversen, 1995).

$$Al^{3+} + 3H_2O \rightarrow Al(OH)_3 + 3H^+ \qquad Eq\ 3.7$$

$$Fe + 2H_2O \rightarrow Fe(OH)_2 + H_2 \qquad Eq\ 3.8$$

3.1.2 Coagulation

Coagulation is the process of chemically changing colloids so that they are able to form bigger particles by coming close to one another (Jarvis et al., 2005). It involves the formation of chemical flocs that absorb, entrap, or otherwise bring together suspended matter such as algal cells (Nemerow, 1978). The aggregation process of these particles to form flocs is described as colloidal destabilization. Four mechanisms of destabilization exist: compression of the double layer, adsorption

for neutralization of charges, entrapment in a precipitate, and adsorption for interparticle bridging (Faust and Aly, 1998).

Algal cells are stable in aqueous systems, by virtue of the electrostatic charge on their surfaces. The charge of an algal cell is typically electronegative for pH 4-10, ranging from -10mV to -35mV (Henderson et al., 2008). The electrostatic charge is formed across the diffuse double layer due to a potential gradient between the shear surface of the cell and the bulk solution. The magnitude of this electrostatic potential is measured by zeta potential (ζ), as seen in the following equation.

$$\zeta = \frac{4\pi q d}{D} \qquad Eq\ 3.9$$

Where: q = charge per unit area

d = layer thickness surrounding the shear surface through the effective charge

D = dielectric constant of the liquid

When a coagulant is added to the culture, its positively charged ions enter the double layer of the cell and reduce the zeta potential. The double layer is physically reduced in size because of this loss in charge. This first mechanism of destabilization is the double layer compression. Charge neutralization is continued with excess absorption of positive ions onto the algal cell. This can reduce the zeta potential to an extent where charge reversal is a possibility. These first two methods of destabilization reduce the repulsive charges and increase the probability of floc formation.

With the zeta potential reduced, the attractive van der Waals forces between cells dominate the interparticle reactions. This interaction is the entrapment of low zeta potential cells with precipitates of no net charge (Faust and Aly, 1998). A physical destabilization of the cell is observed when entrapment occurs. With the repulsive charges overpowered by the van der Waals forces, the particles come into contact and form bonds. This process of bridging the coagulated algal cells to form larger aggregates is known as flocculation (Gregor et al., 1997).

3.1.3 Flocculation

The aggregation process (flocculation) is largely dependent on the duration and amount of agitation applied to the water. The degree of agitation is based on the power imparted on the water, which is measured by the velocity gradient (G) (Reynolds and Richards, 1996).

$$G = \sqrt{\frac{P}{\mu V}} \qquad Eq\ 3.10$$

Where P = power imparted to the water, (N-m/s)

μ = absolute viscosity of the water, (N-s/m^2)

V = basin volume, (m^3)

The typical G values for flocculation in wastewater treatment are 50-100 s^{-1} with a detention time of 30-60 min (Metcalf and Eddy, 2003). Once floc formation is achieved, harvesting costs are reduced significantly and filtration, sedimentation or flotation can be used for harvesting instead of centrifugation (Wiffles, 2010). However, the cost of floc formation must justify the reduced costs for these other harvesting techniques.

Electrocoagulation has shown to be an effective water treatment technique for wastewater (Feng et al., 2003), phosphate removal (Irdemez et al., 2006), distilleries (Kannan et al., 2006) municipalities (Bukhari, 2008), textiles (Cerqueira, 2009), as well as algae (Gao et al., 2010). However, there are not enough proposals reported that provide techniques for reducing the energy and electrode consumption (Martinez et al., 2009). Such techniques are pivotal for electrocoagulation to be an effect algae harvesting technique. The objective of this research was to determine the economic viability of using electrocoagulation to harvest algae for biodiesel. Energy consumption under various salinities and charge densities as well as aluminum and iron charging efficiencies were the main parameters accounted for in this cost analysis.

3.2 Materials and Methods

3.2.1 Salinity of Culture Medium

For electrocoagulation to be an effective algae harvesting technique, sufficient electrolytes must be present within the culture medium to provide efficient conductivity. For brackish or saltwater species the lack of these electrolytes is not an issue, but many freshwater mediums will need additional ions. A freshwater species, *Nannochoris sp*. was cultured in 1 L of standard Guillard's F/2 medium as well as mediums containing 1, 2, and 4 g/L of NaCl. Aeration for all 12 flasks was supplied by a 30 L/min air pump (Hailea V-30) which was split through a 24 port manifold each with its own 0.32 cm brass needle valve for individual air flow control. Attached to each needle valve was 30 cm of 0.48 cm I.D. Tygon tubing with 2.54 cm air diffuser (AquaticEco AA1). After seven days of culturing under florescent lighting, the biomass growth was measured as total suspended solids (TSS) to determine if the added electrolytes had a negative impact on the growth. The zeta potential of these cultures was also measured using a Malvern Zetasizer Nano electrophoretic light scattering unit.

3.2.2 Electrocoagulation Testing

Both *Nannochloris sp* and *Dunaliella sp* were cultured to concentrations of ~100 mg/L for the electrocoagulation testing. The electrochemical cell consisted of 1.3 L acrylic reactor that was 73.5 cm^2 by 18 cm tall. Both the anode and cathode comprised of two (each) perforated (.3175 cm O.D. holes, accounting for 40% of open area) aluminum (milled alloy 3003) or iron (carbon milled steel) plates (0.16 cm thick) connected in parallel. Each plate had a submerged surface area of approximately 90 cm^2 for a total electrode surface area of 361 cm^2 (180.5 cm^2 for anode, 180.5 cm^2 for cathode). The acrylic reactor was set upon a ceramic stir plate (Barnstead Cimarec, SP131325) and filled with 1 L of algal culture and a 3.8 cm magnetic stir bar. The electrodes were separated about 1.3 cm from their nearest counterpart and designed to rest on the edge of reactor. The DC power supply

(Mastech, HY1803DL), which allowed for both amperage and voltage adjustment, was attached to the electrodes by alligator clips (Figure 3.2).

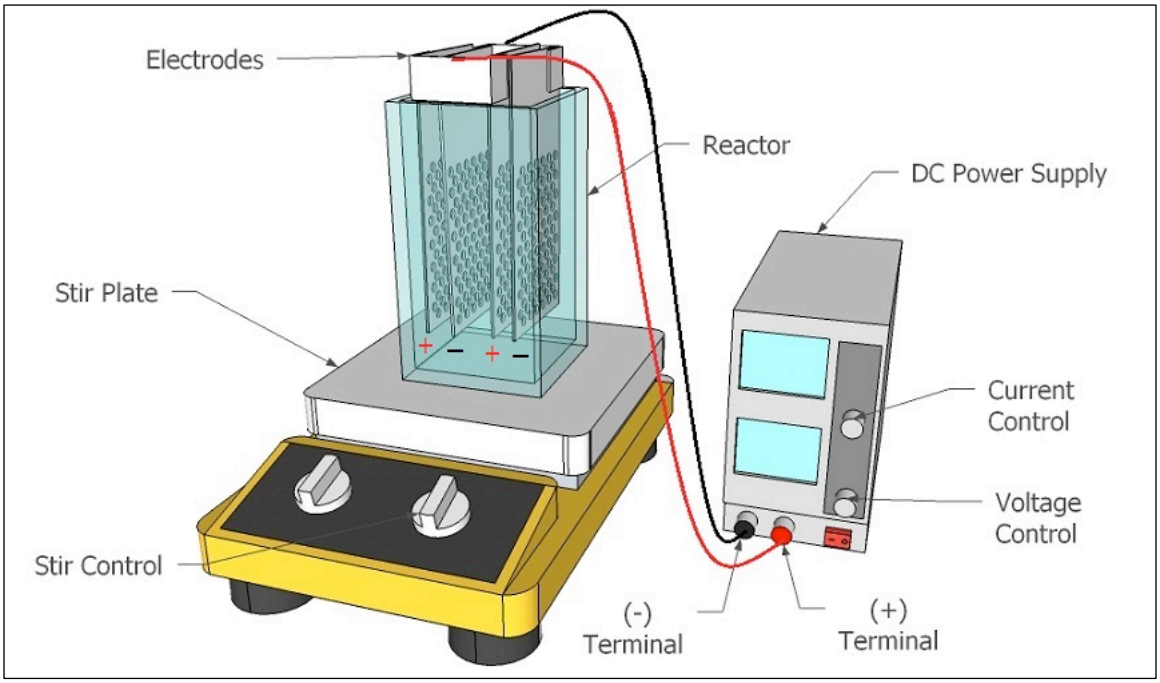

Figure 3.2: The electrocoagulation experimental setup with dual perforated plate electrodes for batch microalgae harvesting

The current control was always adjusted to its maximum setting before the start of all testing so that the applied voltage would be the limiting setting. The stir plate was turned on (level 7 setting) to initiate mixing and a sample of the uniform culture was collected to serve as a baseline for removal efficiency computations. The DC power source was turned on and the voltage was adjusted to obtain the desired amperage. The amperage was maintained for the predetermined electrocoagulation time. For all the experiments, irrespective of the electrocoagulation time, only one minute of rapid mixing ($G = 90\ s^{-1}$) was performed on every sample. For experiments with a 1 min electrocoagulation time, the 1 min flash mixing occurred simultaneously for the entire duration of the minute. However, if the testing required longer applications of amperage (ex: 2 min), then no mixing occurred during the first minute of applied amperage, but was initiated during the final minute of amperage.

After the current was removed from the cell, an additional flocculating mix (level 3 setting, $G = 18\ s^{-1}$) was initiated for 15 min. After the flocculating mix was completed, the reactors were allowed

to rest for 30 min. During this time the flocculated algal cells either floated to the surface or settled to the bottom. An additional sample was taken at the midpoint (about 7.6 cm below the water level) to determine the concentration of any unsettled or non-floating algal cells.

The samples taken were quantified by measuring the absorbance at 680 nm with a spectrophotometer (Genesys 20). These values were converted to TSS using a calibration curve correlating the culture absorbance to the culture density of *Nannochloris sp.* or *Duanliella sp*. (mg/L).

3.3 Results and Discussion

3.3.1 Salinity of Culture Medium

Algae differ in their adaptability to salinity and based on their tolerance extent, they are grouped as halophilic (salt requiring for optimum growth) and halotolerant (having response mechanism that permits their existence in saline medium) (Rao et al., 2007). *Nannochloris sp*., a freshwater algal species, was selected to observe its tolerance to saline medium (Figure 3.3). This tolerance was an indication of the species suitability for electrocoagulation harvesting. Cora and Hung (2009) indicated that additional NaCl was necessary for maximum current efficiency for their electrocoagulation setup.

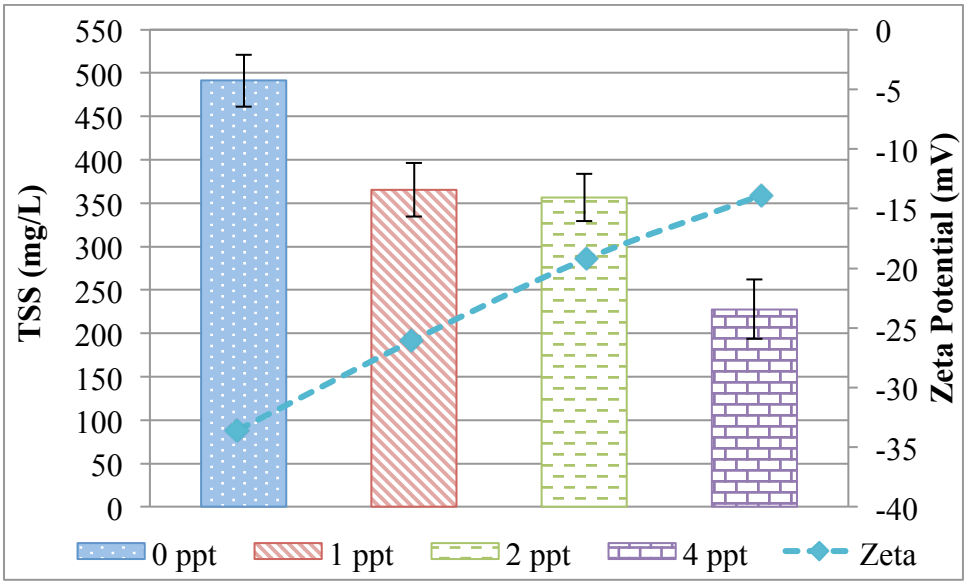

Figure 3.3: The columns represent the final biomass concentration in mg/L after 1 week of culturing *Nannochloris sp.* in various salinities. The dashed line shows the decrease in zeta potential with increased salinity.

The additional salt in the medium showed an average decrease in biomass of 25.7% (±3.8%) for 1 ppt NaCl. At 2 ppt no further loss in biomass of significance was seen ($p>0.05$). However, at 4 ppt NaCl, the biomass decreased by 53.6% (±11.3%) from the original culture. Other authors have indicated that the reduced biomass was offset by increased lipid concentration, which was likely triggered due to the stress of a saline medium. The total fat content of the alga grown in different salinity varied in the range of 24-28% (w/w), whereas in control it was 20% (Rao et al., 2010).

It was also noted that as the salinity increased, the zeta potential of the algal cells decreased. The charge of an algal cell is typically electronegative for pH 4-10, ranging from -10mV to -35mV (Henderson et al., 2008). The zeta potential for the 0 ppt *Nannocholoris* culture measured -33.6 mV and decreased in -13.9 when the species was cultured in 4 ppt solution. The cultures grown in salinity were more likely to form clusters, as complete charge neutralization was not necessary to initiate cell aggregation (Henderson, 2008). The cell aggregation was a potential cause of the reduced growth rates at higher salinities.

The importance of salinity was seen when a current was applied across the electrode setup depicted in Figure 3.2. The energy utilized to maintain these amperages was compared across the various salinities used to culture *Nannochloris sp.* (Figure 3.4). These concentrations were compared with a *Dunaliella sp.* medium (15 ppt NaCl), which was considered to provide maximum conductivity.

When the current was increased to 1.4 A for 1 min, the energy required to maintain said amperage increased by 0.107 kWh/m^3 between 15 ppt and 1 ppt NaCl. More than 18 V was needed to maintain 1.4 A at 0 ppt. This was limited, however, by the capacity of the DC power source. It was postulated by the curve (dotted line in Figure 3.4) that maintaining the same amperage at 0 ppt required an additional 0.285 kWh/m^3 of energy than at 1 ppt. As the amperage was reduced to below 0.6, the additional energy requirements between 1 and 15 ppt was 80% less than the projected energy

difference at 1.4 A. As evidenced by Ofir et al. (2007), adjusting the salinity for electrocoagulation proved beneficial to energy consumption.

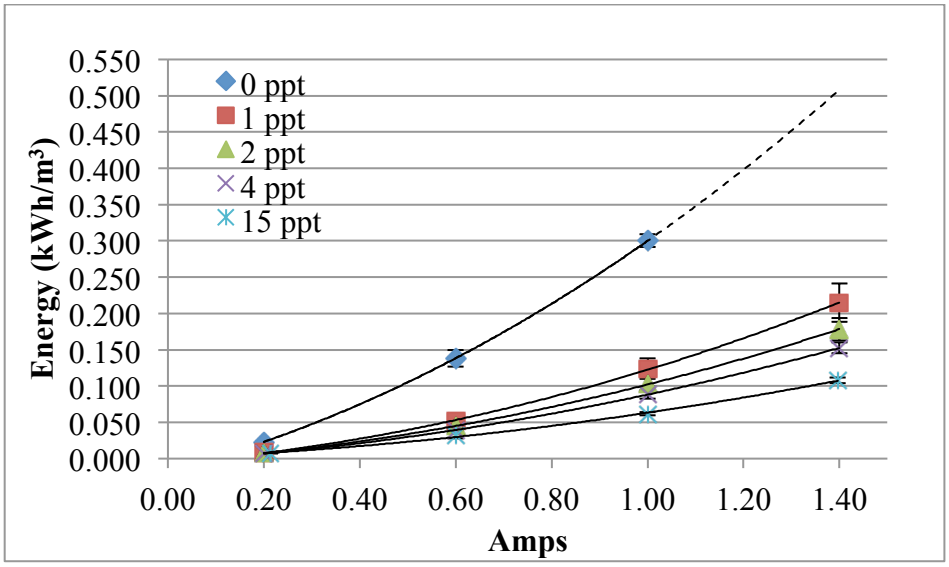

Figure 3.4: The correlation of NaCl concentrations as an electrolyte and the energy consumed per cubic meter to maintain various amperages across aluminum electrodes

The actual effects of harvesting *Nannochloris sp.* under saline conditions by electrocoagulation can be determined when the results of Figures 3.3 and 3.4 are combined to provide a cost per liter value (Figure 3.5). It was noted that when no salinity was added (0 ppt), the culture not only had the highest biomass production, but also the highest energy consumption for electrocoagulation. Conversely, when 4 ppt of NaCl was added to the culture, the lowest biomass growth resulted but the electrocoagulation process was also the most energy efficient. Assuming that 100% of the algal biomass from Figure 3.3 was harvested by the energy requirements in Figure 3.4, a cost value can be applied by the following equation.

$$\frac{L_{culture}}{mg_{algae}} * \frac{1}{\%\ lipids} * \frac{864\ g_{oil}}{L_{oil}} * \frac{m^3{}_{culture}}{g_{algae}} * \frac{X\ kWh}{m^3{}_{culture}} * \frac{\$0.09}{kWh} = \frac{\$}{L_{oil}} \qquad Eq\ 3.11$$

Based on the energy requirements to produce 1 L of oil, a culture medium salinity of 2 ppt was found to be the most cost effective dosage in terms of biomass produced and conductivity achieved for electrocoagulation. Despite the greater biomass produced under non-saline conditions, the lack of conductivity made harvesting by electrocoagulation uneconomical. Likewise, the conductivity

provided by 4 ppt NaCl in the culture medium was offset by the reduction in algal biomass of *Nannochloris*.

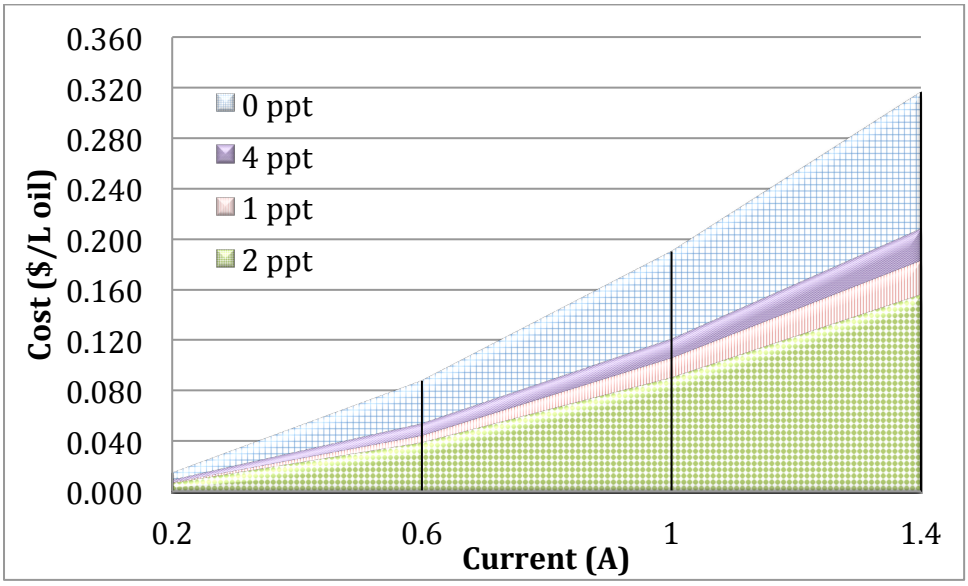

Figure 3.5: The cost per L oil based off of the correlations between the growth densities (Figure 3.3) and the energy consumption (Figure 3.4) due to various salinities

It should also be noted that the addition of salinity, if necessary, for a full scale freshwater operation would only be required during initial culturing due to a recycling of the effluent. It is also possible that the salinity of these freshwater cultures could increase without the addition of chemical salts due to high evaporation rates often seen in open ponds. Additionally, as the species becomes acclimated with the higher salinity, the reduction in biomass would become less prevalent. Therefore, the potential negative effects to produce extra conductivity are anticipated to be minimal.

3.3.2 Electrocoagulation

The main costs associated with electrocoagulation are the energy inputs from current application across the electrodes and the loss of electrodes due to oxidation. Of the two costs, the oxidizing of the electrode typically accounts for over 70% of the total costs (Jiang et al., 2002). Therefore, the most cost effective electrode material must be selected. For harvesting algae, aluminum has often been considered as the more effective electrode material (Aragon et al., 1992; Bukhari, 2008; Vandamme et al., 2011). However, over the course of 2012, the price of aluminum has averaged

$2.187/kg (±$0.12/kg), whereas the price of iron has averaged $0.113/kg (±$0.02/kg). Therefore, both materials were tested to compare the combined effect of efficiency and cost.

Applying the desired amount of aluminum or iron through electrocoagulation can be achieved through various combinations of amperages and times. These combinations produce a certain charge density based on the electrode surface area. Numerous authors have had varying opinions on the most effective charge density for electrocoagulation. These values have ranged from 2-5 A/m^2 under Jiang et al (2002) to 25-125 A/m^2 by Cerqueira et al. (2009) and even 182 A/m^2 from Kannan et al. (2006). After numerous preliminary tests (Appendix C), two sets of charge densities were applied by varying the time of amperage application (1 and 2 min), which would produce the same theoretical concentration of aluminum and iron ions in solution (Figure 3.6).

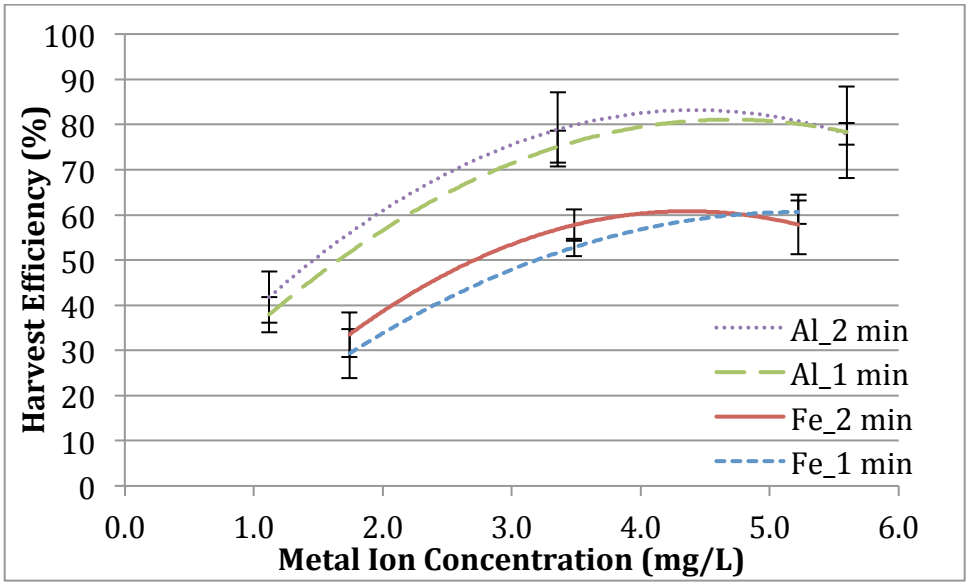

Figure 3.6: The harvest efficiency of *Nannochloris sp.* under various charge densities producing similar concentrations of aluminum and iron from the electrodes

Based on the two sets of charge densities used, it was determined that the charge density did not significantly ($p>0.05$) impact the harvesting efficiency within each metal group. For example, applying 0.6 amps for 1 min or 0.3 amps for 2 min across the aluminum electrodes resulted in approximately 77% harvesting efficiencies by producing similar concentrations of aluminum ions. Similarly, applying 0.2 amps for 1 min or 0.1 amps for 2 min across the iron electrodes resulted in

approximately 55% harvesting efficiencies by producing similar concentrations of iron ions. As other researchers have indicated (Bouhezila et al., 2011; Vandamme, 2011), the aluminum electrodes were more effective than the iron electrodes. The aluminum electrodes harvested nearly 20% more biomass throughout the testing.

However, there were noteworthy variations in the energy required to maintain the currents applied in Figure 3.6. The voltage needed to maintain higher currents for shorter amounts of time consumed more energy than maintaining smaller currents for longer periods of time (Poelman et al., 1997; Sasson et al., 2009). Gao and coworkers (2010) saw similar increases in energy consumption when the charge density was increased in the range of 0.5-5.0 mA/cm^2. When treating large volumes of water, these differences in energy consumption can have a huge impact on the cost of the final product. Figure 3.7 shows the energy consumed per m^3 for the aluminum and iron electrodes under the two charge densities.

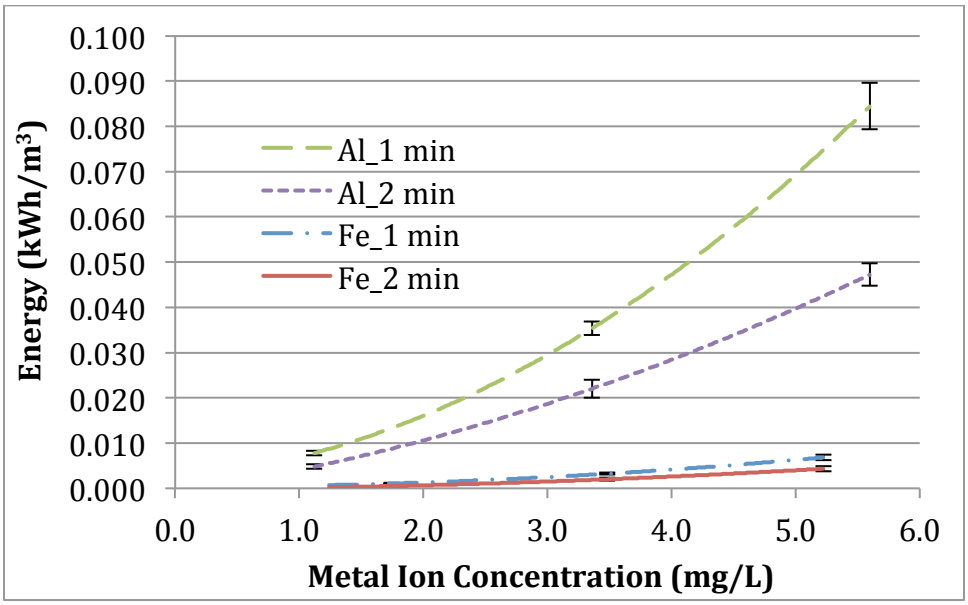

Figure 3.7: The energy requirements to produce aluminum and iron ions under various charge densities

The differences in energy usage were greater when larger concentrations of aluminum were dissolved from the electrode, indicating that a lower charge density would be more economical in terms of harvesting. While the aluminum electrodes proved to be more efficient at harvesting,

however, the iron electrodes showed better conductivity. From an economic standpoint, the ability of the iron electrodes to maintain currents at lower voltages will likely compensate for the lower harvesting efficiency experienced in Figure 3.6.

The final cost to harvest microalgae by electrocoagulation was determined by the harvest efficiency of Figure 3.6, the energy consumption in Figure 3.7, and the cost of the electrode material. The division of harvesting costs was plotted against the metal ion concentration produced by 1 and 2 min current applications from the electrodes (Figure 3.8).

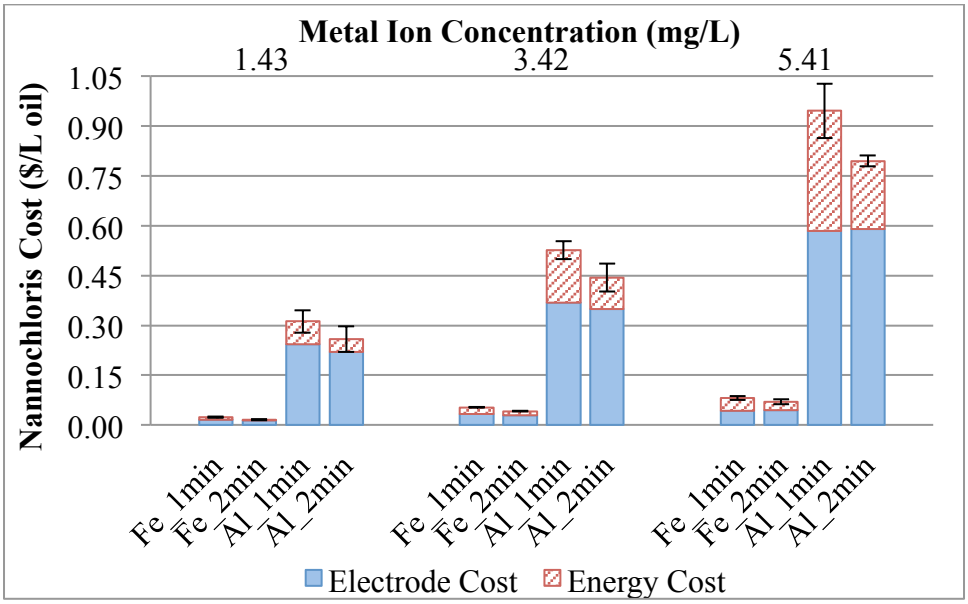

Figure 3.8: The cost (electrode and energy) per L of oil as a function of the *Nannochloris sp.* harvesting efficiencies by aluminum and iron electrodes under multiple charge densities

As seen in Figure 3.8, the electrodes accounted for 50-85% of costs in electrocoagulation, depending on electrode material and charge density. Even though the aluminum electrodes showed better harvesting efficiencies, the material cost was nearly 20 times that of iron electrodes. The 20% higher harvesting efficiency of aluminum was not offset the difference in metal prices. This trend was further confirmed (Figure 3.9) by harvesting *Dunaliella sp.*, a brackish water species (15 ppt), by the said electrocoagulation process at the 2-minute electrocoagulation time.

It was also determined that despite the lower harvesting efficiency achieved at approximately 1.4 mg/L of either aluminum or iron ions, the economics were more favorable at 1.4 mg/L than the

higher harvesting efficiencies achieved at greater metal concentrations (3.42-5.41 mg/L). This strategy was confirmed by Dassey and Theegala (2013) as the preferred harvesting goal through algae harvesting by centrifugation.

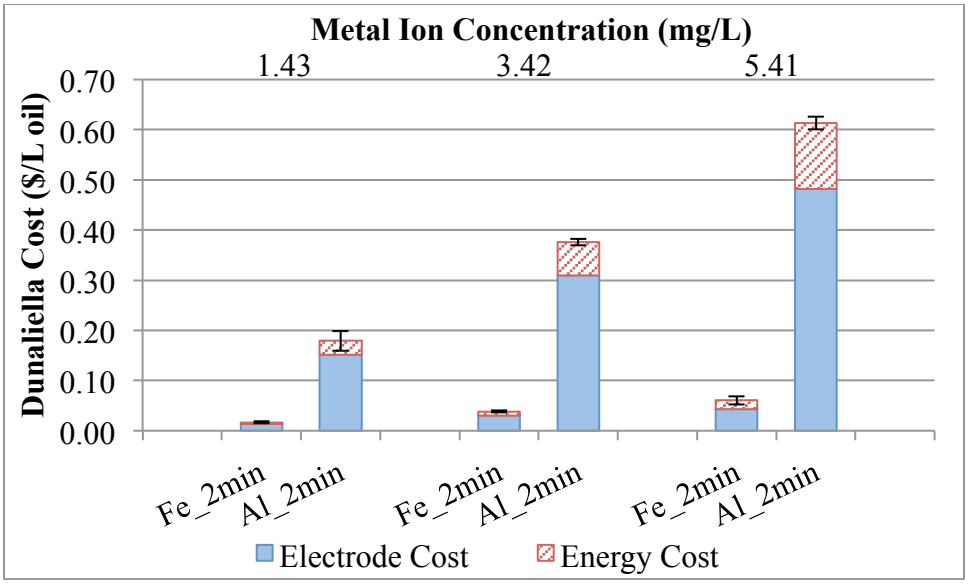

Figure 3.9: The cost per L of oil as a function of the *Dunaliella sp.* harvesting efficiencies by aluminum and iron electrodes under multiple charge densities

3.4 Conclusion

Electrocoagulation proved to be an effective algae pre-concentration technology for both *Nannochloris sp.* and *Dunaliella sp.* Culturing *Nannochloris sp* in 2 ppt NaCl decreased the biomass production by 25.7% but was found to be the most cost effective dosage in terms of biomass produced and conductivity during electrocoagulation batch test. It was anticipated that as the culture became acclimated with the increased salinity, the algal productivity would return to its original growth rates while maintaining the improved conductivity. When comparing iron and aluminum electrodes, aluminum consistently harvested 20% more biomass than the iron electrodes. However, the iron electrodes showed better conductivity when equivalent currents were applied. This energy efficiency, paired with the cost of iron at approximately 20 times less than aluminum, exemplified iron as the more suitable electrode for algal harvesting. By using the appropriate strategy, the pre-concentration of microalgae for biodiesel production by electrocoagulation could see costs less than $0.03/L oil.

Chapter 4: Continuous Microalgae Harvesting

4.1 Introduction

The batch testing in Chapter 3 revealed that electrocoagulation was effective at coagulating microalgal flocs and could be used as the first stage of a 2-stage harvesting system. Applying 0.05 amps for 2 minutes across iron electrodes in a 1 L cell consumed minimal energy and iron ions to form settleable algal flocs for predicted costs less than $0.03/L algal oil. In the electrolytic treatment of algae in a continuous system, a balance between algal loading and electrical current is necessary to achieve high algae removal efficiency and minimum release of excess metal ions (Alfafara et al., 2002; Azarian et al., 2007). Therefore, the objective of Chapter 4 was to design a continuous microalgae harvesting system that could concentrate the flocs formed by a continuous electrocoagulation unit.

Sedimentation is a popular separation method because it operates with minimal maintenance and with little technical costs or expenditures on personnel (Janelt et al., 1997). Gravity settling alone will concentrate microalgal suspensions to 1.5% (w/w) solids at reasonable costs (Amaro et al., 2011). However, algal facilities can be expected to process upwards of 43 m^3 (Table 2.1) of culture to produce 1 L of oil depending on the algae culture's growth and lipid production. The mass cultivation of microalgae requires a high overflow rate that favors flotation as opposed to settling (Amaro et al., 2011). The overflow rate for flotation is approximately 81.5 L/min/m^2 as opposed to the 32.6 L/min/m^2 or less for conventional sedimentation tanks (Aulenbach et al., 2010).

Additional advantages to flotation include better treated water quality, rapid startup, high rate operation, and thicker sludge (Feris et al., 2001). Flotation systems can achieve concentrations of 5-10% biomass for easy surface removal as opposed to 1.25% seen by small batch sedimentation (Greenwell et al., 2005; Dassey and Theegala, 2012). Flotation systems also require a smaller footprint than sedimentation tanks. Dissolved air flotation (DAF) systems are designed with smaller surface areas and larger flow rates than sedimentation tanks, resulting in substantial capital savings

(Leppinen et al., 2001). The DAF floor space and volume requirements are only 15% and 5% of a settling basin respectively (Wang et al., 2005). Therefore, to decrease operational costs, an integrated Stage 1 technology was proposed using: electrocoagulation, flocculation, and dissolved air flotation.

4.1.1 Electrocoagulation

Electrocoagulation (EC) is an electrochemical water treatment technique designed to disperse coagulating metal ions from oxidizing electrodes (typically aluminum or iron). To release these coagulating ions an electric potential between the anode and cathode is needed to drive the forward reaction. The electric potential is determined from the electrochemical half reactions at each electrode. As determined in Chapter 3, iron electrodes were more cost effective than aluminum electrodes despite a lower harvesting efficiency achieved. Iron is also less toxic than aluminum and more acceptable in the agriculture field (Bouhezila et al., 2011). The two independent half-reactions for iron electrodes that were identified in literature are shown below. Oxidation occurs at the anode as electrons increase in energy and flow into solution, resulting in the formation of coagulating iron ions.

$$Fe \rightarrow Fe^{2+} + 2e^{-} \qquad \text{Eq 4.1}$$

Simultaneously, reduction occurs at the cathode as water molecules and free electrons flow towards the electrode to produce hydroxide ions and hydrogen gas.

$$2H_2O + 2e^{-} \rightarrow 2OH^{-} + H_2 \qquad \text{Eq 4.2}$$

The combined reactions result in the formation of ferric hydroxide, which is commonly used in coagulating stabilized colloids.

$$Fe + 2H_2O \rightarrow Fe(OH)_2 + H_2 \qquad \text{Eq 4.3}$$

Coagulation is the process of chemically changing colloids so that they are able to form bigger particles by coming close to one another (Jarvis et al., 2005). The aggregation process of these particles to form flocs is described as colloidal destabilization. Charge neutralization and double layer compression, as described in Chapter 3, initiate colloidal destabilization and make floc formation more

likely. With the repulsive charges overpowered by the attractive van der Waals forces, the particles come into contact and form bonds. This process of bridging the coagulated algal cells to form larger aggregates is known as flocculation (Gregor et al., 1997).

4.1.2 Flocculation

The aggregation process (flocculation) is largely dependent on the duration and amount of agitation applied to the water. The degree of agitation is based on the power imparted on the water, which is measured by the velocity gradient (G) (Reynolds and Richards, 1996). Preliminary testing in Chapter 3 determined that a 15 min flocculating mix ($G = 18\ s^{-1}$) after electrocoagulation was sufficient to develop settleable cell agglomerates in the 1 L batch reactors. Applying a current and velocity gradient (G) induced flocculation, which resulted in precipitation of $Fe(OH)_2$ and formation of algal flocs (Harif and Adin, 2007). The typical G values for flocculation in wastewater treatment are 50-100 s^{-1} with a detention time of 30-60 min (Metcalf and Eddy, 2003). Since the batch testing in Chapter 3 used small concentrations of metal coagulant from the electrodes, long flocculation times coupled with a small velocity gradient was required.

Designing a continuous stirred tank reactor (CSTR) for flocculation, however, requires a different strategy as compared to batch reactors. The goal of this continuous flow system was to harvest algae from a continuous culture flow (Q) of 4 L/min. A single 60 L volume (V) continuous mixed reactor, although would attain the average HRT of 15 minutes, will not ensure 15 minute HRT for each and every algal cell. A single CSTR will allow a portion of the biomass (X) to bypass the reactor before achieving 15 min retention time (discussed below).

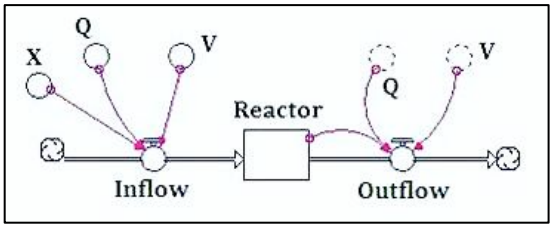

Figure 4.1: Stella model of 1 CSTR

This potential for bypassing the reactor is described by the equation for i[th] complete-mix reactors in series:

$$C_i = \frac{C_o}{(i-1)!}\left(\frac{t}{\tau_i}\right)^{i-1} e^{-t/\tau_i} \qquad Eq\ 4.4$$

Where: C_i = the biomass concentration of reactor i

C_o = the instantaneous biomass concentration in the first reactor (X)

t = time

τ = hydraulic residence time (V/Q)

If a 60 L completely-mixed reactor with an average hydraulic residence time (HRT) of 15 min was used for flocculation, then only 36.8% of the biomass would experience the full 15 min of flocculation. The remaining biomass will have been flushed from the system before the desired flocculation time. The main drawback of the CSTR for flocculation is its mixing field heterogeneity, which requires long retention times (Kurbiel et al., 1991).

The CSTR needs to be over 1000 L with and HRT of 10.4 h to ensure that 95% of the biomass experiences 15 min of flocculation. An alternative solution is to use multiple reactors in series. The output from a plug-flow reactor with axial dispersion is often modeled using 10 complete-mix reactors in series (Theegala et al., 1999; Metcalf and Eddy, 2003).

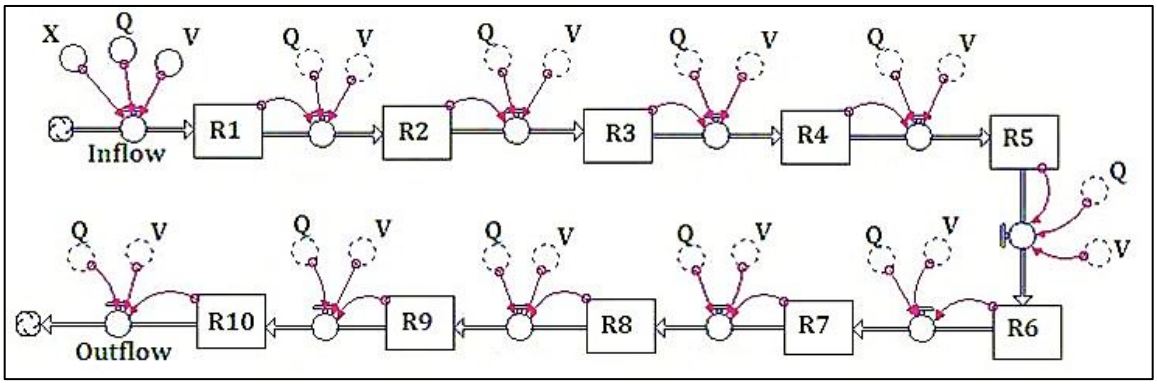

Figure 4.2: Stella model of 10 CSTRs in series representing a plug-flow reactor

Aligning 10 reactors in series with 12 L volumes would provide 99% of the biomass with 15 min of actual flocculation. The resulting HRT would only be twice that of the batch testing at 30 min.

The number of reactors and their volumes can be adjusted based on the length of flocculation and the percentage of biomass retention. Once the algal flocs have formed, they are then suitable for flotation.

4.1.3 Dissolved Air Floatation

Dissolved air flotation (DAF) uses pressure saturation (50-90 psi) to increase the solubility of air in water to produce fine microbubbles for solids removal. Dissolved air flotation is an effective method of particle separation because the high concentration of microbubbles and their slow rise rates allow for more collision opportunities with the particulate matter (Al-Shamrani et al., 2002). The relationship of air solubility with pressure is defined in Henry's Law, which states that the amount of gas that can be dissolved in a given volume of liquid at a constant temperature is directly proportional to the partial pressure of the gas (P), which is given by:

$$P = K_c M \qquad \text{Eq 4.5}$$

Where (K_c) is a variation of Henry's constant as defined by Haarhoff and Steinback (1996) for a specified gas and (M) is the molar concentration of the gas in solution. Since air is mostly composed of nitrogen and oxygen, the molar concentration of air (M_a) with respect to pressure is provided by:

$$M_a = M_n + M_o = P_n/K_{c,n} + P_o/K_{c,o} \qquad \text{Eq 4.6}$$

Where M_n = molar concentration of nitrogen

M_o = molar concentration of oxygen

$K_{c,n}$ = Henry's constant for nitrogen at a given temperature

$K_{c,o}$ = Henry's constant for oxygen at a given temperature

Therefore, as the pressure of the system increases, the amount of air (mostly N_2 and O_2) dissolved into water will also increase. When the pressurized water is released to atmospheric conditions, tiny microbubbles with diameters ranging from 10 to 100 um with typical diameters of 40 um are formed (Edzwald, 1995). The microbubble flow is combined with the flocculated algal culture

in the contact zone of the flotation tank, where the microbubbles produce a dense cloud that carries the light weight particles to the surface where they can be skimmed from the flotation zone.

Pressurizing the recycle flow is the most common technique used during the dissolved air flotation process (Al-Shamrani et al., 2002; Ross et al., 2000, and Schwoyer, 1981). As seen in Figure (4.3), the recycle flow is drawn from the treated effluent exiting the flotation tank and returned to the dissolution tank for re-pressurization and air dissolution. By keeping the incoming algal flow and air saturated flow separate, it is possible to control the volume of air required to treat a specific solids concentration. The recycle ratio (R_r), defined as:

$$R_r = Q_r/Q_a \qquad \text{Eq 4.7}$$

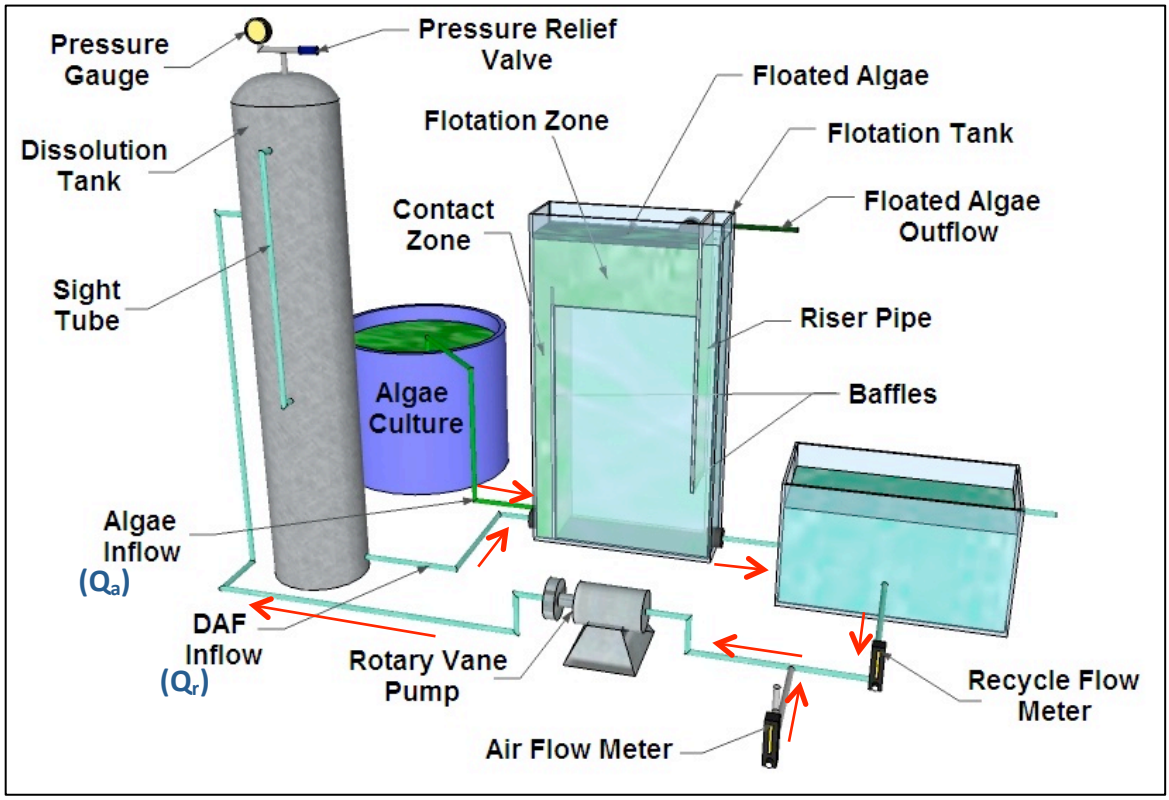

Figure 4.3: The dissolved air flotation system using a recycle flow for pressure saturation and microbubble production in the flotation tank.

Where (Q_r, L/min) is the air saturated recycle flow and (Q_a, L/min) is the algal flow in, is used as a standard measure of the air supplied by a dissolved air flotation unit (Edzwald, 1995). Depending on air solubility and the concentration of solids in the waste flow, recycle ratios vary anywhere from

10 to 100% (Metcalf and Eddy, 2003). The more efficient systems utilize the lowest recycle ratios possible since less pressurized flow is required to maximize the capture efficiency (Ross et al., 2000).

Capture efficiency is defined as the ratio of bubble-captured particles over the number of particles initially present in the treated effluent (Sarrot et al., 2007). Capture efficiency is maximized by increasing the collision opportunity between the microbubbles and particles (Han et al., 2007). The collision opportunity is adjusted by the surface loading of the flotation tank. The overall efficiency, therefore, is determined by relating the rise velocity of bubble/floc agglomerates leaving the contact zone to the surface loading rate of the tank (Jung et al., 2006).

DAF treatment plants are designed and operated applying a wide range of recommended surface loading rates during clarification: 5-15 (Edzwald, 1993), 7.5 m/h (Chung et al., 2000), 20-40 m/h (Amato et al., 2001), 40-98 m/h (Lundh et al., 2002). Regardless of the loading for a DAF system, the formation of buoyant flocs offers a better system than settling for the use of such methods as skimming for final separation of the algal mass (Kumar et al., 1981).

4.2 Materials and Methods

Nannochloris sp., a unicellular green alga, was cultivated outdoors in a 161 cm D x 84 cm H fiberglass tank filled with approximately 1700 L of F/2 medium. The culture was circulated using 2 submerged air lifts made out of 5 cm PVC pipe that stood 109 cm tall with a tee coupling 30.5 cm from the top. Extending from the tee was 61 cm of PVC with an elbow at the end. The bottom of the tee and PVC arm marked the water level in the tank. The air was supplied 2.5 cm from the bottom of the vertical PVC pipe by a Sweetwater air blower (K55JXEPT-395) through 1.3 cm hose barb. This arrangement facilitated gas transfer (CO_2, O_2, and degassing) and brought lower-dwelling cells to the surface for sunlight exposure while providing rotational movement to the culture. The algae was cultured until it reached a density of approximately 100 mg-dry/L.

For the 1 L batch testing performed in Chapter 3, applying (0.05 amps) across the electrodes for 2 min to produce (1.7 mg/L iron) was sufficient in coagulating (65 % ± 5%) of the biomass for harvesting. The objective was to convert these parameters to a continuous system operating at 4 L/min. The incoming algal flow was maintained by a diaphragm pump (Shurflo, 8000-811-288) and a 1.3 cm gate valve and entered 2.5 cm from the base of the electrocoagulation reactor through a 0.95 cm threaded barb fitting.

The electrocoagulation reactor consisted of a 12 cm I.D. acrylic pipe that was 91 cm tall and sealed at the bottom to 0.64 cm acrylic plate (15 cm x 15 cm). Ten (10) perforated iron plates (91 cm x 8.3 cm x 0.16 cm; 0.32 cm diameter holes, 40% open area) were alternated in parallel as cathode and anode and rested 5 cm from the base on a perforated acrylic plate that acted as a diffuser to evenly distribute the incoming flow. The plates were separated by 0.8 cm nylon spacers to maintain the distance between electrodes. Threaded nylon rods (4-40 thread) and nuts were used to keep the spacers in place and provide structure to the electrodes. Reducing the distance between the electrodes reduced the power consumption without changing the degree of separation, since less voltage was needed to maintain the desired current (Koren and Syversen, 1995). This proved to be beneficial because the increased salinity needed in Chapter 3 for improved conductivity was no longer necessary for this arrangement. The flow exited the electrocoagulation reactor through a 1.9 cm barb fitting, 7.6 cm from the top through clear tubing and entered the flocculating system.

The flocculation system (Figure 4.4) used 6 cascading 19 L buckets each with a liquid volume of 15.6 L. The first bucket acted as a rapid mix and used a DC powered servo motor (Allied Motion, 5056-010) and stainless steel shaft with 2 paddles (3.8 cm x 20.3 cm) for a combined surface area of 155 cm^2. The paddles applied a velocity gradient of 405 s^{-1} to the incoming flow. The rapid mix bucket cascaded to 5 flocculation buckets, each with a smaller DC powered servo motor (Molon, CHM-2435-1) and stainless steel shaft/paddle area combination of 103 cm^2 (2.5 cm x 20.3 cm). The

paddles in each of these buckets applied a velocity gradient of 24.2 s^{-1} to the incoming flow. The series of buckets were connected by 1.9 cm bulkhead fittings, with 1.9 cm threaded barbs and clear hosing. A decreasing number of 1.9 cm plywood bases (30.5 cm x 30.5 cm) below the buckets allowed for the gravitational cascading flow between each reactor.

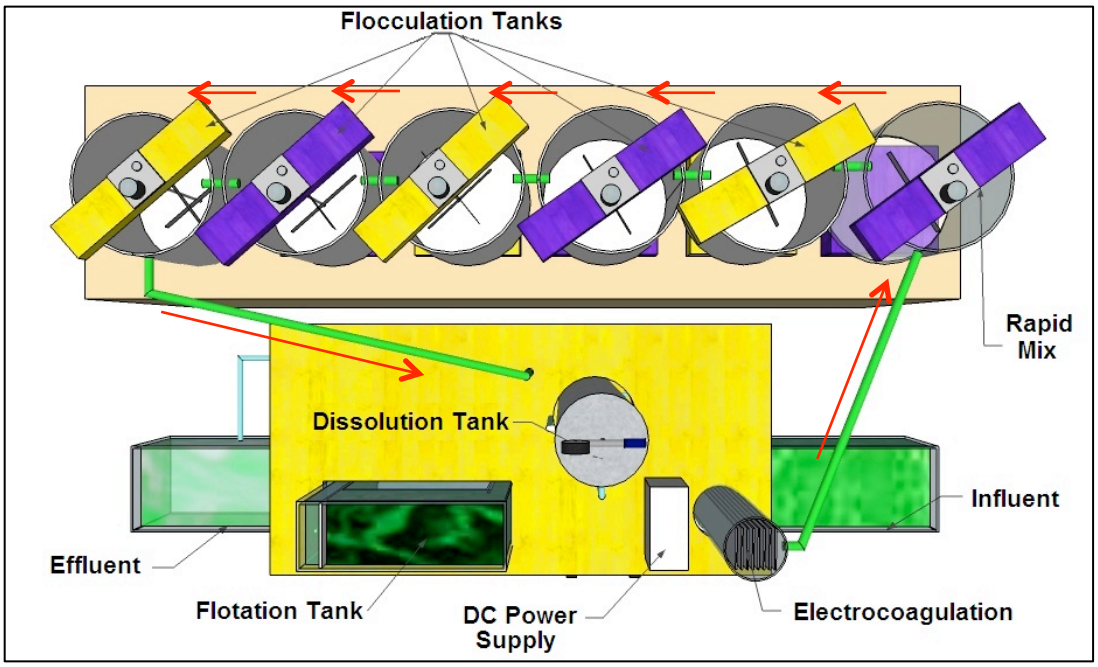

Figure 4.4: A top view of the continuous algae harvesting system showing the flow direction through the 6 CSTRs for coagulation/flocculation.

The dissolution tank was made with a 1.37 m long, 15 cm diameter stainless steel pipe with welded end caps to form a pressure vessel with 25.5 L volume. A stainless steel threaded female couplings with 1.3 cm diameter at the top of the cap accommodated a pressure gauge and continuous pressure relief valve. The pressure gauge could measure up to 1103 kPa, though the system did not exceed 689 kPa, which was previously determined by Dassey and Theegala (2012) to be the most efficient pressure to run the system. The pressure release valve allowed the system to maintain at any pressure ranging from 0 to 689 kPa by expelling any excess air.

Two couplings in the front of the cylinder, separated by about 61 cm, were used to connect a 1.3 cm clear pvc pipe for water level observation (sight tube shown in Fig 4.3 & 4.5). Steady state was maintained between the inflow and outflow by sustaining the water level at a constant height.

A rotary vane pump (Procon, 115B265F31BA) was used to compress a fraction of the recycled effluent into the dissolution tank at potential flows of up to 8.9 L/min at 689 kPa. The incoming line to the pump was split by a barbed tee to merge both the recycled effluent and an incoming air flow to maximize the air saturation in the dissolution tank. The recycle flow was controlled by a variable flow meter with 2.5 L water/min capacity while the air flow was controlled by a variable flow meter with 28 L air/min capacity. The air saturated flow exiting the DAF was maintained at 10% of the incoming 4 L/min algal flow by a gate valve immediately before the flotation tank. The two flows were merged at the contact zone of the flotation tank through (2) 1.3 cm threaded bulkhead fittings.

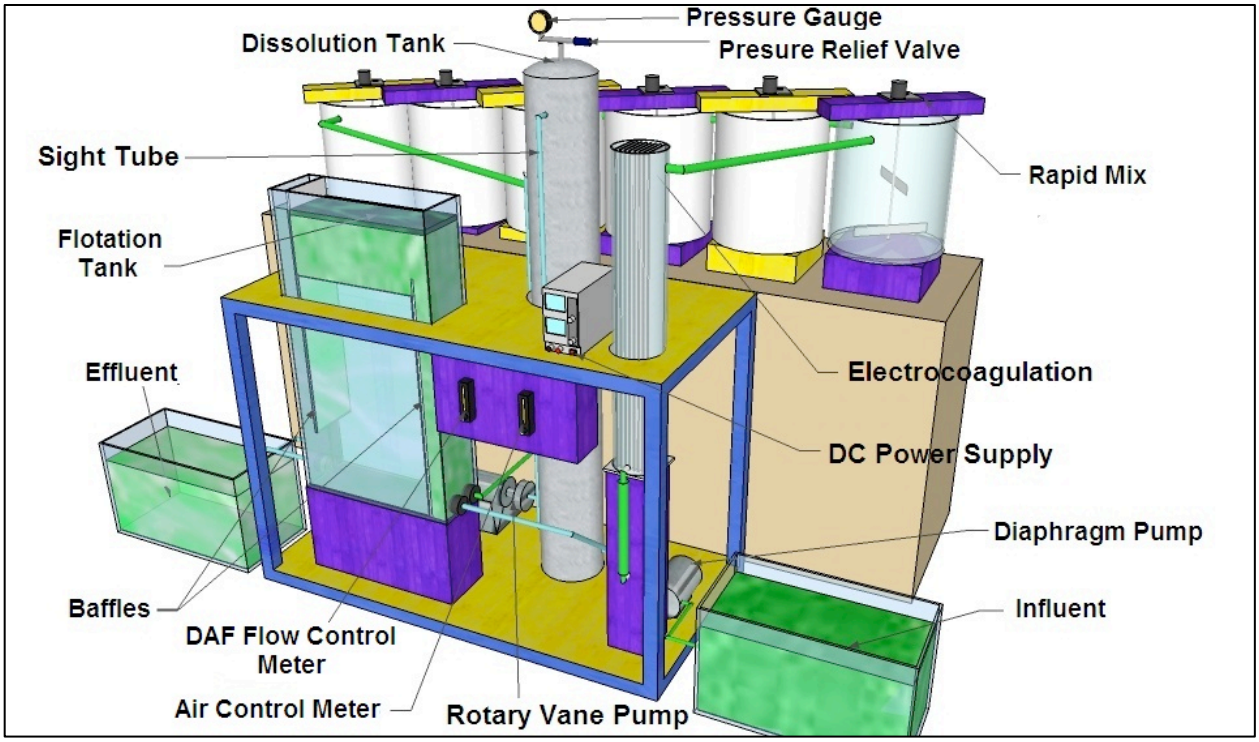

Figure 4.5: Continuous algae harvesting setup; including electrocoagulation unit, CSTRs for coagulation/flocculation, DAF and flotation tank

The flotation tank was made from 0.64 cm thick acrylic to form a rectangular tank that stood 44.5 cm x 14.6 cm x 83.8 cm. The baffle that formed the contact zone was located 4.5 cm from the incoming wall and was attached to the bottom floor and extended to a height of 66 cm. The second baffle that ended the flotation zone was located 4.5 cm from the opposite wall and descended 66 cm from top edge of the tank. A 1.3 cm PVC riser pipe behind the flotation zone baffle stood 76 cm and

maintained a water level of 10 cm above the initial contact zone baffle. This arrangement allowed for the minimum surface loading of 5.1 m/h with a combined flow rate of 4.4 L/min (Figure 4.6).

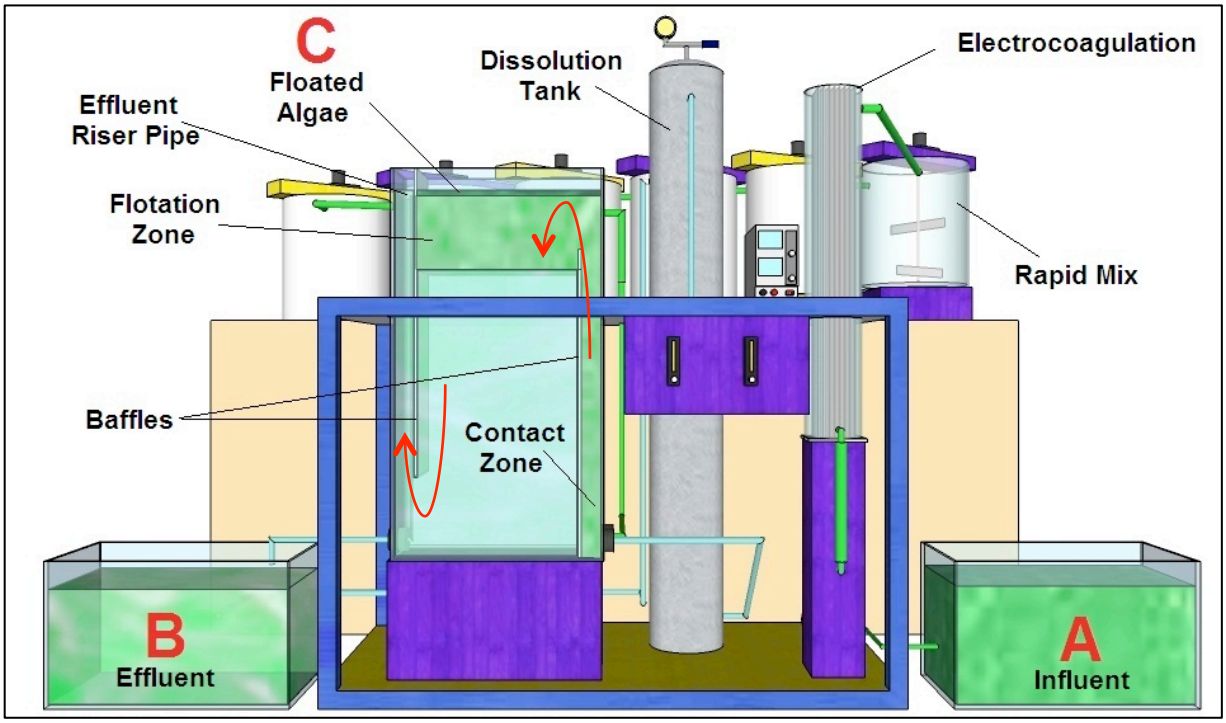

Figure 4.6: Front view of the system showing the locations of sampling

The system was allowed to operate for an hour before sampling began. The samples were taken in 100 mL glass bottles. An influent (A), effluent (B) and floated algal (C) sample were taken every 30 min (Figure 4.6). The floated algal layer was sampled by pipette to avoid excess water content that the float layer would not typically have if removed by a conveyer. Each sample was measured for total suspended solids (TSS) and iron concentration.

4.3 Results and Discussion

4.3.1 Electrocoagulation Harvest Efficiency

A low density (~100 mg/L) *Nannochloris sp* culture was flocculated through a continuous electrocoagulation cell and series of CSTRs before being floated to the surface by the dissolved air flotation unit. The continuous algae harvesting system was effective at low-density algae dewatering by providing a concentrated algal layer at the surface of the flotation tank. As the amperage across the electrodes was increased from 0 to 1 amp, the combined EC/DAF system continued to increase in

efficiency until reaching 55.4% (± 6.9%). Using 2 amps to increase the efficiency showed no improvement, but this was attributed to 40% reduction in expected iron, which is shown in Table 4.1. A maximum harvesting efficiency of 76.2% (± 2.6%) was finally achieved when 3 amps were applied across the iron electrodes. While the harvesting system was able to float flocculated algal cells to the surface for easy removal, the overall efficiency was lower in comparison to the batch testing in Chapter 3.

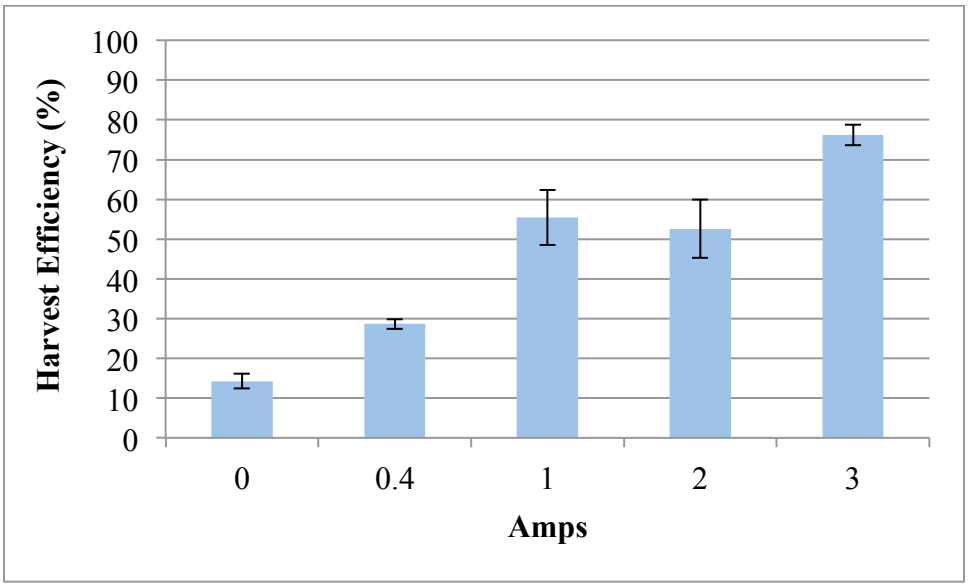

Figure 4.7: The algae harvest efficiency of the continuous system when varying the amperage of the electrocoagulation unit.

Based on the previous experiments in Chapter 3, applying 0.4 amps to the continuous system should have harvested nearly 58% of the incoming biomass as opposed to the 28.6% that was achieved. This 51% decrease in efficiency was attributed to converting the batch parameters to a continuous system as well as flocculation inefficiencies within the series of CSTRs and potential floc degradation upon entering the flotation tank. Despite the reduced floc formation, the majority of the iron deposits were found in the harvested biomass as opposed to being flushed out with the effluent (Table 4.1).

When 0 and 1.0 amp were applied to the electrodes, the harvesting efficiency reduced the effluent iron content by 0.5 and 1.05 mg/L of the influent respectively. However, during the 1.0 amp

run, the incoming biomass content was nearly 300 mg/L as opposed to 140 mg/L seen in the other tests. This increased biomass potentially improved the harvesting efficiency at 1 amp in Figure 4.7. In all other cases, excess iron was found in the effluent. This excess was not anticipated to negatively affect the culture if it were to be recirculated for continuous growth. Liu and coworkers (2008) noted that the addition of 1.2×10^{-5} mol Fe/L (0.67 mg/L) in the initial media suppressed cell growth slightly, but stimulated lipid storage in *C. vulgaris* up to 56.6% by weight of dry biomass, which was 3 to 7-fold higher that in F/2-Si medium supplemented with a lower iron concentration. Increased lipid production was also determined by Amaro et al. (2011) while culturing *C. vulgaris* with excess iron.

Table 4.1: The iron concentration in the influent, effluent, and harvested algal biomass

Amps	Influent[a] (mg Fe/L)	Effluent (mg Fe/L)	Difference (mg Fe/L)	Harvested (mg Fe/L)	Harvested (mg Fe/g biomass)
0	0.7 ± 0.07	0.2 ± 0.09	-0.5	1.5 ± 0.16	0.1 ± 0.02
0.4	1.2 ± 0.02	1.67 ± 0.12	+ 0.47	6.07 ± 1.73	0.35 ± 0.12
1.0	3.6 ± 0.10	2.55 ± 0.32	- 1.05	8.89 ± 3.30	0.4 ± 0.07
2.1	0.8 ± 0.26	2.1 ± 0.38	+ 1.3	9.3 ± 2.19	0.4 ± 0.1
3.1	1.2 ± 0.03	2.7 ± 0.17	+ 1.5	21.3 ± 2.9	0.6 ± 0.12

[a] When accounting for the algae density, the influent iron concentration averaged 8.19 (± 1.57) mg Fe/g biomass for both circumstances.

Investigating the accumulation of lipids as a result of excess iron was outside the scope of this study. However, after the electrocoagulation testing with 3 amps across the iron electrodes, the recycled effluent was used as an inoculum for further culturing in a 100 L clear column under constant aeration and sunlight conditions. The growth of the algae in the effluent was compared to the growth of the algae from the untreated influent, which was diluted so that both cultures would start at the same density. After 4 days of culturing, the recycled effluent showed no signs of reduced cellular production (Figure 4.8). It was determined that the excess iron found in the effluent would have minimal impact on further culturing the algal species.

Despite requiring greater iron content than the batch testing in Chapter 3, the continuous electrocoagulation system still flocculated algal cells with an iron content that was suitable for practical application. When observing the iron content of the harvested biomass on a weight by weight

basis (Table 4.1), the iron content did not exceed 0.6 mg/g of algae. At such a small concentrations, the iron was not anticipated to negatively affect future oil extraction processes.

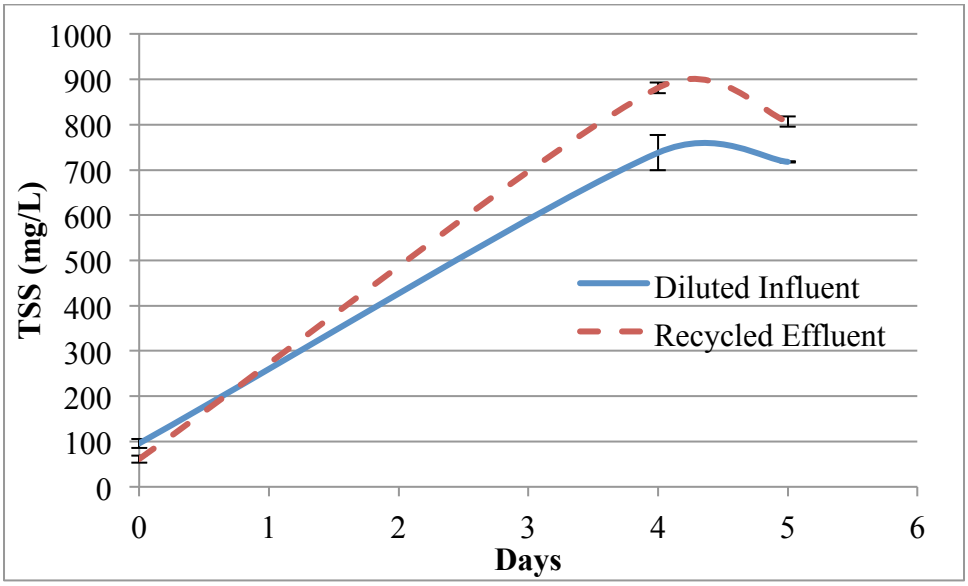

Figure 4.8: Comparing the growth of the *Nannochloris* influent and the effluent after 3 amps of electrocoagulation was applied resulting in an excess of 1.5 mg/L of iron in suspension.

4.3.2 Dissolved Air Flotation Cost Analysis

Dissolved air flotation is often considered too expensive for algae harvesting ventures due to the energy required to pressurize the recycle flow for microbubble production (Feris et al., 2001; Hanotu et al., 2012). For this system, a recycle flow of 10% was deemed acceptable to harvest 100% of the flocs formed during electrocoagulation and reduced operating costs to 0.0466 kWh/m^3 of algae culture treated. Despite using the minimum recycle ratio recommended for DAF operations, its energy consumption remained the most expensive component and therefore the limiting agent for the final costs.

The initial harvesting strategy in Chapter 2 minimized final costs by processing larger volumes at reduced harvest efficiencies to maximize the energy saved. This strategy was applied during electrocoagulation/settling tests in Chapter 3, and showed that by limiting the iron concentrations, the biomass harvested was more affordable despite lower harvesting efficiencies. Since the DAF was a limiting factor for operating costs, however, applying a strategy that focused on reducing

electrocoagulation costs was not practical. Therefore, to reduce the operating costs of the DAF, the amperage was increased to improve the biomass harvesting efficiency until the electrocoagulation costs became inhibiting (Figure 4.9).

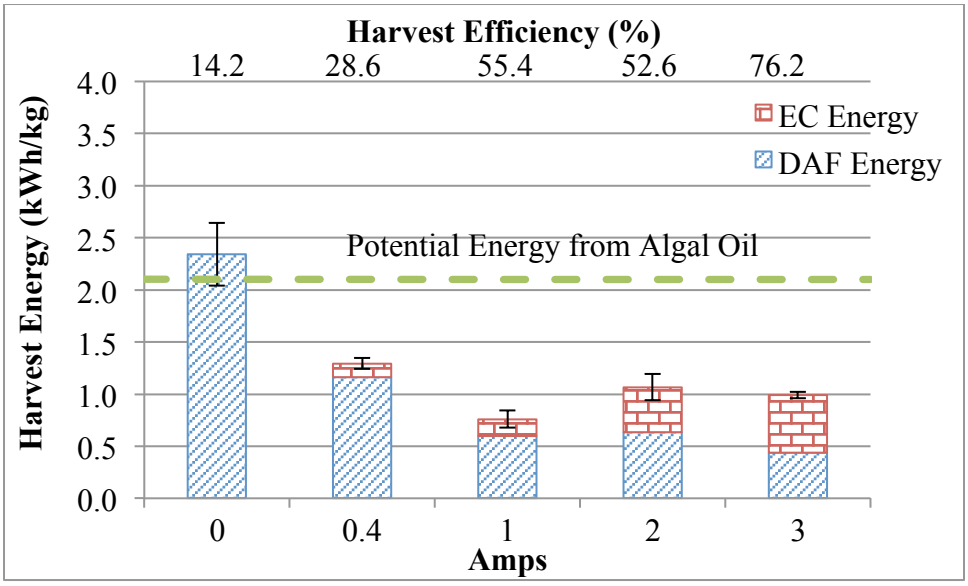

Figure 4.9: A comparison of the electrocoagulation (EC) energy and dissolved air flotation (DAF) energy with respect to the final harvesting efficiency.

As seen from the harvesting efficiencies obtained in Figure 4.9, the increased EC costs due to higher amperages were offset by the decrease in DAF costs up to 1 amp. When comparing the decrease in harvest energy from 0.4 to 1 amp the average EC costs increased by 23.3% but the DAF costs decreased by 48.4%. Despite the increase in EC cost, the overall cost decreased by 41.3%. Due to potential flocculation and scale inefficiencies, increasing the EC unit to 2 and 3 amps became cost inhibiting. The increased costs of the EC system were no longer offset by the increase in harvesting efficiency, which coincides with the energy analysis conducted in both Chapters 2 and 3.

4.3.3 Centrifugation Cost Analysis

The increased harvesting efficiencies achieved during flotation not only provided energy savings for the DAF operations but also increased rate of biomass accumulation at the surface (Figure 4.10). This buildup of solids at the surface continued as flotation continued and compression of the float occurred as a result of drainage of water (Chung and Kim, 1997).

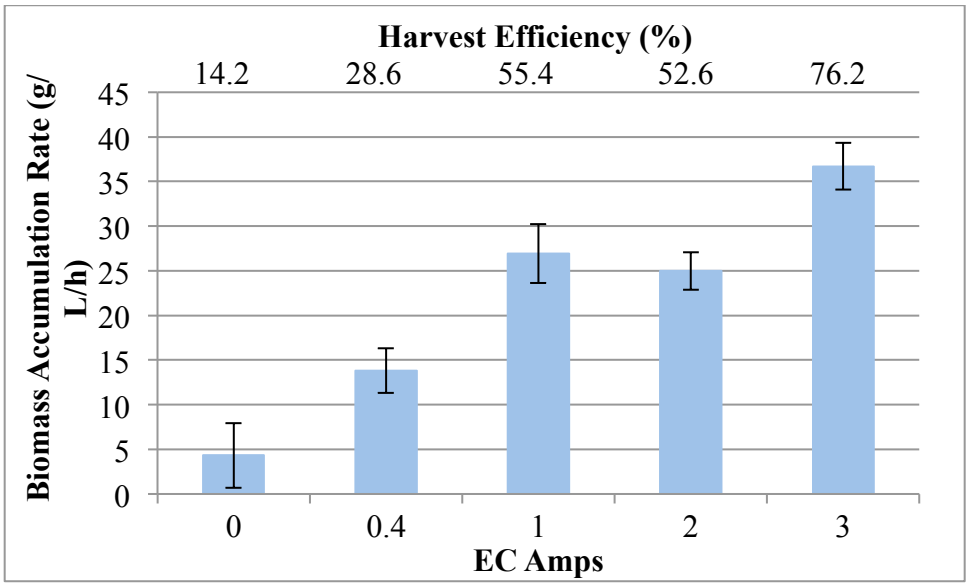

Figure 4.10: The rate of algal biomass accumulation floated to the surface as a result of the combined harvest efficiency of EC/DAF.

When 14.2% of the biomass was harvested by the DAF alone, the average rate of algae accumulation at the surface was 4.3 g/L/h. However, when 76.2% of the biomass was harvested, the rate of accumulation increased to 36.7 g/L/h. If the two-stage system brings the final concentration to 200 g/L (20% solids) by centrifugation, then harvesting 76.2% of the biomass by the integrated EC/DAF system only requires increasing the biomass concentration 5 times as opposed to an increase of 47 times in biomass concentration if only 14.2% were harvested. Considering the centrifuge from Chapter 2 required approximately 20 kWh/m^3 to harvest 100% of the biomass, the resulting centrifuge energy savings was over 4 kWh/kg of algae harvested (Figure 4.11).

For the current harvesting system to consume less energy than what was available as algal oil from a culture grown to approximately 100 mg/L concentration with 20% lipids, it appeared that at least 50% of the biomass needed to be harvested. When the system harvested 55.4% of the biomass, the resulting energy requirement was 1.484 kWh/kg algae. However, it was believed the harvest efficiency was artificially high due to higher biomass concentrations during the 1 amp testing period. Applying 3 amps for 76% harvesting efficiency showed no improvement to the operating costs (1.536 kWh/kg algae), but proved to be effective at harvesting the low concentration algal biomass.

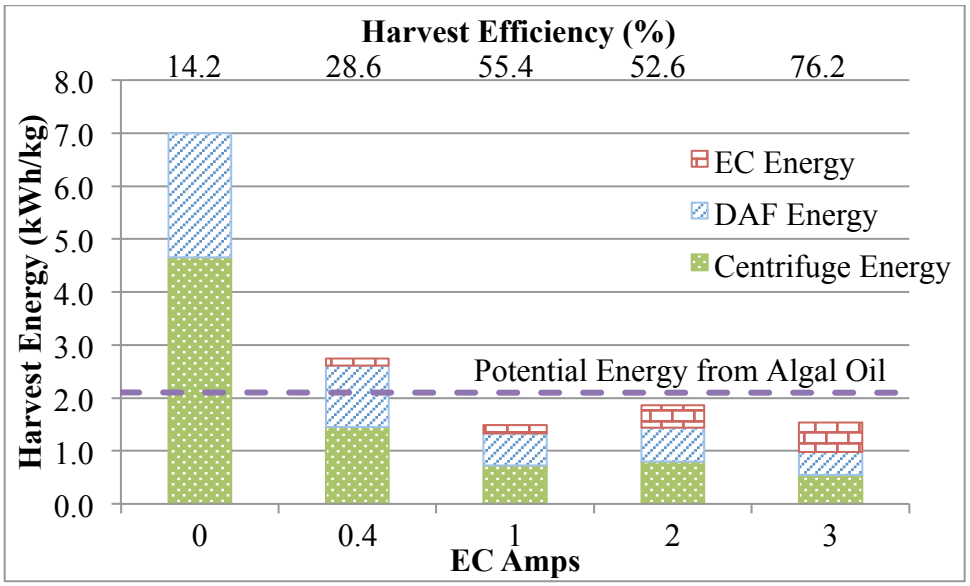

Figure 4.11: A breakdown of the total harvesting energy as a result of applied amperage and harvest efficiency.

4.4 Conclusion

The initial strategy to sacrifice harvesting efficiency for energy savings was practical until the DAF operating costs exceeded the EC costs. Increasing the harvesting efficiency of the electrocoagulation unit to 55% with 1 amp, decreased both DAF and centrifuge energy requirements. Applying 3 amps improved the harvesting efficiency to 76% at a higher cost than when applying 1 amp, but was a more accurate representation of the systems performance. The most cost effective harvesting process was able to dewater a 0.01% algal culture to 20% solids for 1.536 kWh/kg algae. At this energy consumption rate, the system could harvest an algal culture with 20% lipid content for about $0.60/L oil. If the electrocoagulation and flocculation process is improved, then the potential for further energy savings is increased.

Chapter 5: A Life Cycle Analysis Based on the Review of Realistic Algal Biodiesel Production in Louisiana

5.1 Introduction

To assess the sustainability of algal biodiesel as a replacement for petroleum, a life cycle analysis (LCA) was conducted on algae production in Louisiana, which was ranked 3rd in the United States for energy consumption per capita in 2010 (EIA, 2013). Louisiana's transportation sector accounted for 17.1% of its total energy including 52.9 million barrels of motor gasoline and 33.6 million barrels of distillate fuels (EIA, 2010). The energy contained within algal biodiesel is approximately 37.8 MJ/kg (Lardon et al., 2009) as compared to the 43 MJ/kg found in conventional fuels. Therefore, 87.4 million barrels of algal biofuel is needed to potentially replace current transportation fuels in Louisiana. The design of an algae conversion system requires the combination and optimization of several factors such as biomass culturing, growth management, transport to conversion plants, drying, product separation, recycling, waste management, transport of saleable products and marketing (Patil et al., 2008; Singh and Olsen, 2011). Major process engineering accounts for the partial costs associated with biomass culturing, harvesting, oil extraction and oil transesterification (Amaro et al., 2011).

5.2 Biomass Culturing

Algae growth rates, like those of land based plants, are dependent on their photosynthetic efficiency. Photosynthetic efficiency (PE) is the fraction of light energy that can be fixed as chemical energy for biomass production of an algal cell. Oxidative photosynthesis, however, remains somewhat inefficient at converting solar energy to chemical energy and ultimately biomass (Stephenson et al., 2011). The maximum PE that can be achieved is only 10% due to photoinhibition (Beilen, 2010), because the light capturing antennae of algae harvest one photon every 0.5 ms, but the dark phase reaction centers can only process one photon every 5 ms.

Since average solar radiation in the state of Louisiana is 4.6 kWh/m^2/day, the maximum theoretical radiation that can be used by algae for biomass production in a year is:

$$4.6\frac{kWh}{m^2 * day} * \frac{3.6\ MJ}{kWh} * \frac{365\ days}{year} * 10\% = \frac{604\ MJ}{m^2 * year} \qquad Eq\ 5.1$$

Under phototrophic cultivation, there is a large variation in the lipid content of microalgae, ranging from 5% to 68%, depending on the type of microalgae species (Chen et al., 2011). The most common microalgae (*Chlorella, Dunaillea, Isochrysis, Nannochloris, Nannochloropsis, Neochloris, Nitzschia, Phaeodactylum, and Porphyridium*) possess oil levels between 20 and 50% (w/w) and exhibit reasonable productivities (Malcata, 2011). Assuming that the algal cells consist of 20% lipids (triglycerides, (lower heating value) LHV=37.5 MJ/kg) and the remaining 80% to be carbohydrates and proteins (LHV =18MJ/kg), the maximum theoretical biomass production is:

$$\frac{604\ MJ}{m^2 * year} * \frac{kg}{21.9\ MJ} * \frac{4047\ m^2}{acre} * \frac{ton}{1000\ kg} = \frac{111\ mt}{acre * year} \qquad Eq\ 5.2$$

Where 21.9 MJ/kg is the weighted average of LHV for lipids, carbohydrates and proteins. Assuming the algal oil density to be 864 g/L, which falls within the range determined by Kumar and coworkers (2011) for various species (857-892 g/L), the oil production per acre is:

$$\frac{111\ mt}{acre * year} * \frac{1000\ kg}{ton} * 20\%\ lipids * \frac{L}{0.864\ kg} = \frac{25{,}694\ L}{acre * year} \qquad Eq\ 5.3$$

This estimated value is the theoretical ‘‘upper limit’’ of PE, as it does not account for other factors that could decrease efficiency and conversion (e.g. photosaturation, photorespiration, and poor light absorption) (Brennan and Owende, 2010). Due to such impacting factors, most autotrophic organisms attain PE levels typically between 1% and 3% (Vasudevan and Briggs, 2008). Therefore, assuming a PE of 2%, algal production can realistically be expected to produce 5170 L/acre/year. To supply Louisiana’s energy demand of 87.4 million barrels per year of biofuel for transportation purposes, the state would require 710,153 acres of algal ponds. This is less than 2.2% of the total land

surface area in Louisiana. In comparison of land allocation, Louisiana farms approximately 200,000 acres of crawfish ponds during the year (Lutz, 2012).

5.2.1 Pond Design

Most commercial microalgae cultivation systems are carried out in open pond systems using solar energy as the light source, which is the cheapest light source available (Beilen, 2010; Chen et al., 2011). High rate ponds used in commercial algae production are typically operated at 20 to 40 cm (6 to 16 in) liquid depth, mixed with paddlewheels and up to about 0.5 hectares in size (Lundquist et al., 2010). For this discussion, a hypothetical 1 acre oval raceway that was 40 cm deep was assumed to culture an algal species with 20% lipid content and growth rate of 15 $g/m^2/day$.

5.2.2 Mixing

In algal cultivation, the productivity of algal systems, and cost of reactor construction and operation are dependent on the mixing system being able to maintain typical velocities of 8-14 cm/s (Ketheesan and Nirmalakhandan, 2011), with maximum velocities of 20-25 cm/s rarely being exceeded (Lundquist et al., 2010). Mixing by traditional paddlewheel is the most common method of circulation, but Collet et al. (2010) indicated this to be the most energy intensive in algae cultivation, consuming 0.1 kWh/m^3 of culture. Progresses in electricity consumption during cultivation can be achieved by decreasing the mixing costs and circulation between different production steps (Singh and Olsen, 2011). To accomplish this, the minimum energy required to maintain mixing velocities was determined through the headloss (h_L) experienced in the bends (h_b), straightaways (h_s) and carbonation sump (h_c) (Lundquist et al., 2010).

$$h_L = 2h_b + 2h_s + h_c \qquad Eq\ 5.4$$

$$h_L = 2\left(\frac{K_b v^2}{2g}\right) + 2\left(v^2 n^2 \frac{L}{R^{4/3}}\right) + \left(\frac{K_c v^2}{2g}\right) \qquad Eq\ 5.5$$

Where: K = kinetic loss coefficient

v = mean velocity (m/s)

g = acceleration of gravity (9.81 m/s^2)

n = roughness factor (n = 0.018 for clay channels)

L = channel length (m)

R = channel hydraulic radius (m)

$$h_L = 2\left(\frac{2\left(0.25\,\frac{m}{s}\right)^2}{2\left(9.81\,\frac{m}{s^2}\right)}\right) + 2\left(\left(0.25\,\frac{m}{s}\right)^2 (0.018)^2 \frac{109\,m}{(0.39\,m)^{4/3}}\right) + \left(\frac{4\left(0.25\,\frac{m}{s}\right)^2}{2\left(9.81\,\frac{m}{s^2}\right)}\right) = 0.0409\,m$$

The power (P) to maintain a velocity of 0.25 m/s in a 1-acre raceway, was therefore:

$$P = \gamma Q h = \left(9.78\,\frac{kN}{m^3}\right)\left(1.55\,\frac{m^3}{s}\right)(.0409\,m) = 0.620\,kW \qquad Eq\ 5.6$$

Where: γ = specific weight of water (kN/m^3)

Q = flowrate at velocity, v (m^3/s)

h = headloss (m)

Assuming the efficiency of the mixing device, whether paddle wheel or air lift, to be 40% (Weissman and Goebel, 1987), the energy required to mix 1 m^3 of culture at 0.25 m/s fell within the variable range of other authors (Table 5.1).

Table 5.1: A comparison of the daily energy required to maintain a mixing velocity of 0.25 m/s

Author	Collet et al., 2010	Sturm et al., 2010	Lundquist et al., 2010	Jorquera et al., 2010	Current
Energy (kWh/m^{3}d)	0.1	.006	0.016	0.089	0.023

5.2.3 Carbon Dioxide

Microalgae have attracted a great deal of attention for CO_2 fixation and biofuel production because they can convert CO_2 into biomass via photosynthesis at much higher rates than convention biofuel crops (Kumar et al., 2010). Many reports on the potential and bio-economics of algal biomass to generated fuels are based on the premise that CO_2 would be utilized from fossil fuelled power

stations or other industrial sources of CO_2 (Singh and Olsen, 2011). The specific growth rate of *Nannochloropsis* increased 58% when 15% CO_2 (typical concentration of flue gases) was used for aeration (Jiang et al., 2011). Additionally, combustion products such as NO_X or SO_X can be effectively used as nutrients for microalgae, simplifying flue gas scrubbing for combustions systems (Um and Kim, 2009).

Algae require approximately 2 g of CO_2 for every g of biomass generated (Pienkos and Darzins, 2009). To gain a more accurate assessment of the CO_2 required to maximize the algal growth rate, the mass of carbon in the algal cell was determined. As seen in Williams and Laurens (2010) an algal cell composition with 20% lipids was allocated as shown in Table 5.2.

Table 5.2: The elemental composition of an algal cell with 20% lipid content.

	Elemental Components	Percent biomass (%)	C (g)	H (g)	O (g)	N (g)	S (g)	P (g)
Lipids	$C_1H_{1.83}O_{0.17}$	20	2.4	0.37	0.54			
Proteins	$C_1H_{1.56}O_{0.3}N_{0.26}S_{0.006}$	45	5.4	0.70	2.16	1.64	0.09	
Polysaccharide	$C_1H_{1.67}O_{0.83}$	30	3.6	0.50	3.98			
Nucleic acid	$C_1H_{1.23}O_{0.74}N_{0.40}P_{0.11}$	5	0.6	0.06	0.59	0.28		0.08
Total	---	100	12	1.63	7.27	1.92	0.09	0.08
Percent	---	---	52	7.09	31.6	8.35	0.39	0.35

With the algae's composition divided into elemental components, it was seen that carbon accounts for approximately 52% of the cell's biomass. According to Pate el al. (2011), the ratio of carbon dioxide to algal biomass is given by the following:

$$\frac{g(CO_2)}{g(algae)} = \frac{44g/mole * C\%}{1200g/mole} \qquad Eq\ 5.7$$

Therefore, the amount of carbon that was required to be supplied as CO_2 was 1.9 g/g algae. Distributing the carbon dioxide via a 1.5 m counter flow sump ensured 95% diffusion efficiency (Campbell et al., 2011). This flow could be supplied to the 1 acre pond producing 15 g/m^2/day as: (1) pure CO_2 (2.56 m^3/h), (2) flue gas as 15% CO_2 (17.1 m^3/h), or (3) atmospheric CO_2 (6,559 m^3/h). Because of its low concentration, however, atmospheric CO_2 (~0.0387% v/v) is not sufficient to support the high microalgal growth rates and productivities needed for full-scale biofuel production

(Putt, 2007; Kumar et al., 2010). Therefore, flue gas and concentrated carbon dioxide were considered for this analysis (Table 5.3).

Table 5.3: A comparison of the CO_2 and energy requirements for algal cultivation

Author	Lardon et al., 2009	Collet et al., 2011	Kadam 2002	Davis et al., 2011	Campbell et al., 2011		Current	
Growth Rate ($g/m^2/day$)	25	25	45	25	30		15	
CO_2 (kg/kg algae)	2.59	1.172	2.17	1.11	1.69		1.9	
CO_2 (%)	15	15	100	100	15	100	15	100
Energy (kWh/m^3 CO_2)	0.044[a]	0.049[a]	0.065	0.99	---		0.066[b]	1.28[c]

[a] Values based on Kadan 2002 for flue gas with 15% CO_2
[b] 1.5 HP Sweetwater® regenerative blower capable of 68 m^3/hr at 1.65 m water depth
[c] Cost ($58/ton) of post combustion captured CO_2 from coal fired power plant (Finkenrath, 2012)

As seen in Table 5.3, industrial flue gas appeared to be the more affordable option for supplying CO_2 to an algal system. Approximately 115.75 MMT of CO_2 emissions from fossil fuels in Louisiana were produced from the state's industrial sector. By utilizing these carbon emissions, 26% of the industrial sector CO_2 could be recycled in algal production. At a production rate of 15 $g/m^2/d$, biodiesel and electricity produced from the algal biomass could reduce carbon dioxide emissions between 71 and 109 g/MJ compared to ultra-low sulfur diesel (Batan et al., 2010; Campbell et al., 2011).

5.2.4 Water

Managing freshwater use is critical to maintain a positive energy balance in algal cultivation. Open pond systems required a wide range of water (32-656 L/L oil) when considering evaporation, process water, and biodiesel production (Harto et al., 2010). By recycling the harvest water the total water usage was reduced by 84% for every kg of biodiesel generated (Yang et al., 2011). However, evaporation is the most difficult water parameter to address in open pond systems. The most suitable location for algae production on the basis of land area is typically least suitable on the basis of water consumption due to evaporation (Clarens et al., 2010). The projected consumptive water loss from

evaporation could fall into the range of 908 to 2271 L of water for each L of algal oil produced (Pate et al., 2011). Algal producers must plan for water recycling and evaporation control to ensure efficient energy and water usage within their systems (Subhadra and Edwards, 2011).

Table 5.4: A comparison of the water loss due to evaporation and the energy required for pumping

Author	Lardon et al., 2009*	Collet et al., 2011	Davis et al., 2011	Batan et al., 2010*	Sturm and Lamer, 2011	Current
Evaporation (cm/day)	0.082	0.16	0.3	2.5	---	0.33
Pumping (kWh/m^3)	0.05	.049	---	0.012	0.03	0.045

*Includes cm of rainfall per day to account for evaporation losses

Due to evaporation, the potential water loss was 13.3 m^3 per day for a 1 acre pond. Over the past 5 years, the average rainfall in Louisiana has been 55.5 in (0.39 cm/day) (NOAA, 2012), which could potentially offset all evaporative losses. Regardless of evaporation, algal facilities can still expect water losses of 4 to 124 L/kg biomass due to blow down from other operational and downstream processes (Lardon et al., 2009; Davis et al., 2011). While some of these losses may prove detrimental to facilities in areas such as Arizona, Louisiana's lower evaporation rates, higher rainfall rates and easy access to surrounding natural water sources could potentially withstand the resource exhaustion.

5.2.5 Nutrients

In comparison to conventional energetic crops, high photosynthetic yields of microalgae significantly reduce land and pesticide use but not fertilizer needs (Lardon et al., 2009). Using fertilizer to culture microalgae consumed 61% of operating costs, requiring 0.227 kWh/kg of biomass (Liu and Ma, 2009). In some instances, nutrients added as fresh chemicals to the pond produced an overall negative energy balance (Aresta et al., 2005). Nutrient needs are a significant energy barrier for algal culturing, and should be assessed for efficient use.

Previously, the amount of carbon in the cell (52% w/w) was determined for the CO_2 required for maximum biomass production. Using Redfields molar ratio for marine phytoplankton ($C_{106}N_{16}P_1$)

and converting it to mass basis ($C_{1272}N_{224}P_{31}$) it was possible to determine the amount of nitrogen and phosphorus needed for algal cultivation.

$$N = \frac{224\ g * 52\%}{1272\ g} = 9.16\% \qquad Eq\ 5.8$$

$$P = \frac{31\ g * 52\%}{1272\ g} = 1.27\% \qquad Eq\ 5.9$$

These percentages were converted to g/kg of biomass and compared to the estimates of the following authors (Table 5.5). The true impact of nutrients on biomass production could be seen when comparing the costs of the fertilizers in Table 5.6.

Table 5.5: A comparison of the nutrients required to culture 1 kg of algal biomass

Author	Collet et al., 2011	Lardon et al., 2009	Davis et al., 2011	Campbell et al., 2011	Batan et al., 2010	Current
Growth Rate ($g/m^2/day$)	25	25	25	30	25	15
Nitrogen (g/kg algae)	8.85	67.6	32.1	5.61	147	91.6
Phosphorus (g/kg algae)	2.69	14.6	7.38	0.56	20	12.7

Table 5.6: A comparison of the costs for nitrogen and phosphorus

Author	Williams & Laurens, 2010	Davis et al., 2011	Current USDA 2012
Ammonia ($/ton)	300	407	783
$/kg N	0.36	0.50	0.95
Diammonium Phosphate ($/ton)	325	442	726
$/kg P	1.29	1.75	2.76

While fertilizer costs can strain the energy balance, continuously adding 100% of the required nutrients was not expected in most applications. When harvest water was recycled, nitrogen and phosphate usage decreased by 55% to produce 1 kg of biodiesel (Yang et al., 2011). If the used biomass is brought to an anaerobic digester, ~90% of nutrients should fundamentally be recovered (Lundquist et al., 2010). The degree of nutrient recycle had one of the strongest impacts on the cost analysis (Davis et al., 2011).

An alternative option to nutrient addition would be to utilize the wastewater effluent from various treatment facilities. Microalgae ponds used for secondary or tertiary treatment of domestic wastewater would bring advantages such as cost effectiveness, low energy requirements, reductions in sludge formation and pollutants discharged into the environment, greenhouse gas mitigation, and the production of useful microalgal biomass (Kumar et al., 2010; Pittman et al., 2011; Sydney et al., 2011). Small-scale decentralized wastewater treatment could also allow water reuse onsite and reduce the need for transportation of hazardous wastes (Munoz and Guieysse 2006). Using an algal system to treat wastewater for total nitrogen and phosphorus resulted in energy offsets of 0.126 kWh/m^3 (Sturm and Lamer, 2011). Jiang et al. (2011) even showed improved biomass production by 32% over standard f/2 media when a 50% mixture of municipal wastewater and seawater were used to culture *Nannochloropsis*. Despite readily available land, water, and nutrient resources for culturing microalgae in Louisiana, biomass harvesting still remained a serious challenge to practical production of algal biodiesel.

5.3 Harvesting

Given the relatively low biomass concentration in microalgal cultivation systems (<500 mg/L), marginal density difference with culture water (average ~ 1,020 kg/m3), and the small size of microalgal cells (5 to 50 μm in diameter), costs and energy consumption for biomass harvesting are significant concerns that need to be addressed (Li et al., 2008; Theegala, 2009; Kumar et al., 2010). Depending on species, cell density, and culture conditions, harvesting algal biomass is estimated to contribute 20–30% to the production cost (Gudin and Thepenier, 1986; Grima et al., 2003). An efficient algal harvesting process should be applicable for all kinds of algal species, yield a product with a high dry weight percentage, and require minimum investment, energy, and maintenance (Poelman, 1997). This suitable harvesting strategy may involve one or more steps and be achieved in several physical, chemical, or biological ways, in order to perform the desired solid–liquid separation

(Mata et al., 2010). Most harvesting systems employ a 2-stage dewatering process, where stage 1 increases the algae concentration from 0.01% to 1-2% mass and stage 2 brings the final concentration to ~20% biomass (Table 5.7).

The current harvesting strategy used electrocoagulation for charge neutralization, dissolved air flotation to increase the initial concentration, and centrifugation for final dewatering. The current values used the results when applying 1 and 3 amps across the EC unit from Chapter 4 and scaled them for a full size facility. Despite requiring more energy than most of the systems on a per mass basis (kWh/kg), the proposed process was more effective than most other methods when considering the volume treated to harvesting 15g/m^2/day from a 4047 m^2 pond.

$$\frac{kWh}{kg} * \frac{C_o}{1 - \frac{C_o}{C}} * \frac{60705\ g}{day} * \frac{1645\ m^3}{182115\ g} * \frac{1}{\%\ harvest/100} = \frac{kWh}{day} \qquad Eq\ 5.10$$

This additional conversion was necessary considering that the techniques in Table 5.7 treated various initial concentrations (C_o) and dewatered to various final concentrations (C).

Table 5.7: A comparison of potential harvesting techniques and costs for algal biomass.

Harvest Method	Efficiency (%)	Initial C_o (g/L)	Final C (g/L)	Energy (kWh/kg algae)	kWh/day	Author
Centrifugation	100	1.0	200	0.338	186.3	**Batan et al., 2010**
Settle → Centrifuge	65[a]	0.8	120	0.292	198.4	**Liu & Ma, 2009**
Settle → Centrifugation	65	0.5	50	0.235	100.1	**Collet et al., 2011**
Flocculation/pH → Settling → Belt Press	90	0.5	200	0.458	139.9	**Lardon et al., 2009**
Not listed	100[a]	0.5	200	0.879	241.6	**Williams & Laurens, 2010**
Flocculation → DAF → Centrifugation	70	0.1	200	1.440	112.9	**Sturm & Lamer, 2011**
Flocculation → DAF → Belt Press	70	0.1	200	1.086	85.1	**Sturm & Lamer, 2011**
Electrocoagulation → DAF → Centrifugation	55	0.14	200	0.944	131.9	**Current**
Electrocoagulation → DAF → Centrifugation	76	0.14	200	1.133	114.5	**Current**

[a] Values were not listed so they were assumed

5.4 Lipid Extraction and Energy Conversion

The majority of biodiesel today is produced from animal or plant oils through transesterification process following lipid extraction with or without cell disruption (Schenk et al., 2008). The lipid extraction yields vary greatly upon the extraction techniques employed and the algal species harvested (Lewis et al., 2000). Depending on the cell wall and the nature of the product to be obtained, either mechanical methods (cell homogenizers, bead mills, ultrasounds, autoclave, and spray drying) or non-mechanical methods (freezing, organic solvents, osmotic shock, enzyme extraction, thermal liquefaction, and pressure liquid extraction) can be used for cell disruption (Mata et al., 2010; Mercer and Armenta, 2011).

The most likely technology for algal oil recovery involves some form of solvent extraction (Pienkos and Darzins, 2009). Solvents play an important role by lysing cell walls to increase the extraction yield. These extraction solvents should be cheap, easy to remove, free from toxins, insoluble in water, efficient in dissolving targeted components, and recyclable (Chen et al., 2009). The hexane system has been promoted for cell lysing because the hexane and alcohol will readily separate into two separate phases when water is added, thereby improving downstream separation (DOE, 2008). However, hexane could potentially be substituted with biodiesel (methyl soyate) as a less toxic, environmentally acceptable, and biodegradable solvent for algal lipid extraction (Iqbal and Theegala, 2013). Once the lipids have been extracted from the algal biomass, the oils undergo transesterifcation, a multiple-step reaction, where triglycerides are converted to digclycerides, then to monoglycerides, and then converted to esters (biodiesel) and glycerol (Mata et al., 2010).

The continuous flow lipid extraction system (CFLES), which was designed to improve the process economics of microalgae oil extraction while simplifying the overall extraction process used moderate temperatures (80–120 °C) and moderate pressures (ambient to 500 psi) through the extraction cell containing the biomass (Iqbal and Theegala, 2012).

Table 5.8: A comparison of potential algal extraction techniques along with experimental and recovered energies

Lipids (%)	Methods	Energy Consumed (kWh/kg algae)	Biodiesel Energy (kWh/kg algae)	Author
17.5	Hexane extraction → Transesterification	1.77	1.838	**Lardon et al., 2009**
35	Unknown extraction → Transesterification	0.884	3.148	**Williams & Laurens, 2010**
---	Anaerobic digestion → Methane production	0.896	2	**Collet et al., 2011**
10	Unknown extraction → Transesterification	0.875	0.935	**Sturm & Lamer, 2011**
50	Hexane/ethanol extraction → Transesterification	1.996	4.287	**Batan et al., 2010**
---	Methanol conversion	0.658	2.565	**Liu & Ma, 2009**
30	Hexane extraction → Transesterification	0.684	3.247	**Sander and Murthy, 2009**
20	CFLES	4.416	2.083	**Current**

5.5 Shipping

Additional costs were allocated for shipping materials and products to processing or distributing facilities. Assuming that the algal producing facility was centrally located and would complete all processes up until the conversion and processing of algal oil, the following estimates were used for transportation (Table 5.9).

Table 5.9: A comparison of expected shipping costs for crude algal oil and biodiesel

Author	Sander and Murthy 2010	Batan et al., 2010	Liu and Ma 2009	Current
Transportation (kWh/kg)	0.102[a] 0.107[b]	0.093[b]	0.0722[a]	0.105
Distance (km)	150		100	150

a. Transportation from facility to refinery
b. Transportation/distribution of finished fuel product

5.6 Complete Analysis

The major energy components in the life cycle of algal biodiesel were consolidated from various sources to compare the high and low estimates made by other authors. These values were also compared to the predictions and bench scale testing of the dissertation. Values for pumping and shipping were omitted because their effects had minimal impact on the overall cost at all levels. In the

continued scenario, a 1 acre pond growing algae at a conservative rate of 15 g/m^{2}d with 20% lipids was considered (Figure 5.1)

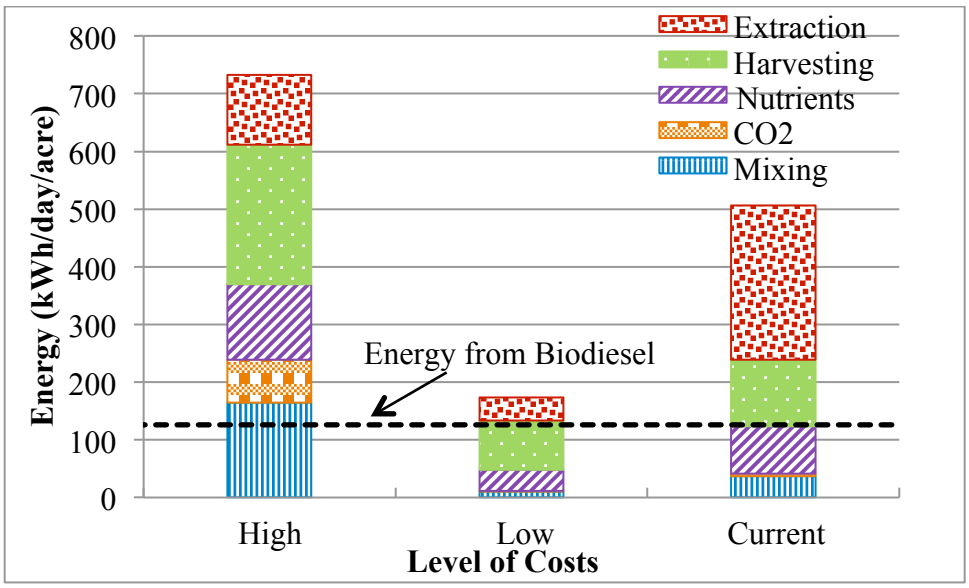

Figure 5.1: Comparison of high, low, and current energy estimates for algal biodiesel production and the available energy from that biodiesel.

Under even the best conditions, the energy consumed on a daily basis for an acre pond continued to exceed the energy extracted as biodiesel. Based on the energy that could be potentially recovered, systems with biomass yields below 20 g/m^2/day were unlikely to make a profit (Williams and Laurens, 2010). The current realistic methods consumed 290% more energy than what was contained in the biodiesel. Harvesting in general continued to be a primary obstacle under all circumstances investigated due to the large quantities of water that were processed for minimal product. Advances in this area should be a priority, but additional improvements to the energy balance could be found through culturing and added value to the algal biomass.

Sturm and Lamer (2011) indicated 0.126 kWh/m^3 in energy offsets were possible after using an algal system to treat wastewater for total nitrogen and phosphorus. Therefore, not only could the cost for supplying fresh nutrients be eliminated, but an additional 207 kWh/day of energy could be credited. This adjustment could provide a 143% energy surplus for the best-case scenario and reduce the energy imbalance for the current scenario to 20% (Figure 5.2)

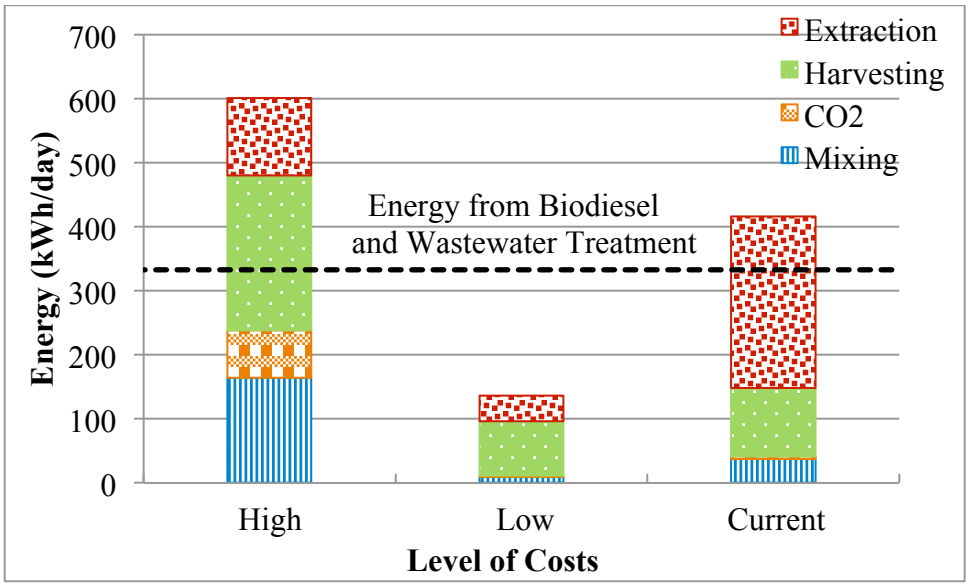

Figure 5.2: Comparison of high, low, and current energy estimates for algal biodiesel production and the available energy from that biodiesel plus supplemental value for wastewater treatment.

The energy imbalance could be further improved by utilizing the algal biomass after lipid extraction. Biomass produced from wastewater would seldom be suitable for the production of food or even high-value chemicals due to high-quality requirements and public acceptance. Therefore, the best option that remained was to use the residual algal biomass after oil extraction for energy production by anaerobic digestion into biogas (Munoz and Guieysse, 2006) (Figure 5.3).

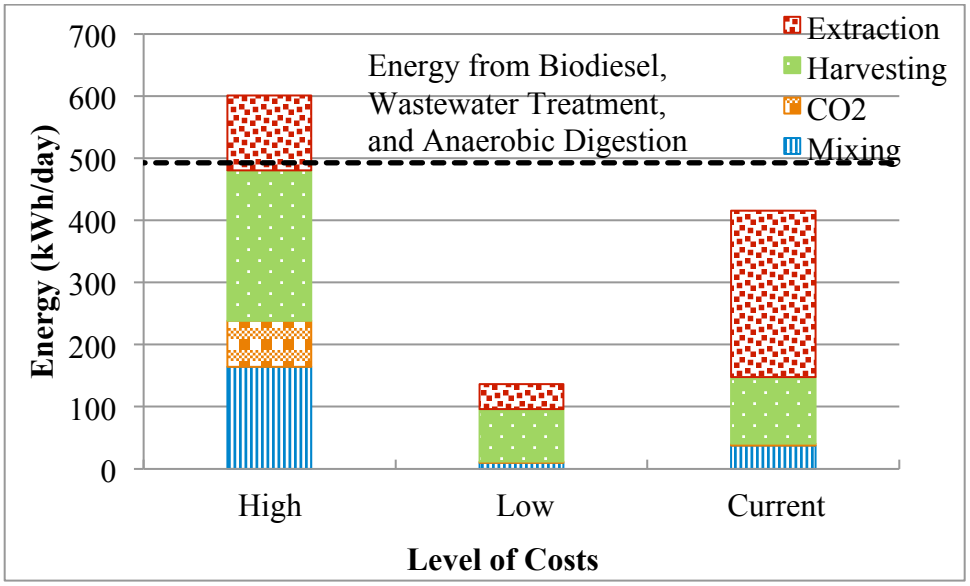

Figure 5.3: Comparison of high, low, and current energy estimates for algal biodiesel production and the available energy from that biodiesel plus supplemental value for wastewater treatment and anaerobic digestion.

Biogas produced from microalgal solids, after their 30% oil content has been removed, could provide at least 9,360 MJ/t (~160 kWh/day) (Chisti, 2008). Co-digesting the microalgae residues with glycerol produced from biodiesel was observed to further methane production by more than 50%, compared to residues digested alone (Ehimen et al., 2011). Assuming these additional energy credits were possible, an 18.5% surplus in energy for the current methods could be achieved.

5.7 Conclusion

Algae have significant potential compared to other biomass feedstocks to supplement the current transportation fossil fuel usage. Considering a highly conservative system with an algal growth rate of 15 g/m^2/day and 20% lipid production, the energy inputs exceeded the outputs from biodiesel production under the most ideal conditions. However, slight improvements to the growth rate (17 g/m^2/day) and lipid content (25%) could provide a positive energy balance for the best-case scenario.

The major costs throughout the chapter were attributed to nutrients, harvesting, and lipid extraction. Harvesting and lipid extraction are the most difficult processing steps to improve upon, but offer substantial potential for energy savings with developing technology. Slight energy improvements for these processes could also provide a positive energy balance for the best-case scenario.

While these slight improvements could potentially make algal biofuels a reality for the best-case scenario, the current technology is less likely to produce a positive energy balance with biofuels as a singular energy provider. However, finding additional value in the algal biomass will greatly supplement the current technology. Obtaining high value antioxidants, nutraceuticals, or pharmaceuticals from algal cultures could easily offset the costs of biodiesel production. In this analysis, it was determined that nutrient supply through wastewater treatment while further using of the residual biomass for methane production could potentially bring the realistic current costs a 18.5% energy surplus. By utilizing the full value of the algal biomass that is cultured, the likelihood of producing a biodiesel feedstock that could compete with petroleum fuels was improved substantially.

Chapter 6: Final Conclusion

Cost effective microalgae harvesting remains one of the most energy intensive processes for algal biodiesel production. Throughout this dissertation it was shown that focusing on the proper strategy was imperative to reduce the harvesting operating costs. The initial strategy of sacrificing biomass harvesting efficiencies for greater process volumes with lower energy consumptions was effective for single Stage 1 harvesting by centrifugation in Chapter 2 as well as the electrocoagulation batch testing in Chapter 3. However, when employing the continuous multistage harvesting system in Chapter 4 that used electrocoagulation and dissolved air flotation as the Stage 1 primary harvesting technique followed by centrifugation as the Stage 2 dewatering technique, the harvesting strategy required an increased biomass harvesting efficiency by the electrocoagulation system to counter the energy consumed by the dissolved air flotation unit. The system reached a maximum harvesting efficiency of 76.2% when 3 amps were applied to the EC unit.

The most cost effective parameters applied to the multistage system harvested 55.4% of the biomass when 1 amp was charged across the electrodes, resulting in an energy consumption of 1.484 kWh/kg algae. However, it was possible that the harvesting efficiency was artificially high during that trial due to higher incoming biomass concentration in comparison to all other tests conducted. The next best applied parameter of 3 amps for 76.2% harvesting efficiency consumed only 1.536 kWh/kg algae. It was anticipated that improvements to the flocculation process could see greater harvesting efficiencies without increasing the final costs. Additionally, the recycle ratio of the dissolved air flotation system could not be reduced below 10% recycle flow due to pump limitations. Using a smaller recycle ratio that will maintain the same harvesting efficiency will significantly improve the energy requirements of the system. Despite the limitations seen in multistage algae harvester, the system achieved its goal of operating costs <$0.80/L oil by harvesting low density (100 mg/L), low lipid (20%) microalgae at a final cost of $0.60/L oil.

Using the data collected from this research and existing literature, a life cycle assessment was assembled to judge the sustainability of microalgal biofuels in Louisiana. High and low cost estimates for culturing (mixing, CO_2, nutrients), harvesting, lipid extraction and energy conversion were compared with the current research. Scaling the EC/DAF system for a full size facility was expected to reduce the harvesting costs to 1.133 kWh/kg algae or $0.44/L oil. Compared to the other systems recommended by authors, this system was one of the most cost effective harvesting strategies that was investigated when considering the amount of energy required per day.

Despite this improvement in harvesting costs, the production of algal biomass for the sole purpose of biodiesel was not anticipated to be economically viable and practically sustainable. Even under the most ideal conditions, the costs for algal biodiesel exceeded the output energy by 36%. However, slight improvements to the aerial productivity (17 $g/m^2/day$) and lipid content (25%) or minor energy improvements to harvesting and lipid extraction processes could potentially provide a positive energy balance for the best-case scenario.

While these slight improvements to the algal culture or processing stages could potentially make algal biofuels a reality for the best-case scenario, the current technology was less likely to produce a positive energy balance with biofuels as a singular energy provider. However, finding additional value in the algal biomass could greatly supplement the current technology. Obtaining high value antioxidants, nutraceuticals, or pharmaceuticals from algal cultures is a common practice that could easily offset the costs of biodiesel production. It was determined that nutrient supply through wastewater treatment while further using the residual biomass for methane production could potentially bring the realistic current costs an 18.5% energy surplus. By utilizing the full value of the algal biomass that was cultured, the likelihood of producing a biodiesel feedstock that could compete with petroleum fuels was improved substantially.

References

1. Ahmad, A., Yasin, N., Derek, C., Lim, J. (2011) Microalgae as a sustainable energy source for biodiesel production: a review. Renewable and Sustainable Energy Reviews, 15, 584-593

2. Alabi, A., Tampier, M. and Bibeau, E. 2009 Microalgae technologies and processes for biofuels/bioenergy production in British Columbia: Current technology, suitability, and barriers to implementation. The British Columbia Innovation Council

3. Alfafara, C., Nakano, K., Nomura, N., Igarashi, T., Matsumura, M. (2002) Operating and scale-up factors for the electrolytic removal of algae from eutrophied lakewater. Journal of Chemical Technology and Biotechnology, 77, 871-876.

4. Al-Shamrani, A., James, A., Xiao, H. (2002) Destabilization of oil-water emulsions and separation by dissolved air flotation. Water Research 36, 1503-1512

5. Al-Shamrani, A., James, A., Xiao, H. (2002) Separation of oil from water by dissolved air flotation. Colloids and Surfaces 209, 15-26

6. Amaro, H., Guedes, A., Malcata, F. (2011) Advances and perspectives in using microalgae to produce biodiesel. Applied Energy, 88, 3402-3410

7. Amato, T., Edzwald, J., Tobiason, J., Dahlquist, J., Hedberg, T. (2001) An integrated approach to dissolved air flotation. Wat. Sci. Tech., 43(8), 19-26.

8. Aulenbach, D., Shammas, N., Wang, L., Marvin, R. (2010) Handbook of Environmental Engineering, Vol. 12: Flotation Technology, Ch 4. Algae removal by flotation. 363-399

9. Aragon B, Padilla R, Ursinos J. 1992. Experimental study of the recovery of algae cultured in effluents form the anaerobic biological treatment of urban wastewaters. Resour Conserv Recy 6(4):293-302.

10. Aresta, M., Dibenedetto, A., Barberio, G. (2005) Utilization of macro-algae for enhanced CO2 fixation and biofuels production: development of a computing software for an LCA study. Fuel Processing Technology, 86, 1679-1693

11. Azarian, G., Mesdaghinia, A., Vaezi, F., Nabizadeh, R., Nematollahi, D. (2007) Algae removal by electro-coagulation process, application for treatment of the effluent from an industrial wastewater treatment plant. Iranian Journal of Public Health, 36(4), 57-64.

12. Babel, S., Takizawa, S., Ozaki, H. (2002) Factors affecting seasonal variation of membrane filtration resistance caused by Chlorella algae. Water Research, 36, 1193-1202

13. Batan, L., Quinn, J., Willson, B., Bradley, T. (2010) Net energy and greenhouse gas emission evaluation of biodiesel derived from microalgae. Environmental Science and Technology, 44, 7975-7980

14. Becker, W (ed) (1994) Microalgae Biotechnology and Microbiology, Cambridge University Press

15. Beilen, J. (2010) Why microalgal biofuels won't save the internal combustion machine. Biofuels, Bioprod. Bioref., 4, 41-52

16. Benemann, J., Olst, J., Massingill, M., Weissman, J., Brune, D. (2002) The controlled eutrophication process: using microalgae for CO2 utilization and agricultural fertilizer recycling

17. Bilad, M., Vandamme, D., Foubert, I., Muylaert, K., Vankelecom, I. 2012 Harvesting microalgal biomass using submerged microfiltration membranes. Bioresour. Technol. 111, 343-352

18. Bouhezila, F., Hariti, M., Lounici, H., Mameri, N. (2011) Treatment of the OUED SMAR town landfill leachate by electrochemical reactor. Desalination, 280, 347-353

19. Brennan, L. and Owende, P. (2010) Biofuels from microalgae – A review of technologies for production, processing, and extractions of biofuels and co-products. Renewable and Sustainable Energy Reviews, 14, 557-577

20. Bukhari A. 2008. Investigation of the electro-coagulation treatment process for the removal of total suspended solids and turbidity from municipal wastewater. Bioresour Technol 99:914-921.

21. Campbell, P., Beer, T., Batten, D. (2011) Life cycle assessment of biodiesel production from microalgae in ponds. Bioresource Technology, 102, 50-56

22. Cerqueira A, Russo C, Marques M. 2009. Electroflocculation for textile wastewater treatment. Braz J Chem Eng 26(4):659-668.

23. Cha, J., Lee, J., Benaim, R., Moon, T., Han, K., Kim, C. (2009) Flexible fibre filter: potential for algae removal. Water Supply: Research and Technology, 58(2), 153-157.

24. Chen, S. and Malone, R. (1991) Suspended solids control in recirculating aquaculture systems. Engineering Aspects of Intensive Aquaculture, NRAES, 170-186

25. Chen, C., Yeh, K., Aisyab, R., Lee, D., Chang, J. 2011 Cultivation, photobioreactor design and harvesting of microalgae for biodiesel production: a critical review. Bioresour. Technol. 102, 71-81.

26. Chen, P., Min, M., Chen, Y., Wang, L., Li, Y. et al. (2009) Review of the biological and engineering aspects of algae to fuel approach. International Journal of Agricultural and Biological Engineering, 2(4), 1-30.

27. Chisti, Y. 2007 Biodiesel from microalgae. Biotechnol. Adv. 25, 294-306

28. Chisit, Y. (2008) Biodiesel from microalgae beats bioethanol. Trends in Biotechnology, 26(3), 126-131)

29. Choi, K. and Dempsey, B. (2004) In-line coagulation with low-pressure membrane filtration. Water Research, 38, 4271-4281.

30. Choi, S., Lee, J., Kwon, D., Cho, K. (2006) Settling characteristics of problem algae in the water treatment process. Wat. Sci. Tech. 53(7), 113-119.

31. Chung Y., Choi, Y.C., Choi, Y.H., Kang, H. (2000) A demonstration scaling-up of the dissolve air flotation. Wat. Res., Vol. 34(3), 817-824

32. Collet, P., Helias, A., Lardon, L., Ras, M., Goy, R., Steyer, J. (2011) Life-cycle assessment of microalgae culture coupled to biogas production. Bioresource Technology, 102, 207-214

33. Contreras, S. (1981) A highly efficient electrolytic method for microorganism flocculation from aqueous cultures. Biotechnology and Bioengineering, 23, 1165-1168

34. Cora M and Hung Y. 2009. Determination of operational parameters for an Electrocoagulation/Flotation (ECF) batch reactor used in the treatment of wastewater with cadmium ions. Inter J Environ Eng 1(1):3-19.

35. Craenenbroeck et al. (1993) Water Supply, 11, 123

36. Dassey, A. and Theegala, C. (2012) Optimizing the air dissolution parameters in an unpacked dissolved air flotation system. Water, 4(1), 1-11.

37. Dassey, A. and Theegala, C. (2012) Evaluating coagulation pretreatment on poultry processing wastewater for dissolved air flotation. Journal of Environmental Science and Health, Part A: Toxic/Hazardous Substances and Environmental Engineering, 47(13), 2069-2076

38. Dassey, A and Theegala, C. (2013) Harvesting Economics and Strategies Using Centrifugation for Cost Effective Separation of Microalgae Cells for Biodiesel Applications. Bioresour Technol 128:241-245.

39. Davis, R., Aden, A., Pienkos, P. (2011) Techno-economic analysis of autotrophic microalgae for fuel production. Applied Energy, 88, 3524-3531

40. Demirbaş, A. (2009) 'Production of Biodiesel from Algae Oils', Energy Sources, Part A: Recovery, Utilization, and Environmental Effects, 31(2), 163-168

41. Demirbas, A. 2010 Use of algae as biofuel sources. Energy Convers. and Manag. 51, 2738-2749.

42. Dismukes, G., Carrieri, D., Bennette, N., Ananyev, G., Posewitz, M. (2008) Aquatic phototrophs: efficient alternatives to land-based crops for biofuels. Current Opinion in Biotechnology, 19, 235-240

43. Donini J, Kan J, Szynkarczuk J, Hassan T, Kar, K. 1994. The operating cost of electrocoagulation. Can J Chem Eng 72:1007-1012.

44. Edzwald, J. (1995) Principles and applications of dissolved air flotation. Wat. Sci. Tech. 31(3-4), 1-23

45. Ehimen, E., Sun, Z., Carrington, C., Birch, J., Rye, J. (2011) Anaerobic digestion of microalgae residues resulting from the biodiesel production process. Applied Energy, 88, 3454-3463.

46. Feng C, Sugiura N, Shimada S, Maekawa T. 2003. Development of a high performance electrochemical wastewater treatment system. J Hazard Mater B103:65-78.

47. Finkenrath, M. (2012) Carbon dioxide capture from power generation – status of cost and performance. Chemical Engineering Technology, 35(3), 482-488

48. Gao S, Yang J, Tian J, Ma F, Tu G, Du, M. 2010. Electro-coagulation-flotation process for algae removal. J Hazard Mater 177: 336-343.

49. Garzon, A., Davis, R., Nikolov, Z. (2012) Harvesting Nannochloris oculata by inorganic electrolyte flocculation: effect of initial cell density, ionic strength, coagulant dosage, and media pH. Bioresource Technology, 118, 418-424

50. Gregor, J., Nokes, C., Fenton, E. (1997) Optimizing natural organic matter removal from low turbidity waters by controlled pH adjustment of aluminum coagulation. Wat. Res. 31, 2949–2958

51. Grima, E. (2003) Recovery of micro algal biomass and metabolites: process options and economics. Biotechnol. Adv. 20, 491-515.

52. Grima, E., Fernandez, F., Camacho, F., Chisti, Y. (1999) Photobioreactors: light regime, mass transfer, and scaleup, 70, 231-247

53. Gudin C and Thepenier C. (1986) Bioconversion of solar energy into organic chemicals by microalgae. Adv. Biotechnol. Process. 6:73–110.

54. Haarhoff, J. and Steinback, S. (1996) A model for the prediction of the air composition in pressure saturators. Wat. Res. 30(12), 3074-3082

55. Han, M., Kim, T., Kim, J. (2007) Effects of floc and bubble size on the efficiency of the dissolved air flotation (DAF) process. Wat. Sci. Tech. 56(1), 109-115.

56. Harif, T. and Adin, A. (2007) Characteristics of aggregates formed by electroflocculation of a colloidal suspension. Water Research, 41, 2951-2961

57. Harto, C., Meyers, R., Williams, E. (2010) Life cycle water use of low-carbon transport fuels. Energy Policy, 38, 4933-4944.

58. Heath, A., Bahri, P., Fawell, P., Farrow, J. (2006) Polymer flocculation of calcite: experimental results from turbulent pipe flow. American Institute of Chemical Engineers, 52, 1284-1293

59. Henderson, R., Parsons, S., Jefferson, B. (2008) Successful removal of algae through the control of zeta potential. Separation Science and Technology, 43, 1653-1666

60. Holtman, S. (1982) An investigation of induced air flotation as an algal removal process. Louisiana State University, Thesis.

61. Hung, Y., Amuda, O., Alade, A., Amoo, I., Tay, S., Li, K. (2010) Handbook of Environmental Engineering, Vol. 11: Environmental Bioengineering, Ch.21: Algae harvest energy conversion. 723-741

62. Hwang, K. and Liu, H. (2002) Cross-flow microfiltration of aggregated submicron particles. Journal of Membrane Science, 201, 137–148.

63. Irdemez S, Demircioglu N, Yildiz Y, Bingul Z. 2006. The effects of current density and phosphate concentration on phosphate removal from wastewater by electrocoagulation using aluminum and iron plate electrodes. Sep Purif Technol 52:P218-223.

64. Iqbal, J. and Theegala, C. (2012) Optimizing a continuous flow lipid extraction system (CFLES) used for extracting microalgal lipids. GCB Bioenergy, 1-11. doi: 10.1111/j.1757-1707.2012.01195.x

65. Iqbal, J. and Theegala, C. (2013) Microwave assisted lipid extraction from microalgae using biodiesel as co-solvent. Algal Research, 2, 34-42.

66. Jameson, G. (1999) Hydrophobicity and floc density in induced-air flotation for water treatment. Colloids and Surfaces A, 151, 269-281

67. Janelt, G., Bolt, P., Gerbsch, N., Buchholz, R., Cho, M. (1997) The lamellar settler – a low-cost alternative for separating the micro-algae Chlorella vulgaris from a cultivation broth? Applied Microbiology Biotechnology, 48, 6-10

68. Jarvis, P., Jefferson, B., Gregory, J., Parsons, S. (2005) A review of floc strength and breakage. Wat. Res. 39, 3121-3137.

69. Jiang J, Graham N, Andre C, Kelsall G, Brandon N, Chipps M. 2002. Comparative performance of an electrocoagulation/flotation system with chemical coagulation/dissolved air flotation: a pilot-scale trial. Wat Sci Technol 2(1):289-297.

70. Jiang, L., Luo, S., Fan, X., Yang, Z., Guo, R. (2011) Biomass and lipid production of marine microalgae using municipal wastewater and high concentration of CO2. Applied Energy, 88, 3336-3341

71. Jorquera, O., Kiperstok, A., Sales, E., Embirucu, M., Ghirardi, M. (2010) Comparative energy life-cycle analyses of microalgal biomass production in open ponds and photobioreators. Bioresource Technology, 101, 1406-1413.

72. Jung, H., Lee, J., Choi, D., Kim, S., Kwak, D. (2006) Flotation efficiency of activated sludge flocs using population balance model in dissolved air flotation. Korean Journal of Chemical Engineering, 23(2), 271-278

73. Kannan N, Karthikeyan G, Tamilselvan N. 2006. Comparison of treatment potential of electrocoagulation of distillery effluent with and without activated Areca catechu nut carbon. J Hazard Mater B137:1803-1809.

74. Ketheesan, B. and Nirmalakhandan, N. (2011) Development of a new airlift-driven raceway reactor for algal cultivation. Applied Energy, 88, 3370-3376

75. Kitchener, J. and Gochin, R. (1981) The mechanism of dissolved air flotation for potable water: basic analysis and a proposal. Wat. Res. 15(5), 585–90

76. Koren, J. and Syversen, U. (1995) State-of-the-art electroflocculation. Filtration and Separation, 153-156

77. Kothandaraman, V. and Evans, R. (1972) Removal of algae from waste stabilization pond effluents – a state of the art. Illinois State Water Survey, Circular 108.

78. Kumar, A., Ergas, S., Yuan, X., Sahu, A., Zhang, Q., Dewulf, J., Malcata, F., Langenhove, H. (2010) Enhanced CO2 fixation and biofuel production via microalgae: recent developments and future directions. Trends in Biotechnology, 28, 371-380

79. Kumar, H., Yadava, P., Gaur, J (1981) Electrical flooculation of the unicellular green alga chlorella vulgaris beijerinck. Aquatic Botany, 11, 187-195

80. Kumar, P., Suseela, M., and Toppo, K. (2011) Physico-chemical characterization of algal oil: a potential biofuel. Asian J. Exp. Biol. Sci. 2(3), 493-497

81. Kurbiel, J., Sapulak, A., Schade, H. (1991) The use of turbulent pipe-flow for rapid flocculation of precipitate in the electroplating wastewater treatment. Water Science and Technology, 24(7), 255-259

82. Lavoie, A. and Noue, J. (1987) Harvesting of Scenedesmus obliquus in wastewaters: auto- or bioflocculation? Biotechnology and Bioengineering, 30, 852-859

83. Lewis T., Nichols P., McMeekin T. (2000) Evaluation of extraction methods for recovery of fatty acids from lipid producing microheterotrophs. J. Microbiol. Methods. 43, 107 – 116

84. Li, Y., Horsman, M., Wu, N., Lan, C., Dubois, N. (2008) Biofuels from microalgae. Biotechnol. Prog. 24, 815-820

85. Liu, J. and Ma, X. (2009) The analysis on energy and environmental impacts of microalgae-based fuel methanol in China. Energy Policy, 37, 1479-1488

86. Liu, Z., Wang, G., Zhou, B. (2008) Effect of iron on growth and lipid accumulation in Chlorella vulgaris. Bioresource Technology, 99, 4717-4722

87. Lundh, M., Jonsson, L., Dahlquist, J. (2000) Experimental studies of the fluid dynamics in the separation zone in dissolved air flotation. Wat. Res. 34(1), 21-30.

88. Lundquist, T., Woertz, I., Quinn, N., Benemann, J. (2010) A realistic technology and engineering assessment of algae biofuel production. Algae Biofuels Assessment from Energy Biosciences Institute at U.C. Berkeley

89. Lutz, C. (2012) Louisiana aquaculture as of 2012: estimated production and value. Aquaculture Research Station. www.lsuagcenter.com

90. Maier, R., Pepper, I., Gerba, C. Environmental Microbiology. 2nd Ed. Burlington, Massachusetts: Academic Press, 2009.

91. Malcata, F. (2011) Microalgae and biofuels: a promising partnership? Trends in Biotechnology, 29(11), 542-549.

92. Martinez J, Montero C, Garcia A. 2009. Energy and electrode consumption analysis of electrocoagulation for the removal of arsenic from underground water. J Hazard Mater 172:1617-1622.

93. Mata, T., Martins, A., Caetano, N. (2010) Microalgae for biodiesel production and other applications: a review. Renewable and Sustainable Energy Reviews, 14, 217-232

94. Mercer P. and Armenta R. (2011) Developments in oil extraction from microalgae. Eur. J. Lipid Sci. Technol. 113, 539 – 547

95. Metcalf & Eddy, Inc. Wastewater Engineering: Treatment and Reuse, 4th ed. New York: McGraw Hill, 2003

96. Mohn F. (1980) Experiences and strategies in the recovery of biomass from mass cultures of microalgae. In: Shelef G, Soeder CJ, editors. Algae biomass. Amsterdam: Elsevier; p. 547– 71

97. Mollah M, Morkovsky P, Gomes J, Kesmez M, Parga J, Cocke D. 2004. Fundamentals, present and future perspectives of electrocoagulation. J Hazard Mater B114:199-210.

98. Munoz, R. and Guieysse, B. (2006) Algal-bacterial processes for the treatment of hazardous contaminants: a review. Water Research, 40, 2799-2815

99. National Renewable Energy Laboratory 1998 A Look Back at the U.S. Department of Energy's Aquatic Species Program – Biodiesel from Algae. By Sheehan, J et al. Golden Colorado,

100. Naghavi, B. (1982) Algae removal by fine sand/silt filtration. Louisiana State University, Thesis

101. Nemerow, N. Industrial Water Pollution: Origins, Characteristics, and Treatment. Addison-Wesley, 1978

102. NOAA (2013) National Climatic Data Center. http://www.ncdc.noaa.gov

103. Ofir, E. Oren, Y., Adin, A. (2007) Comparing pretreatment by iron of electro-flocculation and chemical flocculation. Desalination, 204, 87-93.

104. Olguin, E. (2003) Phycoremediation: key issues for cost effective nutrient removal processes. Biotechnology Advances, 22, 81-91

105. Owen, A., Fawell, P., Swift, J., Labbett, D., Benn, F., Farrow, J. (2008) Using turbulent pipe flow to study the factors affecting polymer-bridging flocculation of mineral systems. International Journal of Mineral Processing, 87, 90-99

106. Patil, V., Tran, K., Giselrod, H (2008) Towards sustainable production of biofuels from microalgae. International Journal of Molecular Sciences, 9, 1188-1195

107. Pate, R., Klise, G., Wu, B. (2011) Resource demand implications for US algae biofuels production scale-up. Applied Energy, 88, 3377-3388

108. Pienkos, P and Darzins, A. 2009 The promise and challenges of microalgal-derived biofuels. Biofuels, Biproducts, and Biorefining, 3, 431-440.

109. Pieterse, A. and Cloot, A. 1997 Algal cells and coagulation, flocculation and sedimentation process. Wat. Sci. Tech. 36(4), 111-118

110. Pittman, J., Dean, A., Osundeko, O. (2011) The potential of sustainable algal biofuel production using wastewater resources. Bioresource Technology, 102, 17-25

111. Poelman, E., Pauw, N., Jeurissen, B. (1997) Potential of electrolytic flocculation for recovery of micro-algae. Resources, Conservation, and Recycling, 19, 1-10

112. Pouet M and Grasmick A. 1995. Urban wastewater treatment by electrocoagulation and flotation. Wat Sci Technol 31(3-4):275-283.

113. Putt, R. 2007 Algae as a biodiesel feedstock: a feasibility assessment. Center for Microfibrous Materials Manufacturing

114. Rao, A., Dayananda, C., Sarada, R., Shamala, T., Ravishankar, G. (2007) Effect of salinity on growth of green alga Botryococcus braunii and its constituents. Bioresource Technology, 98, 560-564

115. Rees, F., Leenheer, J. and Ranville, J. 1991 Use of a single-bowl continuous-flow centrifuge for dewatering suspended sediments: effect on sediment physical and chemical characteristics. Hydrol. Process. 5, 201-214

116. Reynolds, C.S. (1984). Mechanisms of suspension. The Ecology of Freshwater Phytoplankton, Cambridge University Press, pp. 40–82.

117. Reynolds, T. and Richards, P. Unit Operations and Processes in Environmental Engineering. 2nd ed. Boston, Massachusetts: PWS Publishing Co, 1996

118. Ross, C., Smith, B., Valentine, G. (2000) Rethinking dissolved air flotation (DAF) design for industrial pretreatment. Water Environment Federation

119. Rubio, J., Souza, M., Smith, R. (2001) Overview of flotation as a wastewater treatment technique. Minerals Engineering, 15, 139-155.

120. Sander, K. and Murthy, G. (2009) Life cycle analysis of algae biodiesel. Life Cycle Assessment, 15, 704-714.

121. Sarrot, V., Huang, Z., Legendere, D., Guiraud, P. (2007) Experimental determination of particles capture efficiency in flotation. Chemical Engineering Science 62, 7359-7369

122. Sasson, M., Calmano, W., Adin, A. (2009) Iron-oxidation processes in an electroflocculation (electrocoagulation) cell. Journal of Hazardous Materials, 171, 704-709

123. Schenk, P., Thomas, S., Stephens, E., Marx, U., Mussgnug, J., Posten, C., Kruse, O., Hankamer, B. (2008) Second generation biofuels: high-efficiency microalgae for biodiesel production. Bioenerg. Res., 1, 20-43.

124. Schwoyer, W. Polyelectrolytes for Water and Wastewater Treatment. Boca Raton, Florida: CRC Press, 1981

125. Sim, T., Goh, A. and Becker, E. 1988 Comparison of centrifugation, dissolved air flotation and drum filtration techniques for harvesting sewage-grown algae. Biomass, 16, 51-62

126. Singh, A. and Olsen, S. (2011) A critical review of biochemical conversion, sustainability and life cycle assessment of algal biofuels. Applied Energy, 88, 3548-3555

127. Stephenson, P., Moore, C., Terry, M., Zubkov, M., Bibby, T. (2011) Improving photosynthesis for algal biofuels: toward a green revolution. Trends in Biotechnology, 29(12), 615-623

128. Sturm, B. and Lamer, S. (2011) An energy evaluation of coupling nutrient removal from wastewater with algal biomass production. Applied Energy, 88, 3499-3506

129. Subhadra, B. and Edwards, M. (2011) Coproduct market analysis and water footprint of simulated commercial algal biorefineries. Applied Energy, 88, 3515-3523

130. Sukenik, A. and Shelef, G. (1984) Algal autoflocculation – verification and proposed mechanism. Biotechnology and Bioengineering, 26, 142-147

131. Sun A, Davis R, Starbuck M, Amotz A, Pate R, Pienkos P. 2011. Comparative cost analysis of algal oil production for biofuels. Energy 36:5169-5179.

132. Sydney, E., Silva, T., Tokarski, A., Novak, A., Carvalho, J., Woiciecohwski, A., Larroche, C., Soccol, C. (2011) Screening of microalgae with potential for biodiesel production and nutrient removal from treated domestic sewage. Applied Energy, 88, 3291-3294.

133. Theegala, C.S. Microalgal Lipids for Biofuels: Current Status and Recognized Barriers. Book Chapter, pp 133-148, Proceedings of the 2009 Louisiana Natural Resources Symposium. ISBN: 0-9763632-3-2

134. Timmons, M., Ebeling, J., Wheaton, F., Summerfelt, S., Vinci, B. Recirculating Aquaculture Systems. 2nd Ed. Ithaca, New York: Cayuga Aqua Ventures, 2002.

135. Um, B. and Kim, Y. 2009 Review: a chance for Korea to advance algal-biodiesel technology. J. Ind. Eng. Chem, 156, 1-7.

136. U.S. DOE 2010. National Algal Biofuels Technology Roadmap. U.S. Department of Energy, Office of Energy Efficiency and Renewable Energy, Biomass Program.

137. U.S. Energy Information Administration. November 2010. http://www.eia.doe.gov/.

138. Vandamme, D., Pontes, S., Goiris, K., Foubert, I., Pinoy, L., Muylaert, K. (2011) Evaluation of elctro-coagulation-flocculation for harvesting marine and freshwater microalgae. Biotechnology and Bioengineering, 108(10) 2320-2329

139. Vasudevan P, Briggs M. Biodiesel production—current state of the art and challenges. Journal of Industrial Microbiology and Biotechnology 2008;35(5):421–30.

140. Vijayaraghavan, K. and Hemanathan, K. (2009) Biodiesel production from freshwater algae. Energy Fuels, 23, 5448-5453.

141. Wang, L., Fahey, E., Wu, Z. (2005) Handbook of Environmental Engineering, Vol. 3: Physiochemical Treatment Processes, Ch 12. Dissolved Air Flotation. 431-500

142. Wijffels, R., Barbosa, M., Eppink, M. (2010) Microalgae for the production of bulk chemicals and biofuels. Biofuels, Bioproducts, and Biorefining, 4, 287-295

143. Williams, P. and Laurens, L. (2010) Microalgae as biodiesel and biomass feedstocks: review and analysis of the biochemistry, energetics and economics. Energy and Environmental Science,3, 554-590

144. Zouboulis, A. and Avranas, A. (2000) Treatment of oil-in-water emulsions by coagulation and dissolved air flotation. Colloids and Surfaces A. 172, 153-161

Appendix A: Potential Production Values and Culture Volumes of Microalgal Biodiesel

1 Acre pond x 41 cm deep = 1645 m^3

Assuming culture densities of 100 mg/L with oil content of 20%

$$1645\ m^3 * \left(\frac{1000\ L}{m^3}\right) * \left(\frac{100\ mg\ algae}{L}\right)\left(\frac{1\ kg}{1 * 10^6\ mg}\right) * 20\% = 32.9\ kg\ oil\ per\ harvest$$

Density of algal oil, 0.864 kg/L (oilgae)

$$32.9\ kg * \left(\frac{1\ L}{0.864\ kg}\right) = 38\ L$$

$$\frac{1645\ m^3\ culture}{38\ L\ oil} = 43.2 \frac{m^3\ culture}{L\ oil}$$

Table 2.1: Theoretical volume (m^3) of pond culture to be processed to produce 1 L of algal oil as function of culture density and lipid concentration

m^3 of Culture/L of Oil											
		Culture Density in mg/l									
		50	**100**	**150**	**200**	**250**	**300**	**350**	**400**	**450**	**500**
Percent Lipids	**10**	172.80	86.40	57.60	43.20	34.56	28.80	24.69	21.60	19.20	17.28
	15	115.20	57.60	38.40	28.80	23.04	19.20	16.46	14.40	12.80	11.52
	20	86.40	43.20	28.80	21.60	17.28	14.40	12.34	10.80	9.60	8.64
	25	69.12	34.56	23.04	17.28	13.82	11.52	9.87	8.64	7.68	6.91
	30	57.60	28.80	19.20	14.40	11.52	9.60	8.23	7.20	6.40	5.76
	35	49.37	24.69	16.46	12.34	9.87	8.23	7.05	6.17	5.49	4.94
	40	43.20	21.60	14.40	10.80	8.64	7.20	6.17	5.40	4.80	4.32
	45	38.40	19.20	12.80	9.60	7.68	6.40	5.49	4.80	4.27	3.84
	50	34.56	17.28	11.52	8.64	6.91	5.76	4.94	4.32	3.84	3.46
	55	31.42	15.71	10.47	7.85	6.28	5.24	4.49	3.93	3.49	3.14
	60	28.80	14.40	9.60	7.20	5.76	4.80	4.11	3.60	3.20	2.88
	65	26.58	13.29	8.86	6.65	5.32	4.43	3.80	3.32	2.95	2.66

Table 1.1: Predicted yearly oil production from an acre of algal culture based on its culture density and lipid percentage

		Culture Density in mg/l									
		50	**100**	**150**	**200**	**250**	**300**	**350**	**400**	**450**	**500**
Percent Lipids	**10**	1,142	2,285	3,427	4,569	5,712	6,854	7,997	9,139	10,281	11,424
	15	1,714	3,427	5,141	6,854	8,568	10,281	11,995	13,708	15,422	17,135
	20	2,285	4,569	6,854	9,139	11,424	13,708	15,993	18,278	20,563	22,847
	25	2,856	5,712	8,568	11,424	14,280	17,135	19,991	22,847	25,703	28,559
	30	3,427	6,854	10,281	13,708	17,135	20,563	23,990	27,417	30,844	34,271
	35	3,998	7,997	11,995	15,993	19,991	23,990	27,988	31,986	35,984	39,983
	40	4,569	9,139	13,708	18,278	22,847	27,417	31,986	36,556	41,125	45,694
	45	5,141	10,281	15,422	20,563	25,703	30,844	35,984	41,125	46,266	51,406
	50	5,712	11,424	17,135	22,847	28,559	34,271	39,983	45,694	51,406	57,118
	55	6,283	12,566	18,849	25,132	31,415	37,698	43,981	50,264	56,547	62,830
	60	6,854	13,708	20,563	27,417	34,271	41,125	47,979	54,833	61,688	68,542
	65	7,425	14,851	22,276	29,701	37,127	44,552	51,977	59,403	66,828	74,253
		L of Oil/Acre/Year									

Adam Dassey <adasse1@tigers.lsu.edu>

RE: Elsevier.com permissions query

1 message

Permissions Helpdesk <permissionshelpdesk@elsevier.com> Mon, Jun 24, 2013 at 2:23 PM
To: "adasse1@lsu.edu" <adasse1@lsu.edu>

.

Dear Adam,

We hereby grant you permission to reprint the material below at no charge **in your dissertation** subject to the following conditions:

1. If any part of the material to be used (for example, figures) has appeared in our publication with credit or acknowledgement to another source, permission must also be sought from that source. If such permission is not obtained then that material may not be included in your publication/copies.

2. Suitable acknowledgment to the source must be made, either as a footnote or in a reference list at the end of your publication, as follows:

"This article was published in Publication title, Vol number, Author(s), Title of article, Page Nos, Copyright Elsevier (or appropriate Society name) (Year)."

3. Your thesis may be submitted to your institution in either print or electronic form.

4. Reproduction of this material is confined to the purpose for which permission is hereby given.

5. This permission is granted for non-exclusive world **English** rights only. For other languages please reapply separately for each one required. Permission excludes use in an electronic form other than submission. Should you have a specific electronic project in mind please reapply for permission.

6. Should your thesis be published commercially, please reapply for permission.

This includes permission for the Library and Archives of Canada to supply single copies, on demand, of the complete thesis. Should your thesis be published commercially, please reapply for permission.

This includes permission for UMI to supply single copies, on demand, of the complete thesis. Should your thesis be published commercially, please reapply for permission.

Kind regards
Laura

Figure 2.1 Stella model representing the mass balance between growth rate and biomass harvesting

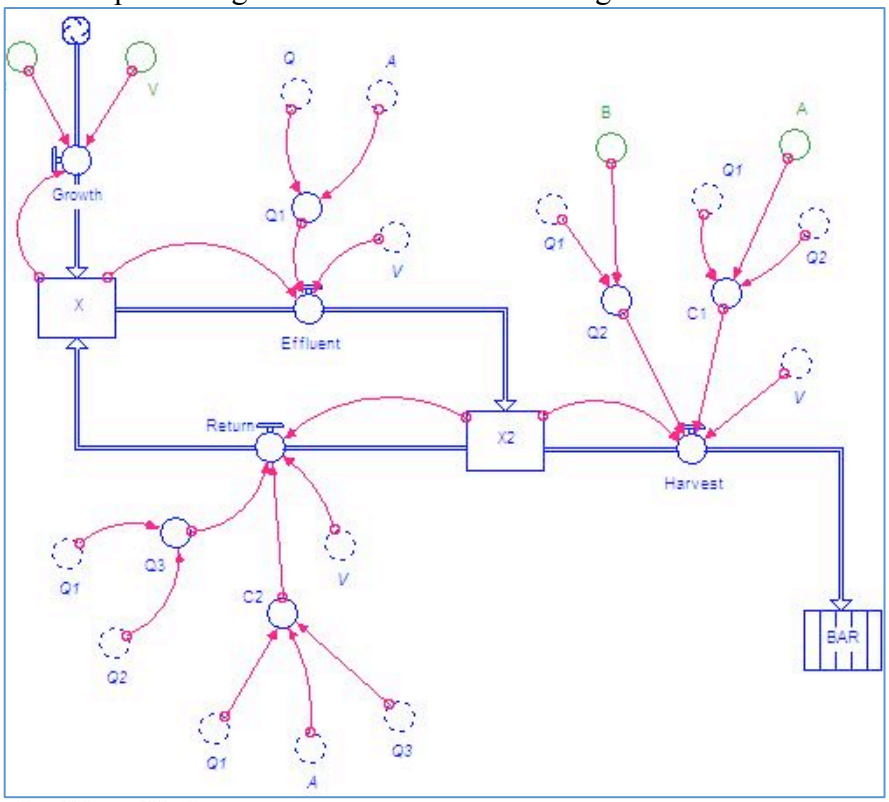

BAR(t) = BAR(t - dt) + (Harvest) * dt
INIT BAR = 0
TRANSIT TIME = 1
INFLOW LIMIT = INF
CAPACITY = INF
INFLOWS:
Harvest = X2*C1*Q2/V

X(t) = X(t - dt) + (Growth + Return - Effluent) * dt
INIT X = 100
INFLOWS:
Growth = X*Q/V
Return = X2*C2*Q3/V
OUTFLOWS:
Effluent = X*Q1/V

X2(t) = X2(t - dt) + (Effluent - Harvest - Return) * dt
INIT X2 = 100
INFLOWS:
Effluent = X*Q1/V
OUTFLOWS:
Harvest = X2*C1*Q2/V
Return = X2*C2*Q3/V

A = .4
B = .3
C1 = Q1/Q2*A
C2 = Q1/Q3*(1-A)
Q = 4
Q1 = Q/A
Q2 = Q1*B
Q3 = Q1-Q2
V = 96

Raw Data for Initial Centrifuge Testing with Varying Flow Rates for Figure 2.3 and 2.4

Influent	**G1**	**G2**	**G3**	**AVG**		
ABS	0.236	0.23	0.237	0.234		
TSS	109.07428	106.3663	109.52561	108.322		
Influent	**A1**	**A2**	**A3**	**AVG**		
ABS	0.232	0.236	0.237	0.235		
TSS	107.26896	109.07428	109.52561	108.623		
Influent	**E1**	**E2**	**E3**	**AVG**		
ABS	0.24	0.238	0.239	0.239		
TSS	110.8796	109.97694	110.42827	110.428		
Average Initial TSS				109.124		
	F1	**F2**	**F3**	**AVG**	**STD DEV**	**95% C.I.**
ABS	0.2	0.193	0.194	0.196	0.00	0.004
TSS (mg/L)	92.8	89.7	90.1	90.9	1.71	1.933
Harvested (mg/L)	16.3	19.5	19.0	18.3	1.71	1.933
Efficiency (%)	15.0	17.9	17.4	16.7	1.57	1.773
Flow Rate (L/min)	24.0	22.8	22.8	23.2	0.69	0.783
Power (kWh/m^3)	0.777	0.818	0.818	0.804	0.02	0.026
Cost ($/L oil)	14.260	12.573	12.872	13.235	0.90	1.018
	D1	**D2**	**D3**	**AVG**	**STD DEV**	**95% C.I.**
ABS	0.164	0.169	0.169	0.167	0.00	0.003
TSS (mg/L)	76.6	78.8	78.8	78.1	1.30	1.474
Harvested (mg/L)	32.5	30.3	30.3	31.0	1.30	1.474
Efficiency (%)	29.9	27.8	27.8	28.5	1.20	1.352
Flow Rate (L/min)	18.2	18.2	18.2	18.2	0.00	
Power (kWh/m^3)	1.022	1.022	1.022	1.022	0.00	
Cost ($/L oil)	9.396	10.096	10.096	9.863	0.40	0.457
	C1	**C2**	**C3**	**AVG**	**STD DEV**	**95% C.I.**
ABS	0.149	0.159	0.161	0.156	0.01	0.007
TSS (mg/L)	69.8	74.3	75.2	73.1	2.90	3.283
Harvested (mg/L)	39.3	34.8	33.9	36.0	2.90	3.283
Efficiency (%)	36.1	31.9	31.1	33.0	2.66	3.012
Flow Rate (L/min)	14.2	14.4	14.2	14.2	0.14	0.156
Power (kWh/m^3)	1.317	1.295	1.317	1.310	0.01	0.014
Cost ($/L oil)	10.019	11.130	11.620	10.923	0.82	0.928
	B1	**B2**	**B3**	**AVG**	**STD DEV**	**95% C.I.**
ABS	0.135	0.131	0.133	0.133	0.00	0.002
TSS (mg/L)	63.5	61.7	62.6	62.6	0.90	1.021
Harvested (mg/L)	45.6	47.4	46.5	46.5	0.90	1.021
Efficiency (%)	41.9	43.5	42.7	42.7	0.83	0.937
Flow Rate (L/min)	7.7	7.6	7.7	7.6	0.07	0.078
Power (kWh /m^3)	2.428	2.467	2.428	2.441	0.02	0.025
Cost ($/L oil)	15.915	15.553	15.606	15.691	0.20	0.221

	H1	H2	H3	AVG	STD DEV	95% C.I.
ABS	0.101	0.099	0.102	0.101	0.00	0.001
TSS (mg/L)	48.1	47.2	48.6	48.0	0.69	0.780
Harvested (mg/L)	61.0	61.9	60.5	61.1	0.69	0.780
Efficiency (%)	55.9	56.8	55.5	56.1	0.63	0.715
Flow Rate (L/min)	5.0	5.1	5.0	5.0	0.05	0.051
Power (kWh/m^3)	3.745	3.679	3.700	3.708	0.03	0.038
Cost ($/L oil)	18.368	17.778	18.284	18.143	0.32	0.360
	I1	**I2**	**I3**	**AVG**	**STD DEV**	**95% C.I.**
ABS	0.085	0.08	0.084	0.083	0.00	0.002
TSS (mg/L)	40.9	38.7	40.5	40.0	1.19	1.351
Harvested (mg/L)	68.2	70.5	68.7	69.1	1.19	1.351
Efficiency (%)	62.6	64.6	63.0	63.4	1.10	1.239
Flow Rate (L/min)	3.9	4.0	4.0	3.9	0.03	0.039
Power (kWh/m^3)	4.782	4.710	4.710	4.734	0.04	0.047
Cost ($/L oil)	20.971	19.991	20.517	20.493	0.49	0.554
	J1	**J2**	**J3**	**AVG**	**STD DEV**	**95% C.I.**
ABS	0.058	0.058	0.061	0.059	0.00	0.001
TSS (mg/L)	28.7	28.7	30.1	29.2	0.78	0.884
Harvested (mg/L)	80.4	80.4	79.0	79.9	0.78	0.884
Efficiency (%)	73.7	73.7	72.5	73.3	0.72	0.811
Flow Rate (L/min)	2.9	3.0	3.0	3.0	0.03	0.033
Power (kWh/m^3)	6.344	6.217	6.279	6.280	0.06	0.071
Cost ($/L oil)	23.601	23.129	23.763	23.498	0.33	0.372
	K1	**K2**	**K3**	**AVG**	**STD DEV**	**95% C.I.**
ABS	0.033	0.032	0.03	0.032	0.00	0.001
TSS (mg/L)	17.5	17.0	16.1	16.9	0.69	0.780
Harvested (mg/L)	91.7	92.1	93.0	92.3	0.69	0.780
Efficiency (%)	84.1	84.5	85.3	84.7	0.63	0.715
Flow Rate (L/min)	2.0	2.0	2.0	2.0	0.00	
Power (kWh/m^3)	9.142	9.142	9.142	9.142	0.00	
Cost ($/L oil)	29.827	29.681	29.393	29.633	0.22	0.249
	L1	**L2**	**L3**	**AVG**	**STD DEV**	**95% C.I.**
ABS	0.009	0.008	0.008	0.008	0.00	0.001
TSS (mg/L)	6.6	6.2	6.2	6.3	0.26	0.294
Harvested (mg/L)	102.5	103.0	103.0	102.8	0.26	0.294
Efficiency (%)	94.0	94.5	94.5	94.3	0.24	0.270
Flow Rate (L/min)	0.9	0.9	0.9	0.9	0.00	
Power (kWh/m^3)	19.840	19.840	19.840	19.840	0.00	
Cost ($/L oil)	57.890	57.636	57.636	57.721	0.15	0.165

Analysis of Raw Data Collected from Centrifuge Testing

algae density (mg/L)	Flow Rate (L/min)	Mass Harvested (mg/L)	Efficiency (%)	Mass Harvested (mg/min)	energy (kWh/m^3)	energy cost ($/gal oil)	energy cost ($/L oil)
109	23.20	18.3	16.75	423.48	0.80	49.883	13.179
109	18.24	31.0	28.48	566.19	1.02	37.288	9.851
109	14.24	36.0	33.03	512.72	1.31	41.179	10.879
109	7.64	46.5	42.69	355.54	2.44	59.383	15.689
109	5.03	61.1	56.08	307.48	3.708	68.664	18.141
109	3.94	69.1	63.40	272.27	4.734	77.545	20.488
109	2.97	79.9	73.33	237.41	6.280	88.933	23.496
109	2.04	92.3	84.65	188.23	9.142	112.158	29.632
109	0.94	102.8	94.31	96.63	19.840	218.472	57.721

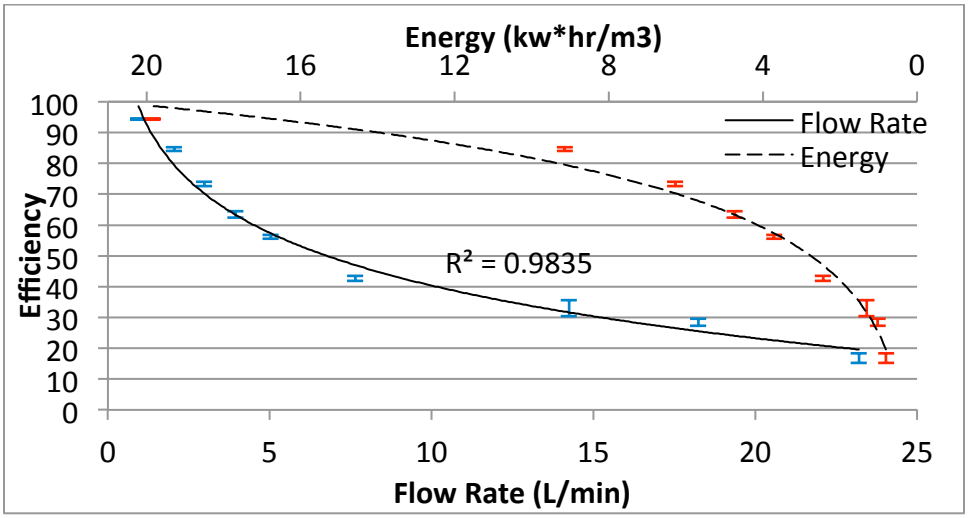

Figure 2.3: Capture efficiency of microalgal cells by centrifugation as a product of various flow rates and the concurrent energy consumed. Red symbols with a dashed trendline correspond to the energy consumed and blue symbols with a solid trendline correspond to the flow rate

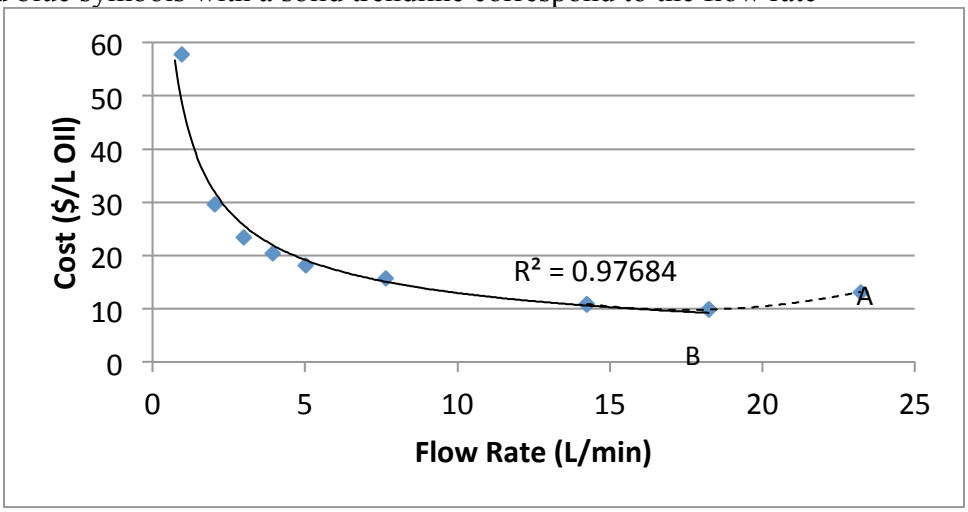

Figure 2.4: Harvesting cost per L of oil as a result of various flow rates. The cost reached a minimum at 18 L/min

Economic Analysis of the Centrifuge Testing

Table 2.2: Theoretical kW required to produce 1 L of oil if a centrifuge operates at 28.5% capture efficiency and harvesting is to be completed within 12 h

KW/L Oil											
		Culture Density in mg/l									
		50	**100**	**150**	**200**	**250**	**300**	**350**	**400**	**450**	**500**
Percent Lipids	**10**	51.78	25.89	17.26	12.94	10.36	8.63	7.40	6.47	5.75	5.18
	15	34.52	17.26	11.51	8.63	6.90	5.75	4.93	4.31	3.84	3.45
	20	25.89	12.94	8.63	6.47	5.18	4.31	3.70	3.24	2.88	2.59
	25	20.71	10.36	6.90	5.18	4.14	3.45	2.96	2.59	2.30	2.07
	30	17.26	8.63	5.75	4.31	3.45	2.88	2.47	2.16	1.92	1.73
	35	14.79	7.40	4.93	3.70	2.96	2.47	2.11	1.85	1.64	1.48
	40	12.94	6.47	4.31	3.24	2.59	2.16	1.85	1.62	1.44	1.29
	45	11.51	5.75	3.84	2.88	2.30	1.92	1.64	1.44	1.28	1.15
	50	10.36	5.18	3.45	2.59	2.07	1.73	1.48	1.29	1.15	1.04
	55	9.41	4.71	3.14	2.35	1.88	1.57	1.34	1.18	1.05	0.94
	60	8.63	4.31	2.88	2.16	1.73	1.44	1.23	1.08	0.96	0.86
	65	7.97	3.98	2.66	1.99	1.59	1.33	1.14	1.00	0.89	0.80

746 W/HP operated for 12 hr at a cost of $.09/kWh

		Culture Density in mg/l									
		50	**100**	**150**	**200**	**250**	**300**	**350**	**400**	**450**	**500**
Percent Lipids	**10**	55.92	27.96	18.64	13.98	11.18	9.32	7.99	6.99	6.21	5.59
	15	37.28	18.64	12.43	9.32	7.46	6.21	5.33	4.66	4.14	3.73
	20	27.96	13.98	9.32	6.99	5.59	4.66	3.99	3.49	3.11	2.80
	25	22.37	11.18	7.46	5.59	4.47	3.73	3.20	2.80	2.49	2.24
	30	18.64	9.32	6.21	4.66	3.73	3.11	2.66	2.33	2.07	1.86
	35	15.98	7.99	5.33	3.99	3.20	2.66	2.28	2.00	1.78	1.60
	40	13.98	6.99	4.66	3.49	2.80	2.33	2.00	1.75	1.55	1.40
	45	12.43	6.21	4.14	3.11	2.49	2.07	1.78	1.55	1.38	1.24
	50	11.18	5.59	3.73	2.80	2.24	1.86	1.60	1.40	1.24	1.12
	55	10.17	5.08	3.39	2.54	2.03	1.69	1.45	1.27	1.13	1.02
	60	9.32	4.66	3.11	2.33	1.86	1.55	1.33	1.16	1.04	0.93
	65	8.60	4.30	2.87	2.15	1.72	1.43	1.23	1.08	0.96	0.86
		$ cost/L oil									

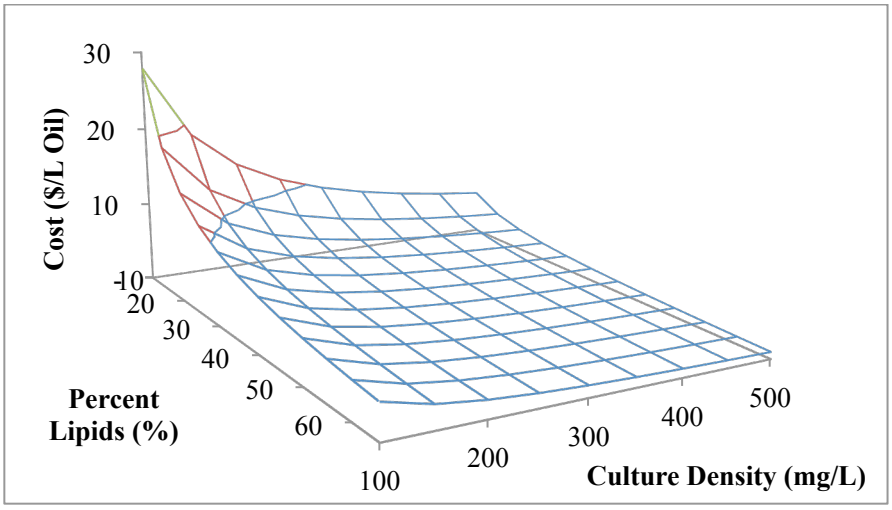

Figure 2.5: Final theoretical cost of harvesting microalgae by centrifugation as a function of culture density and lipid concentration

Appendix C: Initial Electrocoagulation Batch Testing for *Nannochloris* and *Dunaliella*: Including Stella, Salinity, Zeta Potential, Preliminary Testing and Cost Analysis

Figure 3.1 Stella model representing the mass balance between growth rate and a 2-stage biomass harvesting system

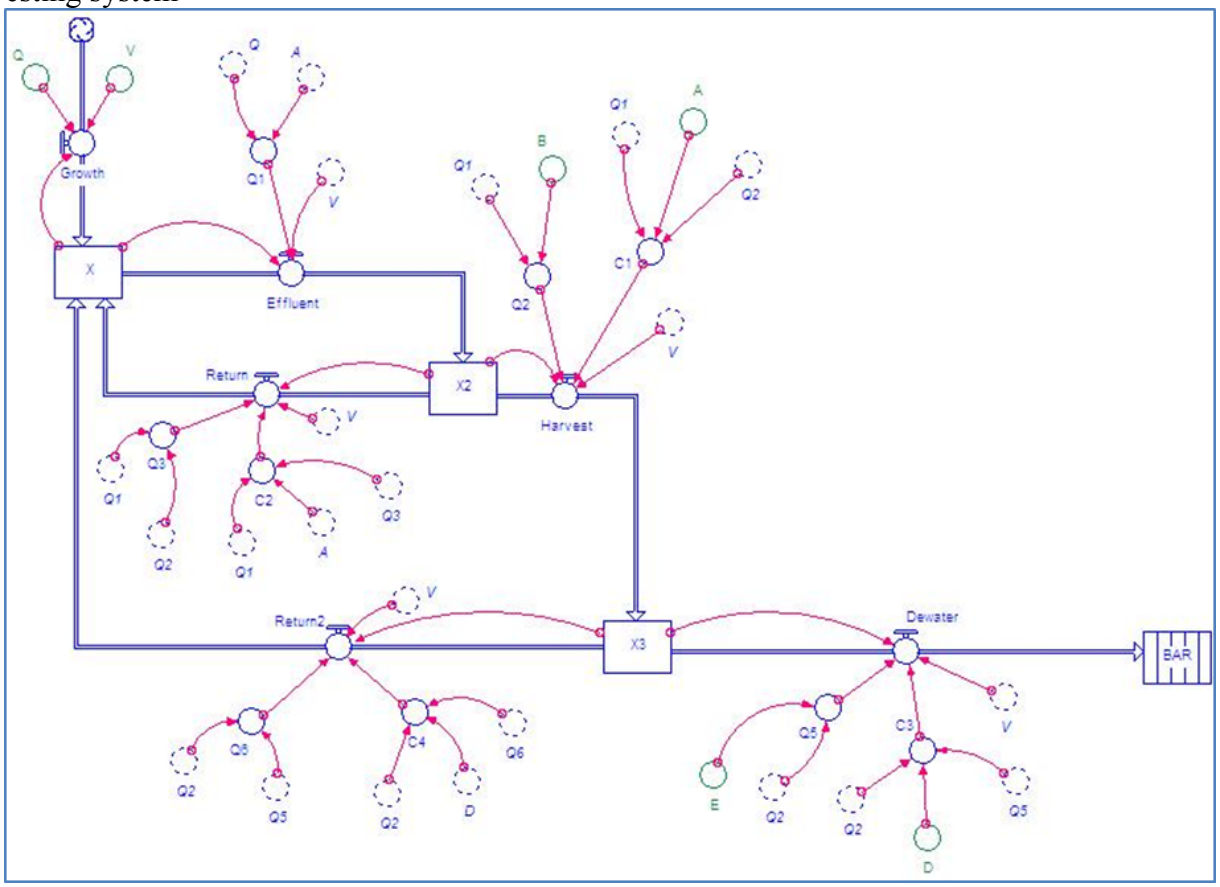

BAR(t) = BAR(t - dt) + (Dewater) * dt
INIT BAR = 0
TRANSIT TIME = 1
INFLOW LIMIT = INF
CAPACITY = INF
INFLOWS:
- Dewater = X3*C3*Q5/V

X(t) = X(t - dt) + (Growth + Return + Return2 - Effluent) * dt
INIT X = 100
INFLOWS:
- Growth = X*Q/V
- Return = X2*C2*Q3/V
- Return2 = X3*C4*Q6/V

OUTFLOWS:
- Effluent = X*Q1/V

X2(t) = X2(t - dt) + (Effluent - Harvest - Return) * dt
INIT X2 = X
INFLOWS:
- Effluent = X*Q1/V

OUTFLOWS:
- Harvest = X2*C1*Q2/V
- Return = X2*C2*Q3/V

X3(t) = X3(t - dt) + (Harvest - Return2 - Dewater) * dt
INIT X3 = C1*100
INFLOWS:
- Harvest = X2*C1*Q2/V

OUTFLOWS:
- Return2 = X3*C4*Q6/V
- Dewater = X3*C3*Q5/V

A = .4
B = .2
C1 = Q1/Q2*A
C2 = Q1/Q3*(1-A)
C3 = Q2/Q5*D
C4 = Q2/Q6*(1-D)
D = 1
E = .001
Q = 4
Q1 = Q/A
Q2 = Q1*B
Q3 = Q1-Q2
Q5 = Q2*E
Q6 = Q2-Q5
V = 96

Raw data salinity variations on the efficiency of batch electrocoagulation units

Sample	Salinity (g/L)	amp	volt	time (min)	energy (kWh/m^3)	Std. Dev.	95% C.I.	aluminum (mg/L)
A	0	0.20	6.9	1	0.023	0.000	0.000	1.119
B	0	0.60	13.8	1	0.138	0.012	0.013	3.358
C	0	1.00	18.0	1	0.300	0.004	0.005	5.597
D	0	0.10	3.2	2	0.011	0.001	0.001	1.119
E	0	0.30	6.7	2	0.067	0.007	0.008	3.358
F	0	0.50	9.8	2	0.163	0.014	0.016	5.597
G	0	0.70	12.8	2	0.299	0.032	0.037	7.835
H	0	0.04	1.8	5	0.006	0.001	0.001	1.119
I	0	0.12	3.1	5	0.031	0.003	0.003	3.358
J	0	0.20	4.6	5	0.077	0.009	0.010	5.597
K	0	0.28	5.9	5	0.138	0.015	0.017	7.835
A	1	0.20	2.4	1	0.008	0.001	0.001	1.119
B	1	0.60	5.2	1	0.052	0.008	0.009	3.358
C	1	1.00	7.4	1	0.124	0.014	0.016	5.597
D	1	1.40	9.2	1	0.215	0.026	0.001	7.835
E	1	0.10	1.5	2	0.005	0.001	0.004	1.119
F	1	0.30	2.9	2	0.029	0.004	0.010	3.358
G	1	0.50	4.1	2	0.068	0.008	0.021	5.597
H	1	0.70	5.2	2	0.121	0.019	0.000	7.835
I	1	0.04	1.1	5	0.004	0.000	0.002	1.119
J	1	0.12	1.7	5	0.017	0.002	0.005	3.358
K	1	0.20	2.3	5	0.038	0.004	0.006	5.597
L	1	0.28	3.1	5	0.073	0.005	0.001	7.835
A	2	0.20	2.2	1	0.007	0.001	0.006	1.119
B	2	0.60	4.4	1	0.044	0.005	0.012	3.358
C	2	1.00	6.2	1	0.103	0.011	0.000	5.597
D	2	1.40	7.6	1	0.178	0.016	0.002	7.835
E	2	0.10	1.4	2	0.005	0.000	0.007	1.119
F	2	0.30	2.5	2	0.025	0.002	0.009	3.358
G	2	0.50	3.5	2	0.058	0.006	0.000	5.597
H	2	0.70	4.3	2	0.101	0.008	0.001	7.835
I	2	0.04	1.1	5	0.004	0.000	0.003	1.119
J	2	0.12	1.5	5	0.015	0.001	0.003	3.358
K	2	0.20	1.9	5	0.032	0.003	0.001	5.597
L	2	0.28	2.4	5	0.055	0.003	0.003	7.835
A	4	0.20	2.0	1	0.007	0.001	0.007	1.119
B	4	0.60	3.9	1	0.039	0.003	0.000	3.358
C	4	1.00	5.3	1	0.088	0.006	0.001	5.597
D	4	1.40	6.5	1	0.152	0.008	0.002	7.835
E	4	0.10	1.3	2	0.004	0.000	0.003	1.119
F	4	0.30	2.2	2	0.022	0.001	0.000	3.358
G	4	0.50	3.1	2	0.052	0.002	0.000	5.597
H	4	0.70	3.8	2	0.089	0.002	0.001	7.835
I	4	0.04	1.0	5	0.003	0.000	0.002	1.119
J	4	0.12	1.4	5	0.014	0.000	0.001	3.358

K	4	0.20	1.7	5	0.029	0.001	0.004	5.597
L	4	0.28	2.2	5	0.051	0.001	0.003	7.835
A	15	0.21	2.1	1	0.008	0.001	0.001	1.194
B	15	0.60	3.1	1	0.031	0.004	0.004	3.358
C	15	1.00	3.7	1	0.062	0.002	0.003	5.597
D	15	1.40	4.6	1	0.108	0.004	0.004	7.817
E	15	0.11	1.3	2	0.005	0.001	0.001	1.269
F	15	0.30	1.9	2	0.019	0.001	0.001	3.321
G	15	0.50	2.4	2	0.040	0.001	0.001	5.597
H	15	0.71	3.1	2	0.073	0.004	0.004	7.873
I	15	0.04	1.0	5	0.003	0.000	0.000	1.119
J	15	0.12	1.3	5	0.013	0.002	0.002	3.265
K	15	0.20	1.5	5	0.025	0.003	0.003	5.503
L	15	0.28	1.9	5	0.044	0.006	0.007	7.835

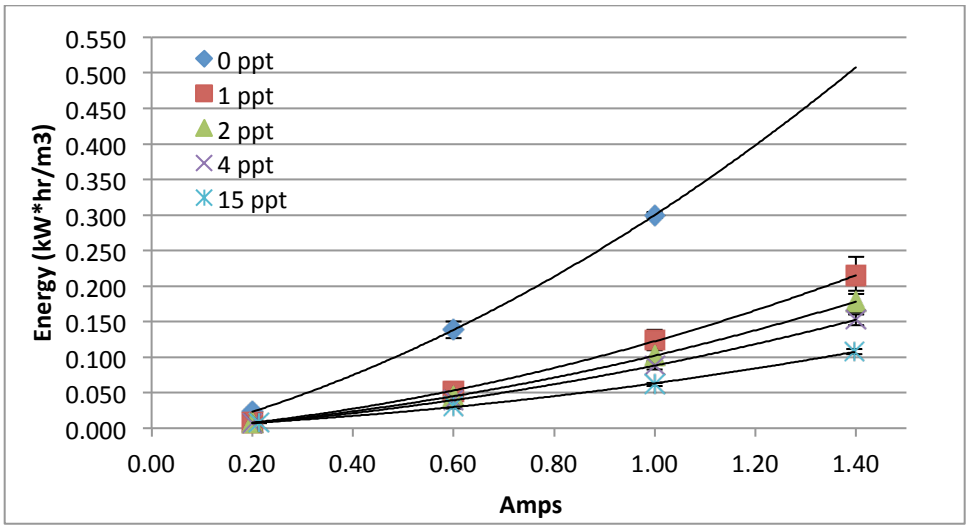

Figure 3.4 The correlation of NaCl concentrations as an electrolyte and the energy consumed per cubic meter to maintain various amperages

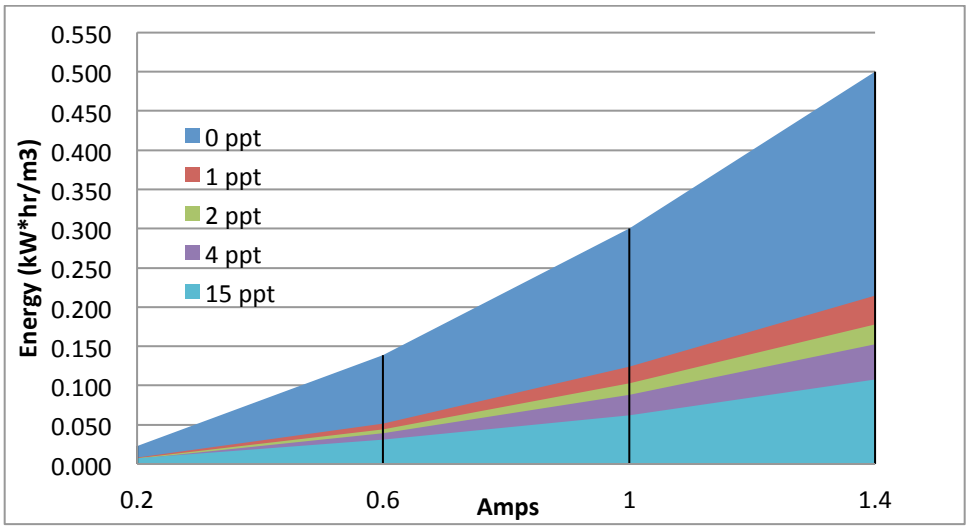

Raw data for the growth of *Nannochloris* under various salinities

0 ppt	a1	a2	a3	AVG	Std Dev	95% C.I.	Zeta
pH	7.19	7.14	7.1	7.143333	0.045092	0.051026	
0 mL	0.0844	0.0851	0.0844	0.084633	0.000404	0.000457	
30 mL	0.1	0.0999	0.0982	0.099367	0.001012	0.001145	
TSS (mg/L)	520	493.3333	460	491.1111	30.06167	34.01735	-33.6
1 ppt	b1	b2	b3	AVG	Std Dev	95% C.I.	
pH	8.29	9	8.39	8.56	0.384318	0.434888	
0 mL	0.0849	0.0855	0.087	0.0858	0.001082	0.001224	
30 mL	0.0963	0.0971	0.0969	0.096767	0.000416	0.000471	
TSS (mg/L)	380	386.6667	330	365.5556	30.97191	35.04737	-26.1
2 ppt	c1	c2	c3	AVG	Std Dev	95% C.I.	
pH	8.08	8.57	7.95	8.2	0.326956	0.369978	
0 mL	0.0851	0.0838	0.0854	0.084767	0.00085	0.000962	
30 mL	0.0956	0.0938	0.097	0.095467	0.001604	0.001815	
TSS (mg/L)	350	333.3333	386.6667	356.6667	27.28451	30.87476	-19.2
4 ppt	d1	d2	d3	AVG	Std Dev	95% C.I.	
pH	8.48	8.23	8.58	8.43	0.180278	0.204	
0 mL	0.0852	0.0821	0.0857	0.084333	0.00195	0.002207	
30 mL	0.0913	0.0901	0.0921	0.091167	0.001007	0.001139	
TSS (mg/L)	203.3333	266.6667	213.3333	227.7778	34.0479	38.52811	-13.9

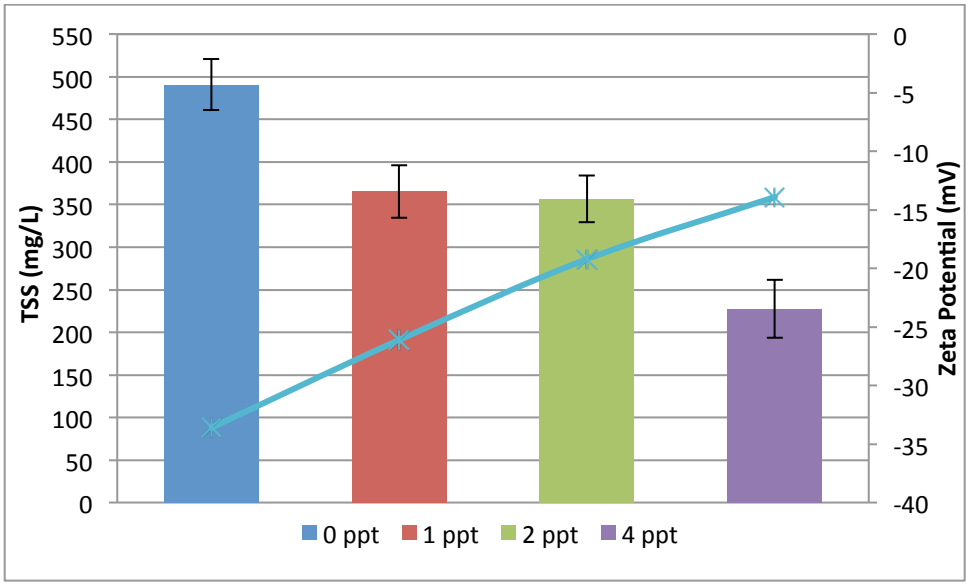

Figure 3.3 The columns represent the final biomass concentration in mg/L after 1 week of culturing *Nannochloris sp.* in various salinities. The line shows the decrease in zeta potential with increased salinity

Cost comparison of salinity on electrocoagulation and growth of *Nannochloris*

Biomass (mg/L)	Salinity (g/L)	Amps	energy (kWh/m^3)	$/L oil
491	0	0.2	0.0230	0.015
491	0	0.6	0.1383	0.088
491	0	1	0.3000	0.190
491	0	1.4	0.5000	0.317
366	1	0.2	0.0081	0.007
366	1	0.6	0.0517	0.044
366	1	1	0.1239	0.105
366	1	1.4	0.2147	0.182
357	2	0.2	0.0074	0.006
357	2	0.6	0.0443	0.039
357	2	1	0.1028	0.090
357	2	1.4	0.1781	0.155
228	4	0.2	0.0068	0.009
228	4	0.6	0.0393	0.054
228	4	1	0.0883	0.121
228	4	1.4	0.1524	0.208

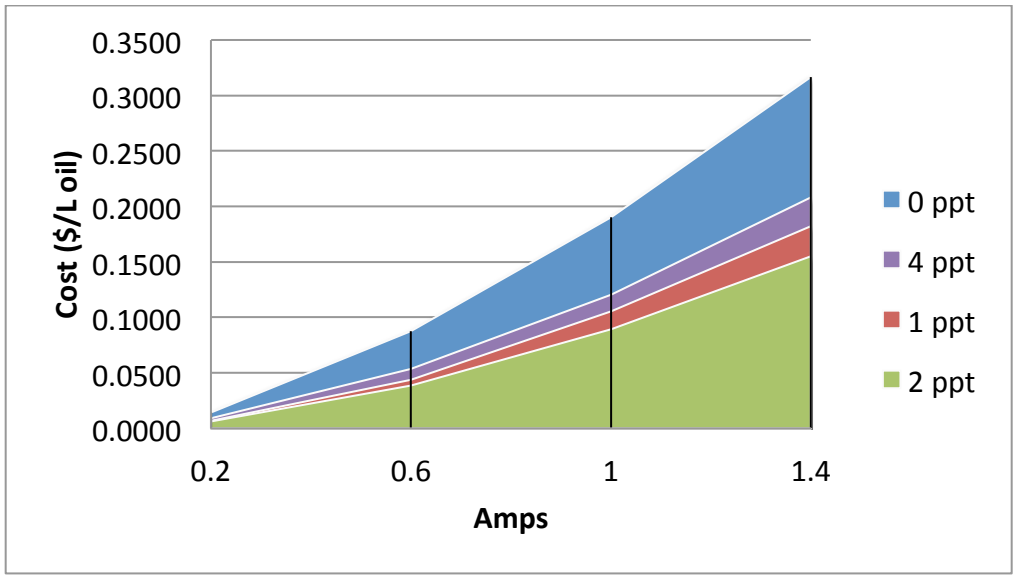

Figure 3.5 The cost per L oil based off of the correlations between the growth densities (Figures 3.3) and the energy consumption (Figure 3.4) due to various salinities

Zeta Potential Report

v2.2

Sample Details

Sample Name: A3 1
SOP Name: mansettings.nano
General Notes:

File Name: Salinity.dts
Record Number: 10
Date and Time: Thursday, October 11, 2012 1:44:...
Dispersant Name: Adam - water-0ppt
Dispersant RI: 1.330
Viscosity (cP): 0.8891
Dispersant Dielectric Constant: 78.5

System

Temperature (°C): 25.0
Count Rate (kcps): 81.8
Cell Description: Clear disposable zeta cell
Zeta Runs: 13
Measurement Position (mm): 2.00
Attenuator: 7

Results

		Mean (mV)	Area (%)	Width (mV)
Zeta Potential (mV): -33.6	**Peak 1:**	-27.5	70.4	5.66
Zeta Deviation (mV): 11.3	**Peak 2:**	-49.0	29.6	5.03
Conductivity (mS/cm): 0.648	**Peak 3:**	0.00	0.0	0.00

Result quality : Good

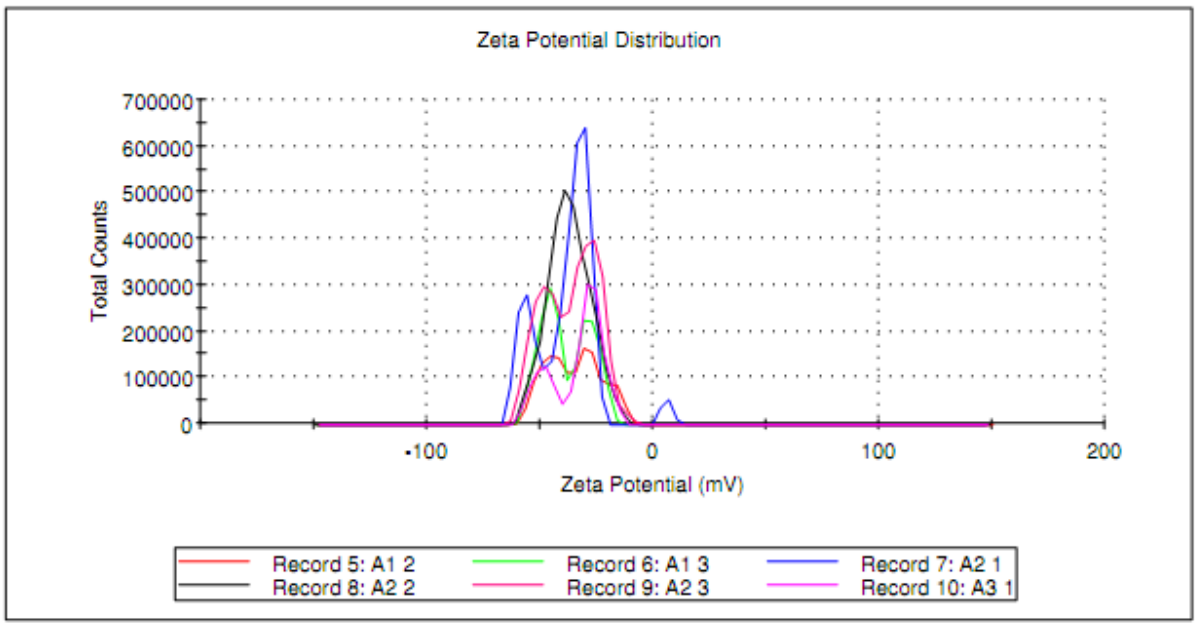

Zeta Potential Report

v2.2

Malvern

Sample Details

Sample Name: B3 2

SOP Name: mansettings.nano

General Notes:

File Name: Salinity.dts

Record Number: 20

Date and Time: Thursday, October 11, 2012 2:05:...

Dispersant Name: Adam - water-1ppt

Dispersant RI: 1.330

Viscosity (cP): 0.8901

Dispersant Dielectric Constant: 78.5

System

Temperature (°C): 25.0

Count Rate (kcps): 175.1

Cell Description: Clear disposable zeta cell

Zeta Runs: 12

Measurement Position (mm): 2.00

Attenuator: 8

Results

		Mean (mV)	Area (%)	Width (mV)
Zeta Potential (mV): -26.1	**Peak 1:**	-26.1	100.0	5.07
Zeta Deviation (mV): 5.07	**Peak 2:**	0.00	0.0	0.00
Conductivity (mS/cm): 2.75	**Peak 3:**	0.00	0.0	0.00

Result quality : Good

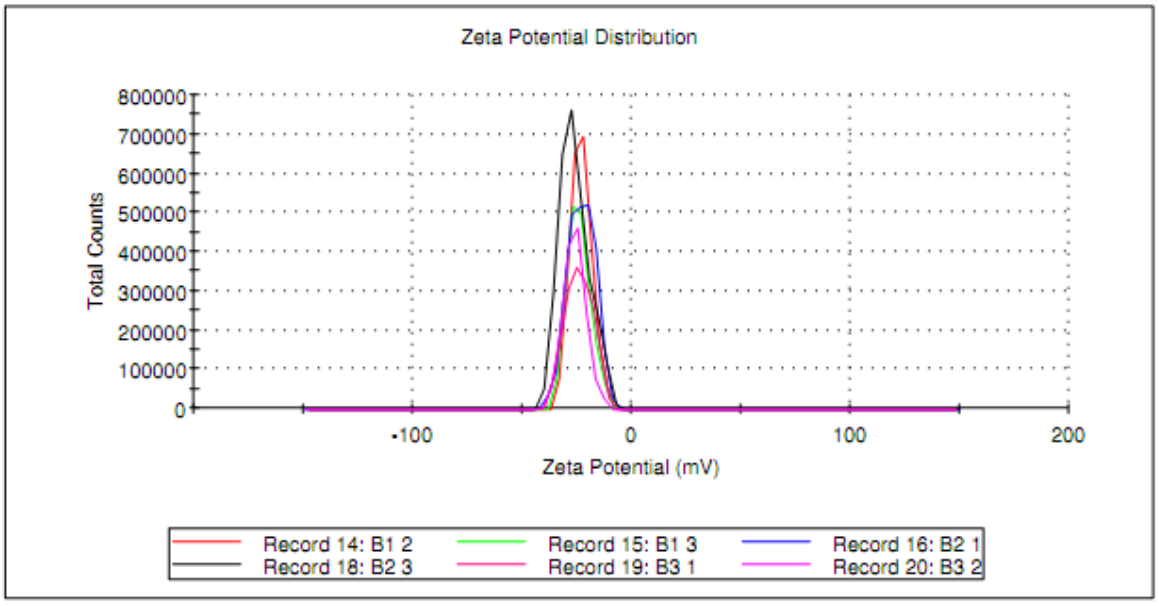

Zeta Potential Report

v2.2

Malvern

Sample Details

Sample Name: C3 2

SOP Name: mansettings.nano

General Notes:

File Name: Salinity.dts

Record Number: 29

Date and Time: Thursday, October 11, 2012 2:23:...

Dispersant Name: Adam - water-2 ppt

Dispersant RI: 1.330

Viscosity (cP): 0.8916

Dispersant Dielectric Constant: 78.5

System

Temperature (°C): 25.0

Count Rate (kcps): 204.4

Cell Description: Clear disposable zeta cell

Zeta Runs: 14

Measurement Position (mm): 2.00

Attenuator: 8

Results

		Mean (mV)	Area (%)	Width (mV)
Zeta Potential (mV): -19.2	**Peak 1:**	-19.2	100.0	8.10
Zeta Deviation (mV): 8.10	**Peak 2:**	0.00	0.0	0.00
Conductivity (mS/cm): 4.98	**Peak 3:**	0.00	0.0	0.00

Result quality : Good

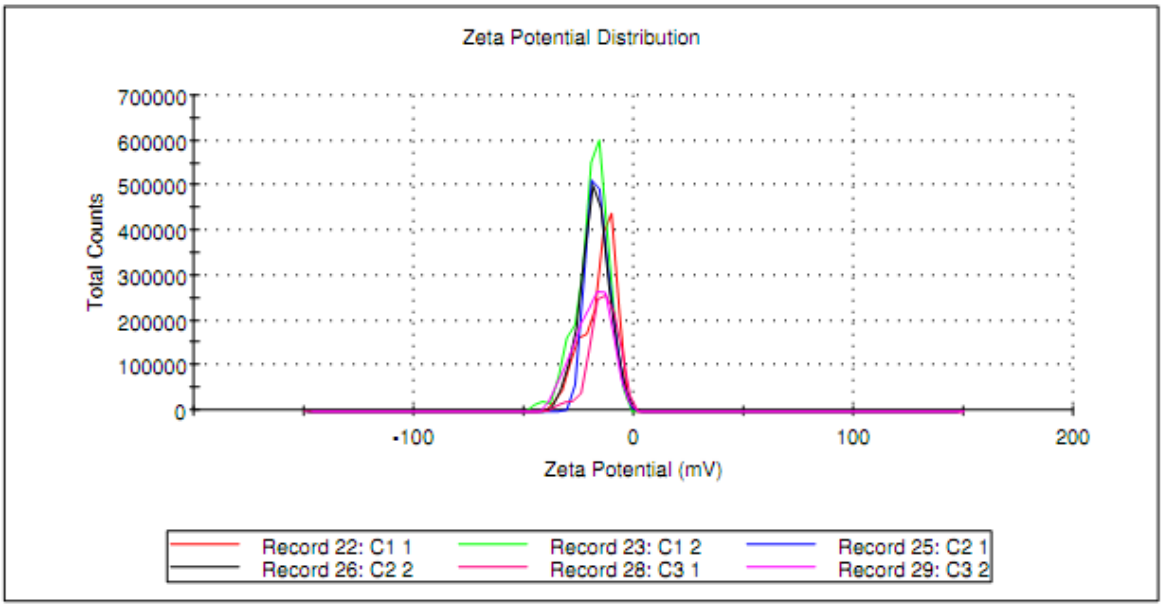

Zeta Potential Report

v2.2

Sample Details

Sample Name: D3 3

SOP Name: mansettings.nano

General Notes:

File Name:	Salinity.dts	**Dispersant Name:**	Adam - water-4ppt
Record Number:	39	**Dispersant RI:**	1.331
Date and Time:	Thursday, October 11, 2012 2:42:...	**Viscosity (cP):**	0.8947
		Dispersant Dielectric Constant:	78.5

System

Temperature (°C):	25.0	**Zeta Runs:**	14
Count Rate (kcps):	304.4	**Measurement Position (mm):**	2.00
Cell Description:	Clear disposable zeta cell	**Attenuator:**	10

Results

		Mean (mV)	**Area (%)**	**Width (mV)**
Zeta Potential (mV):	-13.9	**Peak 1:**	0.00	0.0	0.00
Zeta Deviation (mV):	0.00	**Peak 2:**	0.00	0.0	0.00
Conductivity (mS/cm):	7.39	**Peak 3:**	0.00	0.0	0.00

Result quality : Good

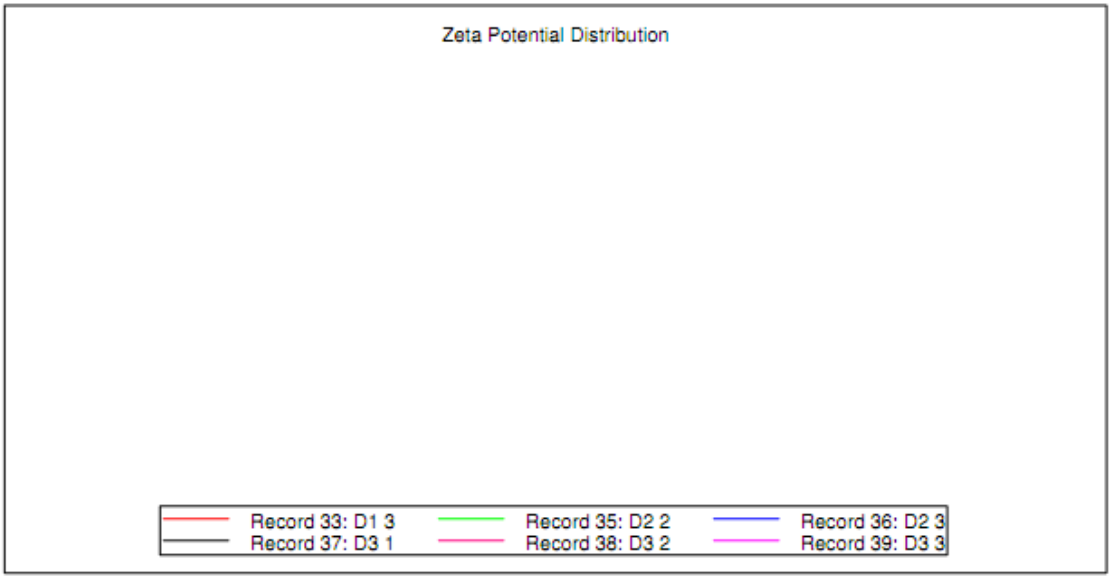

Preliminary *Nannochloris* Testing with Aluminum Plates: Flocculation Times

algae density (mg/L)	Floc (min)	arvest eff. (%)	Mass (mg)	amp	volt	time min	energy (kWh/m^3)	AL (mg/L)	energy ($/gal oil)	AL ($/gal oil)	Total ($/gal oil)
122	15	49.79	60.74	0.60	3.43	1	0.034	3.358	0.640	1.836	2.476
122	15	77.71	94.81	1.00	5.47	1	0.091	5.615	1.092	1.967	3.058
122	15	85.42	104.21	1.40	6.57	1	0.154	7.854	1.668	2.503	4.171
122	10	48.55	59.23	0.61	3.40	1	0.034	3.395	0.657	1.903	2.561
122	10	67.78	82.69	1.00	5.17	1	0.086	5.615	1.183	2.255	3.438
122	10	80.94	98.75	1.40	6.70	1	0.157	7.854	1.796	2.641	4.437
122	5	35.58	43.40	0.60	3.70	1	0.037	3.377	0.970	2.583	3.554
122	5	61.23	74.71	1.00	5.07	1	0.084	5.597	1.280	2.488	3.767
122	5	82.12	100.19	1.40	7.07	1	0.165	7.854	1.868	2.603	4.471
122	0	26.79	32.69	0.60	3.57	1	0.036	3.358	1.235	3.411	4.646
122	0	39.88	48.65	1.00	5.13	1	0.086	5.597	1.991	3.820	5.811
122	0	60.84	74.22	1.40	6.50	1	0.152	7.854	2.319	3.514	5.833

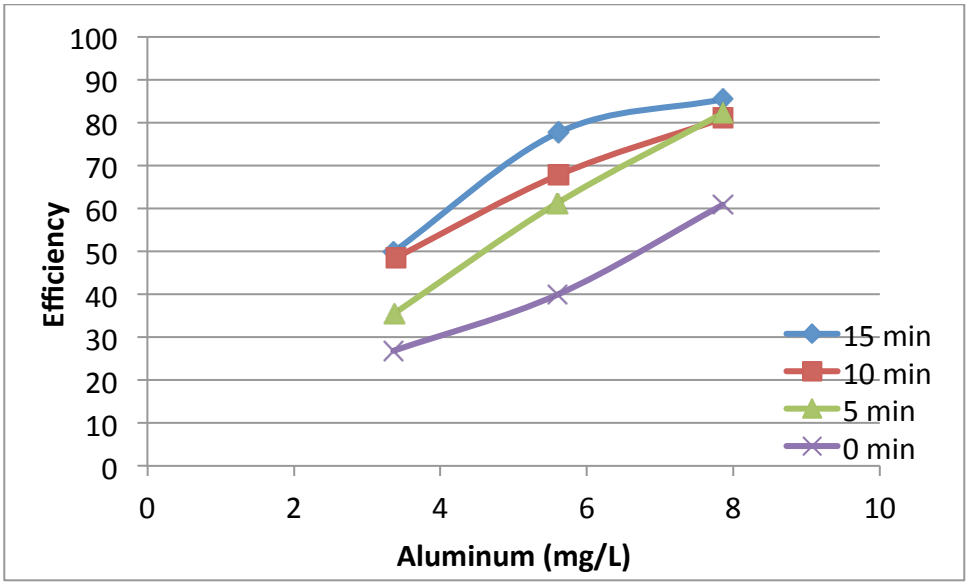

Figure C1: Harvesting efficiency of *Nannochloris* with aluminum plates in comparison to flocculation times

Preliminary *Nannochloris* Testing with Aluminum Plates: Charge Density Variation

algae density (mg/L)	harvest eff. (%)	Std Dev	Mass (mg)	amp	volt	time min	energy kwh/m^3	AL (mg/L)	energy ($/gal oil)	AL ($/gal oil)	Total ($/gal oil)
123	59.4	6.6	73.0	0.15	1.90	4	0.019	3.358	0.295	1.527	1.821
123	73.7	3.0	90.6	0.25	2.53	4	0.042	5.522	0.520	2.023	2.544
123	77.2	7.5	94.9	0.35	3.17	4	0.073	7.761	0.873	2.715	3.588
123	65.5	5.6	80.5	0.30	2.87	2	0.028	3.321	0.398	1.369	1.768
123	74.6	0.5	91.8	0.51	4.03	2	0.068	5.671	0.840	2.052	2.892
123	82.8	6.1	101.8	0.70	4.73	2	0.110	7.798	1.222	2.543	3.764
123	71.7	5.6	88.2	0.61	4.20	1	0.042	3.395	0.545	1.279	1.824
123	80.4	2.1	98.9	1.01	6.50	1	0.109	5.653	1.252	1.897	3.149
123	81.4	2.7	100.1	1.40	8.30	1	0.194	7.835	2.190	2.599	4.790
123	66.5	7.4	81.8	1.20	7.23	0.5	0.072	3.358	1.001	1.363	2.363
123	74.2	3.1	91.3	2.00	11.00	0.5	0.184	5.606	2.276	2.038	4.315
123	81.2	2.9	99.9	2.80	15.50	0.5	0.362	7.845	4.104	2.608	6.712

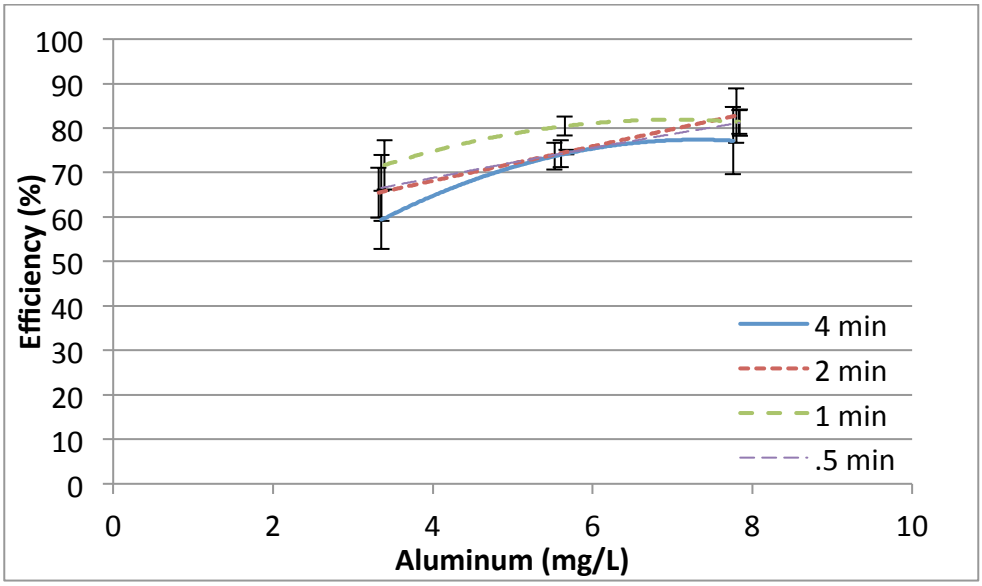

Figure C2: Harvesting efficiency of *Nannochloris* with aluminum plates in comparison to various charge densities

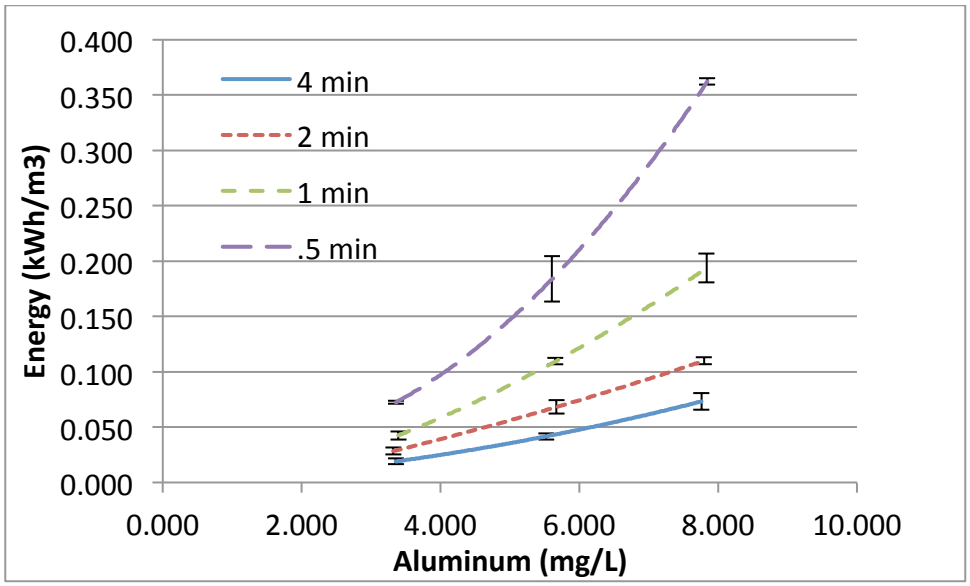

Figure C3: The energy requirements of various charge densities across aluminum plates

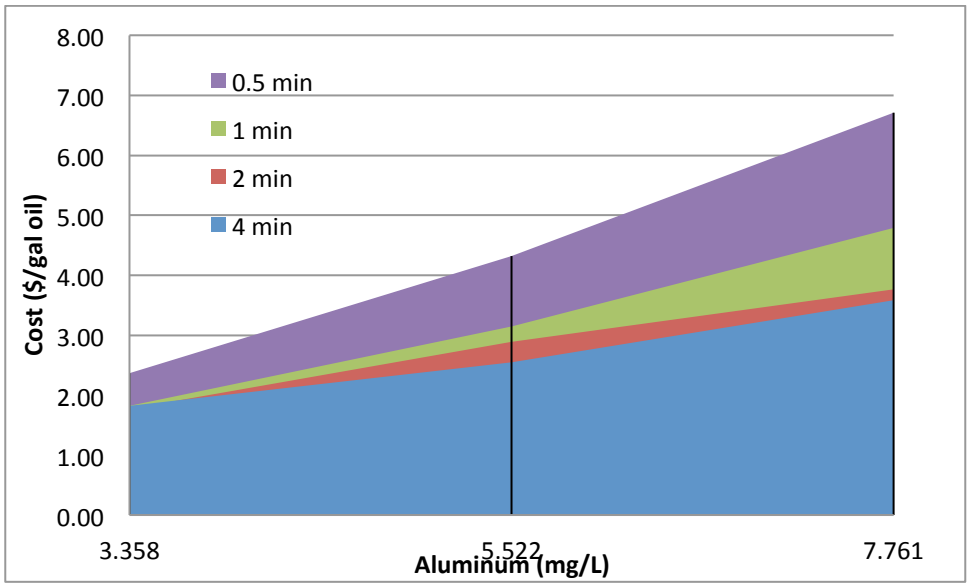

Figure C4: The cost per gal of oil for harvesting *Nannochloris* with aluminum plates under various charge densities

Preliminary *Dunaliella* Testing with Aluminum Plates: Flocculation Time

algae density (mg/L)	Floc (min)	harvest eff. (%)	Std. Dev. (%)	Mass (mg)	amp	volt	energy kwh/m^3	AL (mg/L)	energy ($/gal oil)	AL ($/gal oil)	Total ($/gal oil)
98.3	15	70.5	3.0	69.3	0.60	3.17	0.032	3.377	0.520	1.617	2.137
98.3	15	84.9	1.7	83.5	1.01	3.73	0.063	5.634	0.849	2.241	3.091
98.3	15	94.8	1.2	93.2	1.40	4.97	0.116	7.854	1.410	2.797	4.207
98.3	10	53.7	7.9	52.8	0.60	2.97	0.030	3.358	0.636	2.113	2.749
98.3	10	68.5	5.5	67.4	1.00	3.73	0.062	5.578	1.042	2.748	3.790
98.3	10	80.4	4.6	79.0	1.40	4.77	0.111	7.835	1.593	3.291	4.884
98.3	5	23.5	7.3	23.1	0.60	2.77	0.028	3.358	1.355	4.822	6.177
98.3	5	57.4	8.6	8.6	1.00	3.87	0.064	5.597	1.293	3.294	4.587
98.3	5	68.6	8.6	67.5	1.40	4.50	0.105	7.835	1.762	3.857	5.619
98.3	0	0.0	0.0	0.0	0.60	2.83	0.028	3.358	0.000	0.000	0.000
98.3	0	9.6	0.9	9.4	1.00	3.67	0.061	5.615	7.382	19.830	27.211
98.3	0	24.6	7.7	24.1	1.40	4.57	0.107	7.835	4.995	10.775	15.770

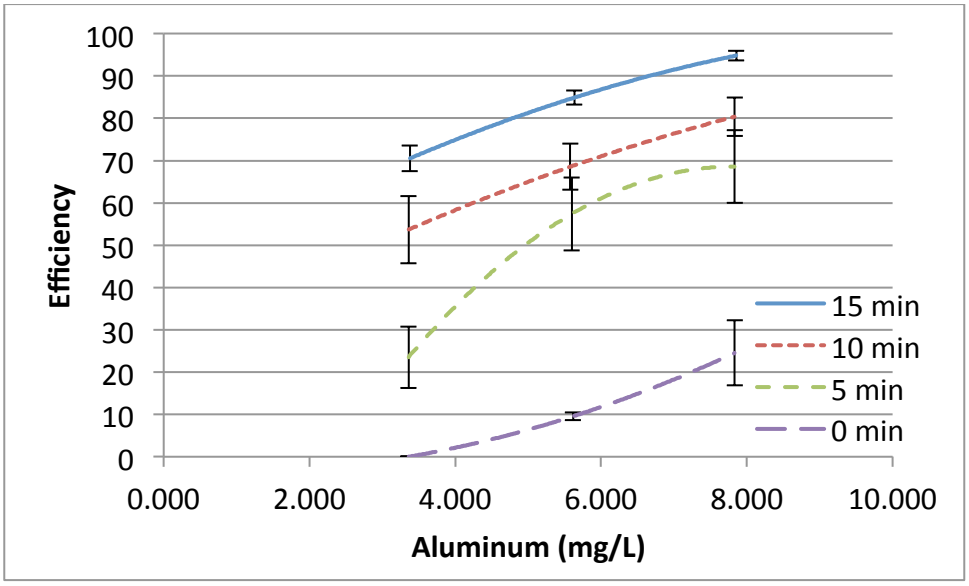

Figure C5: Harvest efficiency of *Dunaliella* with aluminum plates with various flocculation times

Preliminary *Dunaliella* Testing with Aluminum Plates: Charge Density Variation

algae density (mg/L)	Harvest eff. (%)	Std. Dev (%)	Mass (mg)	amp	volt	time min.	energy kwh/m^3	AL mg/L	energy ($/gal oil)	AL ($/gal oil)	Total ($/gal oil)
99	54.6	4.0	54.1	1.20	4.10	0.5	0.041	3.367	0.860	1.597	2.458
99	84.0	4.7	83.1	2.00	5.90	0.5	0.098	5.597	1.339	1.727	3.066
99	87.4	2.2	86.5	2.81	7.87	0.5	0.184	7.854	2.408	2.330	4.737
99	0.0	0.0	0.0	0.00	0.00	1	0.000	0.000	0.000	0.000	0.000
99	5.7	1.6	5.7	0.21	2.13	1	0.008	1.194	1.515	5.405	6.919
99	60.4	2.9	59.8	0.60	2.95	1	0.030	3.358	0.558	1.441	1.999
99	76.7	3.6	75.9	1.00	3.70	1	0.062	5.597	0.919	1.891	2.811
99	88.7	2.6	87.8	1.40	4.63	1	0.108	7.817	1.391	2.285	3.675
99	4.7	3.4	4.7	0.11	1.33	2	0.005	1.269	1.220	6.963	8.182
99	66.5	1.3	65.8	0.30	1.90	2	0.019	3.321	0.323	1.295	1.618
99	79.3	4.7	78.5	0.50	2.40	2	0.040	5.597	0.577	1.830	2.407
99	87.8	3.7	87.0	0.71	3.13	2	0.074	7.910	0.961	2.334	3.295
99	38.5	7.5	38.2	0.12	1.30	5	0.013	3.265	0.375	2.195	2.570
99	72.1	3.0	71.4	0.20	1.50	5	0.025	5.503	0.390	1.977	2.367
99	73.1	1.0	72.3	0.28	1.90	5	0.044	7.835	0.694	2.780	3.474
99	43.2	3.7	42.7	0.06	1.10	10	0.011	3.358	0.291	2.016	2.307
99	57.9	3.5	57.3	0.10	1.17	10	0.019	5.597	0.384	2.504	2.888
99	81.9	4.7	81.1	0.14	1.37	10	0.032	7.835	0.445	2.479	2.924
99	13.6	12.3	13.5			1		2.35			8.571
99	74.3	17.3	73.6			1		4.7			3.141
99	83.6	7.7	82.8			1		7.05			4.187

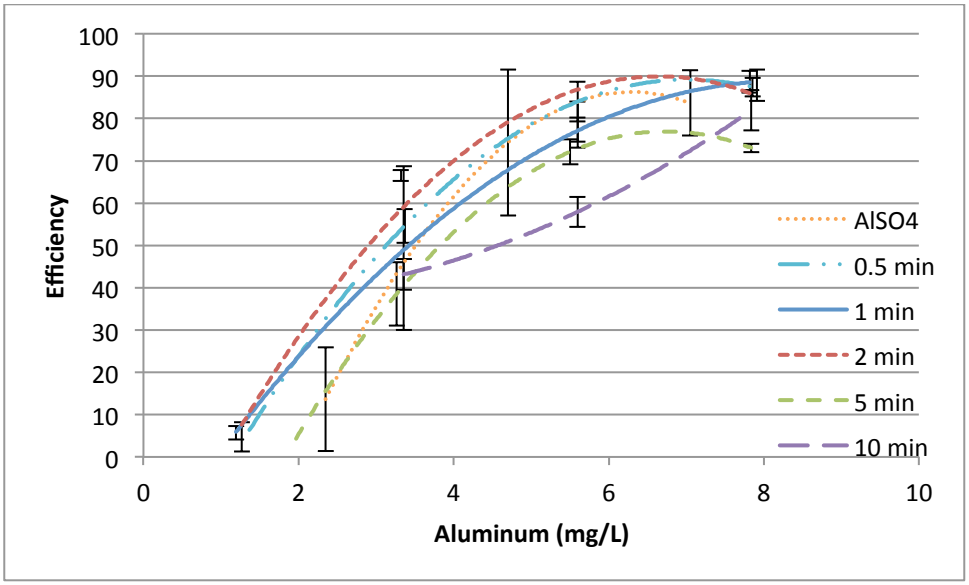

Figure C6: Harvest efficiency of *Dunaliella* with aluminum plates under various charge densities

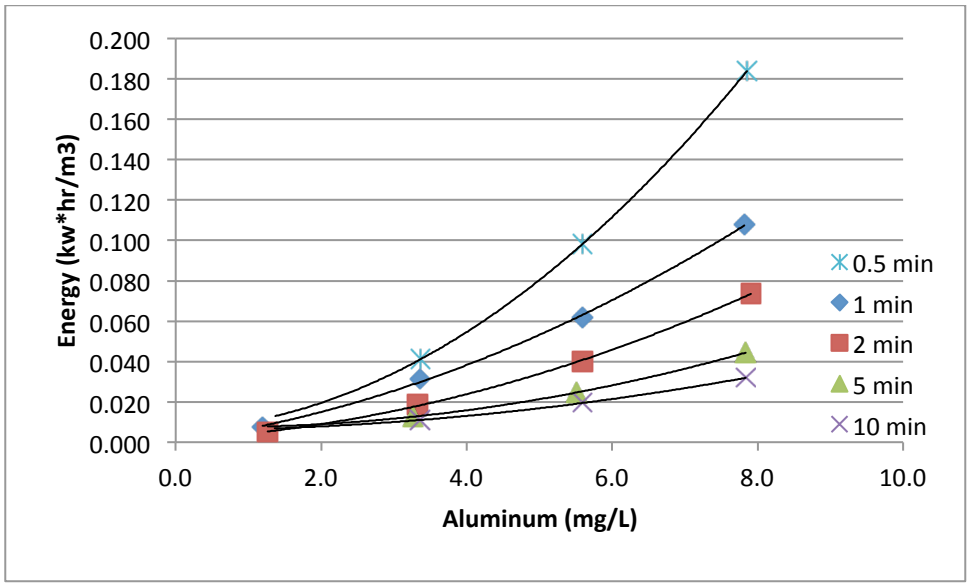

Figure C7: The energy requirements of various charge densities across aluminum plates

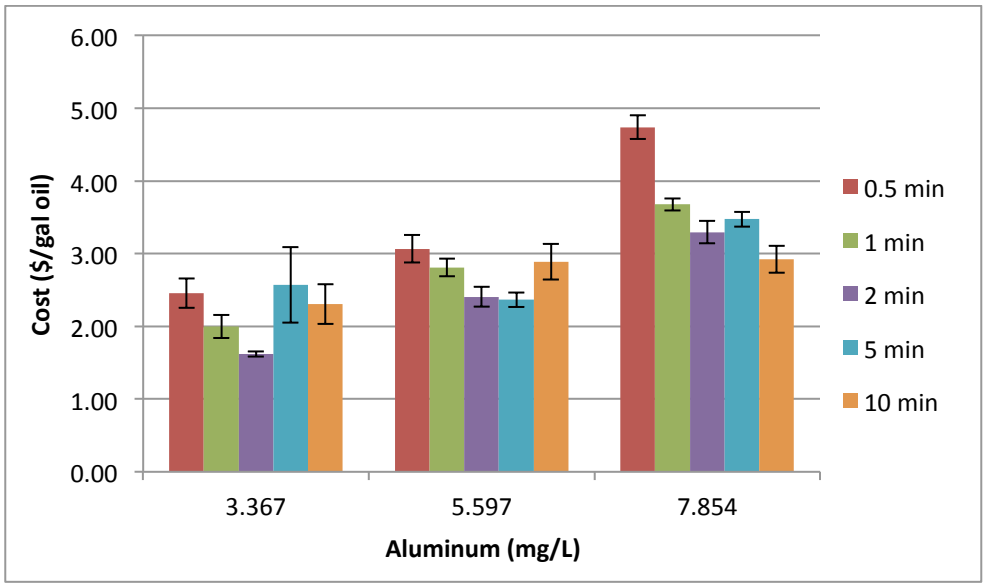

Figure C8: The cost per gal of oil for harvesting *Dunaliella* with aluminum plates under various charge densities

Raw data for *Nannochloris* cultured in 2 ppt
Perforated Iron Plates; 15 min flocculation, 30 min settle

	a1	a2	a3	AVG	Std Dev	95% C.I.
abs1	0.21	0.207	0.195	0.204	0.0079	0.0090
abs2	0.185	0.182	0.17	0.179	0.0079	0.0090
Efficiency	11.90	12.08	12.82	12.268	0.4866	0.5506
	b1	**b2**	**b3**	**AVG**	**Std Dev**	**95% C.I.**
amp	0.1	0.1	0.1	0.100	0.0000	0.0000
volt	0.6	0.7	0.6	0.633	0.0577	0.0653
abs1	0.209	0.207	0.2	0.205	0.0047	0.0053
abs2	0.109	0.087	0.101	0.099	0.0111	0.0126
Efficiency (%)	47.85	57.97	49.50	51.773	5.4312	6.1459
Energy (kWh/m3)	0.0010	0.0012	0.0010	0.001	0.0001	0.0001
Iron (mg/L)	1.741	1.741	1.741	1.741	0.0000	#NUM!
Energy ($/L oil)	0.005	0.005	0.005	0.005	0.0001	0.0001
Fe. ($/L oil)	0.014	0.011	0.013	0.013	0.0013	0.0015
Total Cost	0.019	0.017	0.019	0.018	0.0014	0.0015
	d1	**d2**	**d3**	**AVG**	**Std Dev**	**95% C.I.**
amp	0.2	0.2	0.2	0.200	0.0000	0.0000
volt	1	1	0.9	0.967	0.0577	0.0653
abs1	0.213	0.194	0.197	0.201	0.0102	0.0116
abs2	0.1	0.088	0.097	0.095	0.0062	0.0071
Efficiency (%)	53.05	54.64	50.76	52.817	1.9495	2.2060
Energy (kWh/m3)	0.0033	0.0033	0.0030	0.003	0.0002	0.0002
Iron (mg/L)	3.482	3.482	3.482	3.482	0.0000	#NUM!
Energy ($/L oil)	0.016	0.016	0.015	0.016	0.0005	0.0005
Fe. ($/L oil)	0.025	0.024	0.026	0.025	0.0009	0.0011
Total Cost	0.041	0.040	0.042	0.041	0.0007	0.0008
	f1	**f2**	**f3**	**AVG**	**Std Dev**	**95% C.I.**
amp	0.3	0.3	0.3	0.300	0.0000	#NUM!
volt	1.5	1.3	1.3	1.367	0.1155	0.1307
abs1	0.207	0.221	0.217	0.215	0.0072	0.0082
abs2	0.084	0.091	0.079	0.085	0.0060	0.0068
Efficiency (%)	59.42	58.82	63.59	60.613	2.5994	2.9415
Energy (kWh/m3)	0.0075	0.0065	0.0065	0.007	0.0006	0.0007
Iron (mg/L)	5.224	5.224	5.224	5.224	0.0000	#NUM!
Energy ($/L oil)	0.033	0.029	0.027	0.029	0.0032	0.0036
Fe. ($/L oil)	0.034	0.034	0.031	0.033	0.0014	0.0016
Total Cost	0.066	0.063	0.058	0.062	0.0042	0.0048

Raw data for *Nannochloris* cultured in 2 ppt
Perforated Aluminum Plates; 15 min flocculation, 30 min settle

	a1	a2	a3	AVG	Std Dev	95% C.I.
abs1	0.21	0.207	0.195	0.204	0.0079	0.0090
abs2	0.185	0.182	0.17	0.179	0.0079	0.0090
Efficiency (%)	11.90	12.08	12.82	12.268	0.4866	0.5506
	c1	**c2**	**c3**	**AVG**	**Std Dev**	**95% C.I.**
amp	0.2	0.2	0.2	0.200	0.0000	0.0000
volt	2.5	2.3	2.2	2.333	0.1528	0.1729
abs1	0.206	0.211	0.218	0.212	0.0060	0.0068
abs2	0.135	0.122	0.137	0.131	0.0081	0.0092
Efficiency (%)	34.47	42.18	37.16	37.934	3.9155	4.4307
Energy (kWh/m3)	0.0083	0.0077	0.0073	0.008	0.0005	0.0006
Al (mg/L)	1.119	1.119	1.119	1.119	0.0000	#NUM!
Energy ($/L oil)	0.063	0.047	0.051	0.054	0.0081	0.0092
Al ($/L oil)	0.205	0.168	0.190	0.188	0.0189	0.0214
Total Cost	0.268	0.215	0.242	0.242	0.0266	0.0301
	e1	**e2**	**e3**	**AVG**	**Std Dev**	**95% C.I.**
amp	0.6	0.6	0.6	0.600	0.0000	#NUM!
volt	3.5	3.7	3.4	3.533	0.1528	0.1729
abs1	0.217	0.203	0.218	0.213	0.0084	0.0095
abs2	0.062	0.05	0.047	0.053	0.0079	0.0090
Efficiency (%)	71.43	75.37	78.44	75.079	3.5149	3.9774
Energy (kWh/m3)	0.0350	0.0370	0.0340	0.035	0.0015	0.0017
Al (mg/L)	3.358	3.358	3.358	3.358	0.0000	0.0000
Energy ($/L oil)	0.127	0.128	0.113	0.123	0.0086	0.0097
Al ($/L oil)	0.297	0.282	0.271	0.283	0.0133	0.0151
Total Cost	0.425	0.409	0.383	0.406	0.0209	0.0236
	f1	**f2**	**f3**	**AVG**	**Std Dev**	**95% C.I.**
amp	1	1	1	1.000	0.0000	#NUM!
volt	5.4	4.8	5	5.067	0.3055	0.3457
abs1	0.201	0.222	0.219	0.214	0.0114	0.0129
abs2	0.058	0.058	0.022	0.046	0.0208	0.0235
Efficiency (%)	71.14	73.87	89.95	78.324	10.1641	11.5015
Energy (kWh/m3)	0.0900	0.0800	0.0833	0.084	0.0051	0.0058
Al (mg/L)	5.597	5.597	5.597	5.597	0.0000	#NUM!
Energy ($/L oil)	0.329	0.282	0.241	0.284	0.0441	0.0499
Al ($/L oil)	0.497	0.479	0.393	0.456	0.0555	0.0628
Total Cost	0.826	0.760	0.634	0.740	0.0976	0.1104

Raw data for *Nannochloris* cultured in 2 ppt
Perforated Iron Plates; 15 min flocculation, 30 min settle

	a1	a2	a3	AVG	Std Dev	95% C.I.
abs1	0.21	0.207	0.195	0.204	0.0079	0.0090
abs2	0.185	0.182	0.17	0.179	0.0079	0.0090
Efficiency	11.90	12.08	12.82	12.268	0.4866	0.5506
	h1	**h2**	**h3**	**AVG**	**Std Dev**	**95% C.I.**
amp	0.05	0.05	0.05	0.050	0.0000	0.0000
volt	0.3	0.3	0.3	0.300	0.0000	#NUM!
abs1	0.224	0.23	0.214	0.223	0.0081	0.0091
abs2	0.067	0.077	0.085	0.076	0.0090	0.0102
Efficiency (%)	70.09	66.52	60.28	65.630	4.9648	5.6181
Energy (kWh/m3)	0.0005	0.0005	0.0005	0.0005	0.0000	#NUM!
Iron (mg/L)	1.741	1.741	1.741	1.741	0.0000	#NUM!
Energy ($/L oil)	0.002	0.002	0.003	0.002	0.0002	0.0002
Fe. ($/L oil)	0.009	0.010	0.011	0.010	0.0008	0.0009
Total Cost	0.012	0.012	0.014	0.013	0.0010	0.0011
	j1	**j2**	**j3**	**AVG**	**Std Dev**	**95% C.I.**
amp	0.1	0.1	0.1	0.100	0.0000	0.0000
volt	0.6	0.7	0.5	0.600	0.1000	0.1132
abs1	0.204	0.224	0.219	0.216	0.0104	0.0118
abs2	0.088	0.086	0.099	0.091	0.0070	0.0079
Efficiency (%)	56.86	61.61	54.79	57.755	3.4928	3.9524
Energy (kWh/m3)	0.0020	0.0023	0.0017	0.002	0.0003	0.0004
Iron (mg/L)	3.482	3.482	3.482	3.482	0.0000	#NUM!
Energy ($/L oil)	0.011	0.012	0.009	0.011	0.0012	0.0013
Fe. ($/L oil)	0.023	0.022	0.024	0.023	0.0014	0.0015
Total Cost	0.034	0.033	0.034	0.034	0.0005	0.0006
	m1	**m2**	**m3**	**AVG**	**Std Dev**	**95% C.I.**
amp	0.15	0.15	0.15	0.150	0.0000	#NUM!
volt	1	0.8	0.8	0.867	0.1155	0.1307
abs1	0.227	0.211	0.217	0.218	0.0081	0.0091
abs2	0.086	0.082	0.108	0.092	0.0140	0.0158
Efficiency (%)	62.11	61.14	50.23	57.827	6.5974	7.4655
Energy (kWh/m3)	0.0050	0.0040	0.0040	0.004	0.0006	0.0007
Iron (mg/L)	5.224	5.224	5.224	5.224	0.0000	#NUM!
Energy ($/L oil)	0.025	0.020	0.025	0.023	0.0026	0.0030
Fe. ($/L oil)	0.032	0.033	0.040	0.035	0.0042	0.0048
Total Cost	0.057	0.053	0.064	0.058	0.0058	0.0066

Raw data for *Nannochloris* cultured in 2 ppt
Perforated Aluminum Plates; 15 min flocculation, 30 min settle

	a1	a2	a3	AVG	Std Dev	95% C.I.
abs1	0.21	0.207	0.195	0.204	0.0079	0.0090
abs2	0.185	0.182	0.17	0.179	0.0079	0.0090
Efficiency	11.90	12.08	12.82	12.268	0.4866	0.5506
	i1	**i2**	**i3**	**AVG**	**Std Dev**	**95% C.I.**
amp	0.1	0.1	0.1	0.100	0.0000	0.0000
volt	1.6	1.3	1.4	1.433	0.1528	0.1729
abs1	0.211	0.228	0.226	0.222	0.0093	0.0105
abs2	0.134	0.119	0.133	0.129	0.0084	0.0095
Efficiency (%)	36.49	47.81	41.15	41.817	5.6864	6.4347
Energy (kWh/m3)	0.0053	0.0043	0.0047	0.005	0.0005	0.0006
Al (mg/L)	1.119	1.119	1.119	1.119	0.0000	#NUM!
Energy ($/L oil)	0.038	0.024	0.029	0.030	0.0073	0.0082
Al ($/L oil)	0.194	0.148	0.172	0.171	0.0229	0.0260
Total Cost	0.232	0.172	0.201	0.202	0.0302	0.0341
	k1	**k2**	**k3**	**AVG**	**Std Dev**	**95% C.I.**
amp	0.3	0.3	0.3	0.300	0.0000	#NUM!
volt	2.4	2.2	2	2.200	0.2000	0.2263
abs1	0.224	0.216	0.212	0.217	0.0061	0.0069
abs2	0.042	0.031	0.064	0.046	0.0168	0.0190
Efficiency (%)	81.25	85.65	69.81	78.903	8.1751	9.2508
Energy (kWh/m3)	0.0240	0.0220	0.0200	0.022	0.0020	0.0023
Al (mg/L)	3.358	3.358	3.358	3.358	0.0000	0.0000
Energy ($/L oil)	0.077	0.067	0.075	0.073	0.0052	0.0059
Al ($/L oil)	0.261	0.248	0.304	0.271	0.0294	0.0332
Total Cost	0.338	0.315	0.378	0.344	0.0323	0.0366
	n1	**n2**	**n3**	**AVG**	**Std Dev**	**95% C.I.**
amp	0.5	0.5	0.5	0.500	0.0000	#NUM!
volt	3	2.8	2.7	2.833	0.1528	0.1729
abs1	0.222	0.225	0.215	0.221	0.0051	0.0058
abs2	0.043	0.054	0.049	0.049	0.0055	0.0062
Efficiency (%)	80.63	76.00	77.21	77.947	2.4018	2.7178
Energy (kWh/m3)	0.0500	0.0467	0.0450	0.047	0.0025	0.0029
Al (mg/L)	5.597	5.597	5.597	5.597	0.0000	#NUM!
Energy ($/L oil)	0.161	0.160	0.152	0.158	0.0052	0.0059
Al ($/L oil)	0.439	0.465	0.458	0.454	0.0138	0.0156
Total Cost	0.600	0.625	0.610	0.612	0.0127	0.0143

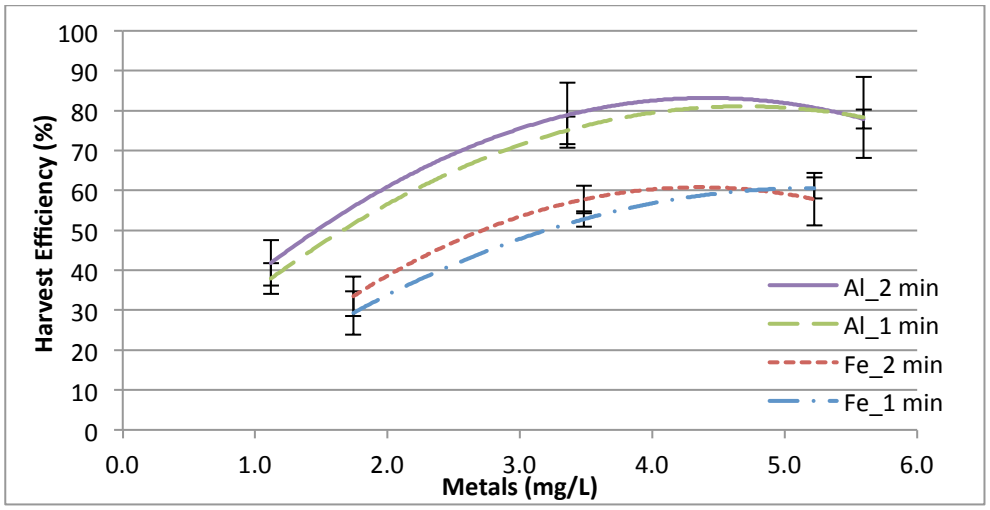

Figure 3.6 The harvest efficiency of *Nannochloris sp.* under various charge densities producing similar concentrations of aluminum and iron from the electrodes

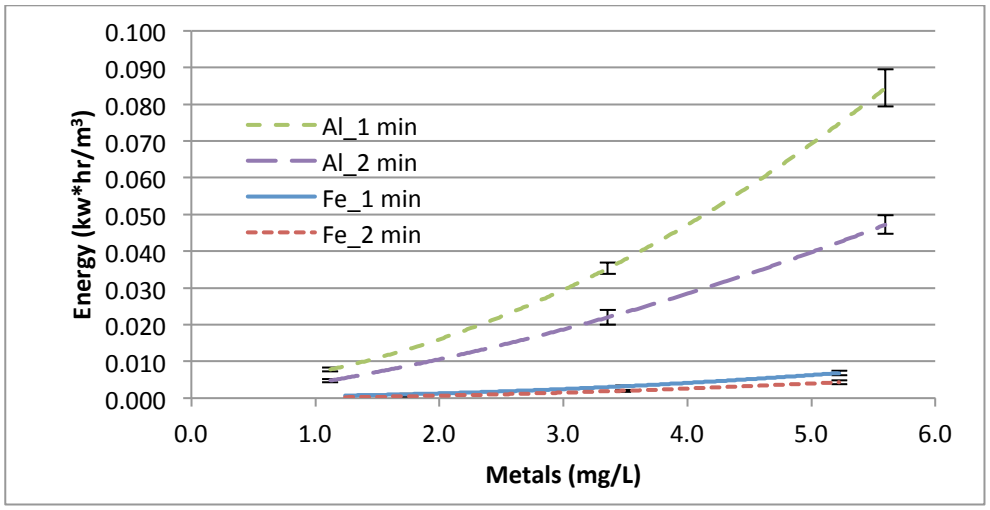

Figure 3.7 The energy requirements to produce aluminum and iron ions under various charge densities

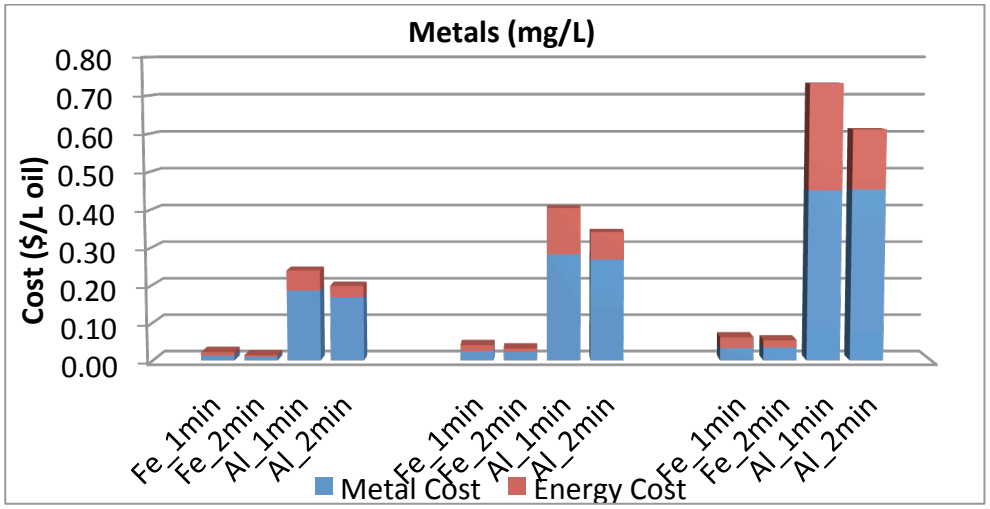

Figure 3.8 The cost (electrode and energy) per L of oil as a function of the *Nannochloris sp.* harvesting efficiencies by aluminum and iron electrodes under multiple charge densities

Raw data for Perforated Iron Plates

Dunaliella, 15 min flocculation, 30 min settle

	a1	a2	a3	AVG	Std Dev	95% C.I.
abs1	0.22	0.231	0.237	0.229	0.0086	0.0098
abs2	0.209	0.225	0.222	0.219	0.0085	0.0096
Efficiency	5.00	2.60	6.33	4.642	1.8914	2.1403
	b1	**b2**	**b3**	**AVG**	**Std Dev**	**95% C.I.**
amp	0.05	0.05	0.04	0.047	0.0058	0.0065
volt	0.5	0.3	0.2	0.333	0.1528	0.1729
abs1	0.223	0.212	0.223	0.219	0.0064	0.0072
abs2	0.094	0.101	0.101	0.099	0.0040	0.0046
Efficiency (%)	57.85	52.36	54.71	54.972	2.7540	3.1163
Energy (kWh/m3)	0.0008	0.0005	0.0003	0.0005	0.0003	0.0003
Iron (mg/L)	1.741	1.741	1.393	1.625	0.2011	0.2275
Energy ($/L oil)	0.003	0.002	0.001	0.002	0.0009	0.0010
Fe. ($/L oil)	0.008	0.009	0.007	0.008	0.0011	0.0012
Total Cost	0.011	0.011	0.008	0.010	0.0018	0.0020
	d1	**d2**	**d3**	**AVG**	**Std Dev**	**95% C.I.**
amp	0.1	0.09	0.09	0.093	0.0058	0.0065
volt	0.5	0.4	0.3	0.400	0.1000	0.1132
abs1	0.222	0.218	0.21	0.217	0.0061	0.0069
abs2	0.107	0.105	0.116	0.109	0.0059	0.0066
Efficiency (%)	51.80	51.83	44.76	49.466	4.0741	4.6102
Energy (kWh/m3)	0.0017	0.0012	0.0009	0.001	0.0004	0.0004
Iron (mg/L)	3.482	3.134	3.134	3.250	0.2011	0.2275
Energy ($/L oil)	0.006	0.004	0.004	0.005	0.0012	0.0013
Fe. ($/L oil)	0.018	0.017	0.019	0.018	0.0013	0.0015
Total Cost	0.024	0.021	0.023	0.023	0.0018	0.0020
	f1	**f2**	**f3**	**AVG**	**Std Dev**	**95% C.I.**
amp	0.15	0.14	0.15	0.147	0.0058	0.0065
volt	0.7	0.6	0.6	0.633	0.0577	0.0653
abs1	0.22	0.224	0.21	0.218	0.0072	0.0082
abs2	0.114	0.094	0.084	0.097	0.0153	0.0173
Efficiency (%)	48.18	58.04	60.00	55.406	6.3328	7.1661
Energy (kWh/m3)	0.0035	0.0028	0.0030	0.003	0.0004	0.0004
Iron (mg/L)	5.224	4.875	5.224	5.108	0.2011	0.2275
Energy ($/L oil)	0.014	0.009	0.009	0.011	0.0025	0.0029
Fe. ($/L oil)	0.030	0.023	0.024	0.026	0.0036	0.0041
Total Cost	0.043	0.032	0.033	0.036	0.0062	0.0070

Raw data for Perforated Aluminum Plates

Dunaliella, 15 min flocculation, 30 min settle

	a1	a2	a3	AVG	Std Dev	95% C.I.
abs1	0.22	0.231	0.237	0.229	0.0086	0.0098
abs2	0.209	0.225	0.222	0.219	0.0085	0.0096
Efficiency	5.00	2.60	6.33	4.642	1.8914	2.1403
	c1	**c2**	**c3**	**AVG**	**Std Dev**	**95% C.I.**
amp	0.1	0.1	0.11	0.103	0.0058	0.0065
volt	1.6	1.2	1.3	1.367	0.2082	0.2356
abs1	0.236	0.234	0.222	0.231	0.0076	0.0086
abs2	0.106	0.096	0.112	0.105	0.0081	0.0091
Efficiency (%)	55.08	58.97	49.55	54.536	4.7363	5.3595
Energy (kWh/m3)	0.0053	0.0040	0.0048	0.005	0.0007	0.0008
Al (mg/L)	1.119	1.119	1.231	1.157	0.0646	0.0731
Energy ($/L oil)	0.018	0.013	0.018	0.016	0.0031	0.0035
Al ($/L oil)	0.086	0.080	0.105	0.091	0.0130	0.0147
Total Cost	0.104	0.093	0.123	0.107	0.0153	0.0173
	e1	**e2**	**e3**	**AVG**	**Std Dev**	**95% C.I.**
amp	0.3	0.31	0.31	0.307	0.0058	0.0065
volt	1.6	1.7	1.6	1.633	0.0577	0.0653
abs1	0.206	0.23	0.216	0.217	0.0121	0.0136
abs2	0.042	0.046	0.046	0.045	0.0023	0.0026
Efficiency (%)	79.61	80.00	78.70	79.438	0.6653	0.7528
Energy (kWh/m3)	0.0160	0.0176	0.0165	0.017	0.0008	0.0009
Al (mg/L)	3.358	3.470	3.470	3.433	0.0646	0.0731
Energy ($/L oil)	0.038	0.041	0.039	0.039	0.0017	0.0020
Al ($/L oil)	0.179	0.184	0.187	0.183	0.0041	0.0046
Total Cost	0.216	0.225	0.226	0.222	0.0053	0.0060
	g1	**g2**	**g3**	**AVG**	**Std Dev**	**95% C.I.**
amp	0.5	0.5	0.5	0.500	0.0000	#NUM!
volt	2.2	2	2	2.067	0.1155	0.1307
abs1	0.205	0.222	0.22	0.216	0.0093	0.0105
abs2	0.035	0.033	0.041	0.036	0.0042	0.0047
Efficiency (%)	82.93	85.14	81.36	83.142	1.8949	2.1443
Energy (kWh/m3)	0.0367	0.0333	0.0333	0.034	0.0019	0.0022
Al (mg/L)	5.597	5.597	5.597	5.597	0.0000	#NUM!
Energy ($/L oil)	0.083	0.073	0.077	0.077	0.0048	0.0054
Al ($/L oil)	0.286	0.279	0.291	0.285	0.0065	0.0073
Total Cost	0.369	0.352	0.368	0.363	0.0096	0.0108

Graphs for *Dunaliella* Electrocoagulation Tests

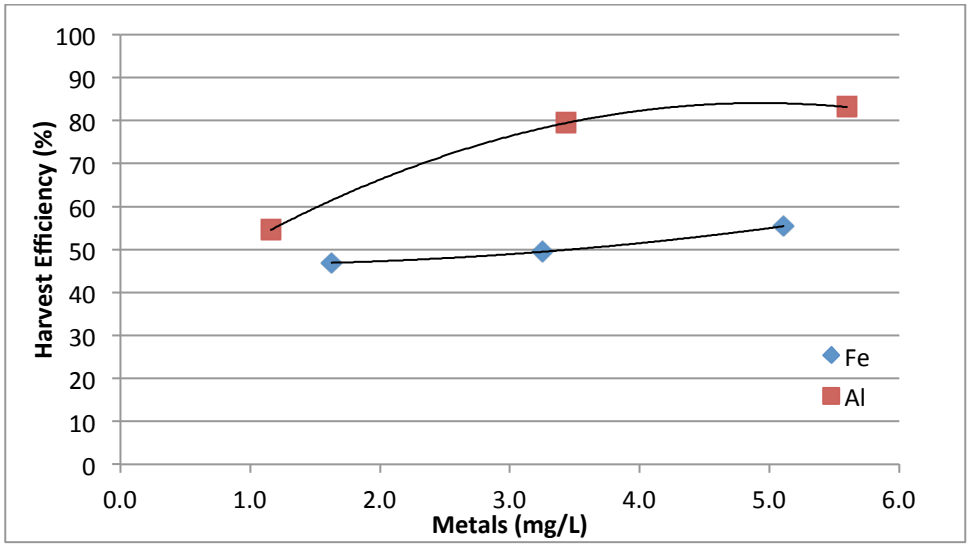

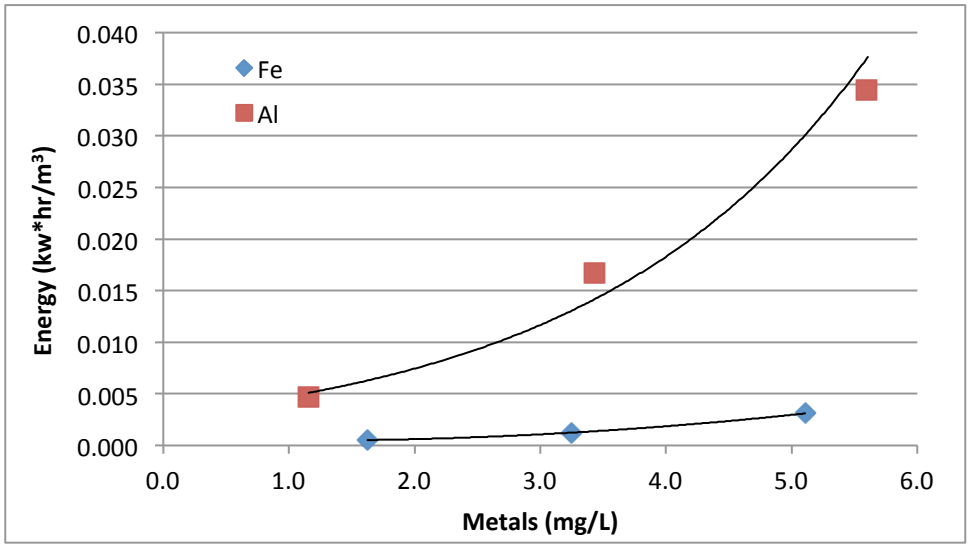

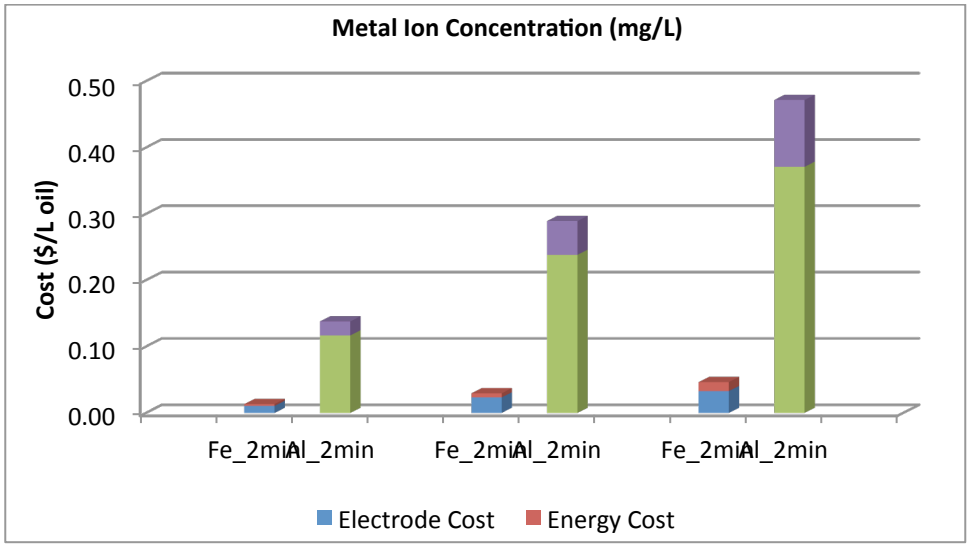

Figure 3.9 The cost per L of oil as a function of the *Dunaliella sp.* harvesting efficiencies by aluminum and iron electrodes under multiple charge densities

Appendix D: Continuous Full Scale Setup with Nannochloris and Economic Analysis on Electrocoagulation, Dissolved Air Flotation, and Centrifugation Energy Usage

Raw data for full scale setup using *Nannochloris* (0.70 ppt NaCl) and 0 amps applied to EC unit

	Influent					
	A1	**B1**	**C1**	**AVG**	**Std Dev**	**95% C.I.**
Time	0	0.5	1			
Vol (mL)	30	30	30	30	0.00	
Mass 1 (g)	0.1265	0.1264	0.1289	0.1273	0.00	
Mass 2 (g)	0.1292	0.1295	0.1319	0.1302	0.00	
TSS (mg/L)	90.0	103.3	100.0	97.8	6.94	7.851
Iron (mg/L)	0.596	0.700	0.717	0.7	0.07	0.074
Iron (mg/g algae)	6.631	6.782	7.178	6.9	0.28	0.319
	Effluent					
	A2	**B2**	**C2**	**AVG**	**Std Dev**	**95% C.I.**
Time	0	0.5	1			
Vol (mL)	30	30	30	30	0.00	
Mass 1 (g)	0.1260	0.1262	0.1262	0.1261	0.00	
Mass 2 (g)	0.1286	0.1282	0.1284	0.1284	0.00	
TSS (mg/L)	86.7	66.7	73.3	75.6	10.18	11.523
Iron (mg/L)	0.14	0.066	0.248	0.2	0.09	0.103
Iron (mg/g algae)	1.568	1.000	3.386	2.0	1.25	1.410
	Floated					
	A3	**B3**	**C3**	**AVG**	**Std Dev**	**95% C.I.**
Time	0	0.5	1			
Vol (mL)	5	5	5	5	0.00	
Mass 1 (g)	0.1258	0.1258	0.1271	0.1262	0.00	
Mass 2 (g)	0.1695	0.1896	0.1914	0.1835	0.01	
TSS (g/L)	8.7	12.8	12.9	11.5	2.35	2.659
Iron (mg/L)	130.81	200.93	209.53	180.4	43.18	48.862
Corrected (mg/L)	1.35	1.63	1.63	1.5	0.16	0.183
Iron (mg/g algae)	0.154	0.127	0.126	0.1	0.02	0.017
	30 minute settle					
	G1	**G2**	**G3**	**AVG**	**Std Dev**	**95% C.I.**
Vol (mL)	30	30	30	30	0.00	
Mass 1 (g)	0.1263	0.1265	0.1268	0.1265	0.00	
Mass 2 (g)	0.1297	0.1295	0.1306	0.1299	0.00	
TSS (mg/L)	113.3	100.0	126.7	113.3	13.33	15.08781

Raw data for full scale setup using *Nannochloris* (0.70 ppt NaCl) and 0.4 amps applied to the EC unit

	Influent					
	D1	**E1**	**F1**	**AVG**	**Std Dev**	**95% C.I.**
Time	0	0.5	1			
Vol (mL)	30	30	30	30	0.00	
Mass 1 (g)	0.0950	0.0964	0.0946	0.0953	0.00	
Mass 2 (g)	0.0997	0.1008	0.0998	0.1001	0.00	
TSS (mg/L)	156.7	146.7	173.3	158.9	13.47	15.244
Iron (mg/L)		1.153	1.183	1.2	0.02	0.0295
Iron (mg/g algae)		7.862	6.827	7.345		
	Effluent					
	D2	**E2**	**F2**	**AVG**	**Std Dev**	**95% C.I.**
Time	0	0.5	1			
Vol (mL)	30	30	30	30	0.00	
Mass 1 (g)	0.0952	0.0945	0.0943	0.0947	0.00	
Mass 2 (g)	0.0989	0.0977	0.0976	0.0981	0.00	
TSS (mg/L)	123.3	106.7	110.0	113.3	8.82	9.979
Iron (mg/L)	1.809	1.648	1.565	1.67	0.12	0.140
Iron (mg/g algae)	14.670	15.454	14.233	14.79	0.62	0.700
	Floated					
	D3	**E3**	**F3**	**AVG**	**Std Dev**	**95% C.I.**
Time	0	0.5	1			
Vol (mL)	5	5	5	5	0.00	
Mass 1 (g)	0.0943	0.0947	0.1314	0.1068	0.02	
Mass 2 (g)	0.1518	0.1623	0.2139	0.1760	0.03	
TSS (g/L)	11.5	13.5	16.5	13.8	2.52	2.846
Iron (mg/L)	392.62	445.07	765.66	534.46	201.95	228.518
Corrected (mg/L)	5.348	4.828	8.043	6.07	1.73	1.952
Iron (mg/g algae)	0.465	0.357	0.487	0.44	0.07	0.078

Raw data for full scale setup using *Nannochloris* (0.70 ppt) and 1 amp applied to EC unit

	Influent					
	H1	**I1**	**J1**	**AVG**	**Std Dev**	**95% C.I.**
Time	0	0.5	1			
Vol (mL)	30	30	30	30	0.00	
Mass 1 (g)	0.0949	0.1327	0.1310	0.1195	0.02	
Mass 2 (g)	0.1026	0.1434	0.1418	0.1293	0.02	
TSS (mg/L)	256.7	356.7	360.0	324.4	58.72	66.4477718
Iron (mg/L)		3.5454135	3.686554	3.6	0.10	0.1383147
Iron (mg/g algae)		9.9404116	10.24043	10.090	0.21	0.29400912
	Effluent					
	H2	**I2**	**J2**	**AVG**	**Std Dev**	**95% C.I.**
Time	0	0.5	1			
Vol (mL)	30	30	30	30	0.00	
Mass 1 (g)	0.1313	0.0950	0.0953	0.1072	0.02	
Mass 2 (g)	0.1354	0.0990	0.1000	0.1115	0.02	
TSS (mg/L)	136.7	133.3	156.7	142.2	12.62	14.2803815
Iron (mg/L)	2.1798228	2.7955366	2.663695	2.55	0.32	0.36685552
Iron (mg/g algae)	15.949923	20.966525	17.00231	17.97	2.65	2.99349575
	Floated					
	H3	**I3**	**J3**	**AVG**	**Std Dev**	**95% C.I.**
Time	0	0.5	1			
Vol (mL)	5	5	5	5	0.00	
Mass 1 (g)	0.1319	0.1310	0.0945	0.1191	0.02	
Mass 2 (g)	0.2530	0.2945	0.2244	0.2573	0.04	
TSS (g/L)	24.2	32.7	26.0	27.6	4.48	5.06411272
Iron (mg/L)	480.29806	977.60576	788.2685	748.7	251.00	284.029268
Corrected (mg/L)	5.0898639	10.662978	10.92289	8.89	3.30	3.72883791
Iron (mg/g algae)	0.2101513	0.326085	0.420435	0.32	0.11	0.11918549

Raw data for full scale setup using *Nannochloris* (0.70 ppt) and 2 amps applied to the EC unit

	Influent					
	D1	**E1**	**F1**	**AVG**	**Std Dev**	**95% C.I.**
Time	0	0.5	1			
Vol (mL)	30	30	30	30	0.00	
Mass 1 (g)	0.1269	0.1264	0.1266	0.1266	0.00	
Mass 2 (g)	0.1301	0.1310	0.1298	0.1303	0.00	
TSS (mg/L)	106.7	153.3	106.7	122.2	26.94	30.488
Iron (mg/L)	0.718	1.091	0.597	0.802	0.258	0.292
Iron (mg/g algae)	6.730	7.117	5.595	6.481	0.791	0.895
	Effluent					
	D2	**E2**	**F2**	**AVG**	**Std Dev**	**95% C.I.**
Time	0	0.5	1			
Vol (mL)	30	30	30	30	0.00	
Mass 1 (g)	0.1259	0.1271	0.1259	0.1263	0.00	
Mass 2 (g)	0.1277	0.1288	0.1275	0.1280	0.00	
TSS (mg/L)	60.0	56.7	53.3	56.7	3.33	3.771
Iron (mg/L)	1.734	2.496	2.205	2.145	0.384	0.435
Iron (mg/g algae)	28.901	44.046	41.338	38.095	8.076	9.139
	Floated					
	D3	**E3**	**F3**	**AVG**	**Std Dev**	**95% C.I.**
Time	0	0.5	1			
Vol (mL)	5	5	5	5	0.00	
Mass 1 (g)	0.1250	0.1258	0.1261	0.1256	0.00	
Mass 2 (g)	0.2606	0.2501	0.2408	0.2505	0.01	
TSS (g/L)	27.1	24.9	22.9	25.0	2.09	2.367
Iron (mg/L)	1881.159	1898.723	1920.354	1900.079	19.633	22.216
Corrected (mg/L)	7.399	11.711	8.929	9.346	2.186	2.474
Iron (mg/g algae)	0.273	0.471	0.389	0.378	0.100	0.113

Raw data for the full scale setup using *Nannochloris* (0.70 ppt) using 3 amps applied to EC unit

	Influent					
	H1	**I1**	**J1**	**AVG**	**Std Dev**	**95% C.I.**
Time	0	0.5	1			
Vol (mL)	30	30	30	30	0.00	
Mass 1 (g)	0.1236	0.1279	0.1259	0.1258	0.00	
Mass 2 (g)	0.1260	0.1329	0.1312	0.1300	0.00	
TSS (mg/L)	80.0	166.7	176.7	141.1	53.16	60.154
Iron (mg/L)		1.254	1.210	1.232	0.031	0.036
Iron (mg/g algae)		7.525	6.847	7.186	0.479	0.543
	Effluent					
	H2	**I2**	**J2**	**AVG**	**Std Dev**	**95% C.I.**
Time	0	0.5	1			
Vol (mL)	30	30	30	30	0.00	
Mass 1 (g)	0.1257	0.1278	0.1276	0.1270	0.00	
Mass 2 (g)	0.1270	0.1291	0.1281	0.1281	0.00	
TSS (mg/L)	43.3	43.3	16.7	34.4	15.40	17.421
Iron (mg/L)	2.695	2.481	2.827	2.668	0.175	0.198
Iron (mg/g algae)	62.191	57.257	169.640	96.362	63.508	71.865
	Floated					
	H3	**I3**	**J3**	**AVG**	**Std Dev**	**95% C.I.**
Time	0	0.5	1			
Vol (mL)	5	5	5	5	0.00	
Mass 1 (g)	0.1268	0.1262	0.1262	0.1264	0.00	
Mass 2 (g)	0.3242	0.3086	0.2972	0.3100	0.01	
TSS (g/L)	39.5	36.5	34.2	36.7	2.65	2.996
Iron (mg/L)	4690.570	4564.834	4716.873	4657.426	81.258	91.950
Corrected (mg/L)	18.613	20.855	24.366	21.278	2.899	3.281
Iron (mg/g algae)	0.471	0.572	0.712	0.585	0.121	0.137

Graph displaying the harvesting efficiency of the EC/DAF unit with increasing amperage

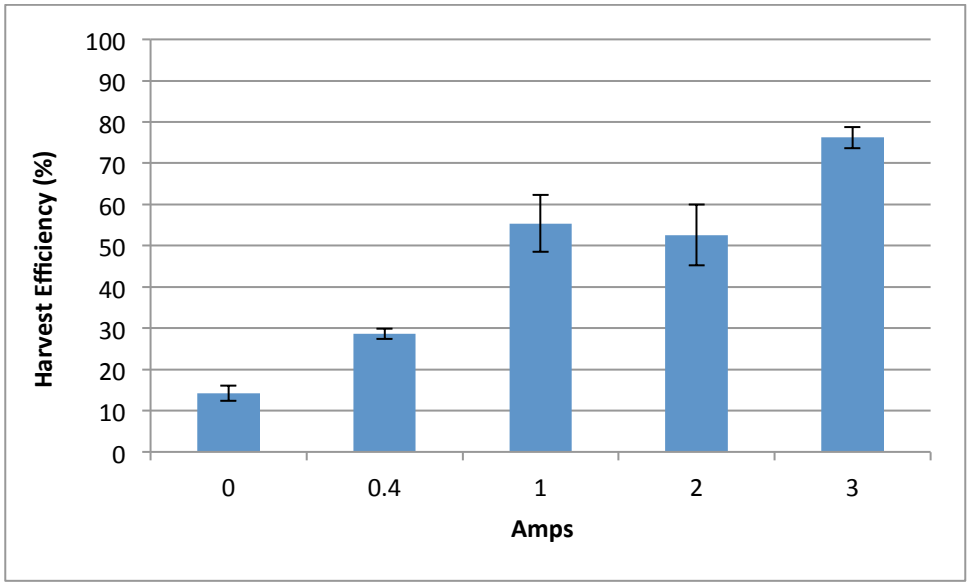

Figure 4.7: The algae harvest efficiency of the continuous system when varying the amperage of the electrocoagulation unit comparing the energy of the DAF and EC systems

Amps	Harvested Biomass (mg/L)	Std Dev	DAF Energy	Std Dev	EC Energy	Std Dev	Total (kWh/kg)	Std Dev
0	19.9	2.5	2.342	0.301	0.000	0.000	2.342	0.301
0.4	40.0	1.8	1.165	0.053	0.129	0.008	1.294	0.054
1	77.6	9.7	0.601	0.076	0.159	0.028	0.760	0.081
2	73.2	10.4	0.637	0.092	0.428	0.087	1.065	0.126
3	106.7	3.6	0.437	0.015	0.554	0.026	0.991	0.030

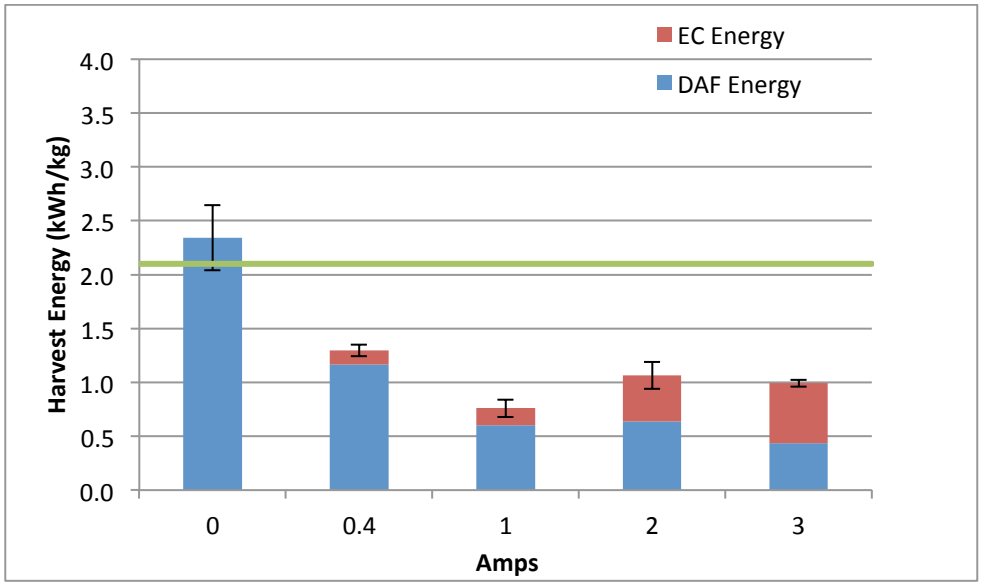

Figure 4.9: A comparison of the electrocoagulation (EC) energy and dissolved air flotation (DAF) energy with respect to the final harvesting efficiency TSS of the floated algal mass at the surface of the flotation tank

Raw data for the accumulation of harvested biomass at the surface of the flotation tank

	A3	B3	C3	AVG	Std Dev	95% C.I.
Time	0	0.5	1			
Vol (mL)	5	5	5	5	0.00	
Mass 1 (g)	0.1316	0.0945	0.0956	0.1072	0.02	0.023887
Mass 2 (g)	0.1372	0.1123	0.1370	0.1288	0.01	0.016203
TSS (g/L)	1.1	3.6	8.3	4.3	3.64	4.118972
	D3	**E3**	**F3**	**AVG**	**Std Dev**	**95% C.I.**
Time	0	0.5	1			
Vol (mL)	5	5	5	5	0.00	
Mass 1 (g)	0.0943	0.0947	0.1314	0.1068	0.02	0.024109
Mass 2 (g)	0.1518	0.1623	0.2139	0.1760	0.03	0.037613
TSS (g/L)	11.5	13.5	16.5	13.8	2.52	2.846292
	H3	**I3**	**J3**	**AVG**	**Std Dev**	**95% C.I.**
Time	0	0.5	1			
Vol (mL)	5	5	5	5	0.00	
Mass 1 (g)	0.1319	0.1310	0.0945	0.1191	0.02	0.024146
Mass 2(g)	0.2530	0.2840	0.2244	0.2538	0.03	0.03373
TSS (g/L)	24.2	30.6	26.0	26.9	3.30	3.728697
	D3	**E3**	**F3**	**AVG**	**Std Dev**	**95% C.I.**
Time	0	0.5	1			
Vol (mL)	5	5	5	5	0.00	
Mass 1 (g)	0.1250	0.1258	0.1261	0.1256	0.00	0.000643
Mass 2 (g)	0.2606	0.2501	0.2408	0.2505	0.01	0.01121
TSS (g/L)	27.1	24.9	22.9	25.0	2.09	2.367621
	H3	**I3**	**J3**	**AVG**	**Std Dev**	**95% C.I.**
Time	0	0.5	1			
Vol (mL)	5	5	5	5	0.00	
Mass 1 (g)	0.1268	0.1262	0.1262	0.1264	0.00	0.000392
Mass 2 (g)	0.3242	0.3086	0.2972	0.3100	0.01	0.015338
TSS (g/L)	39.5	36.5	34.2	36.7	2.65	2.99663

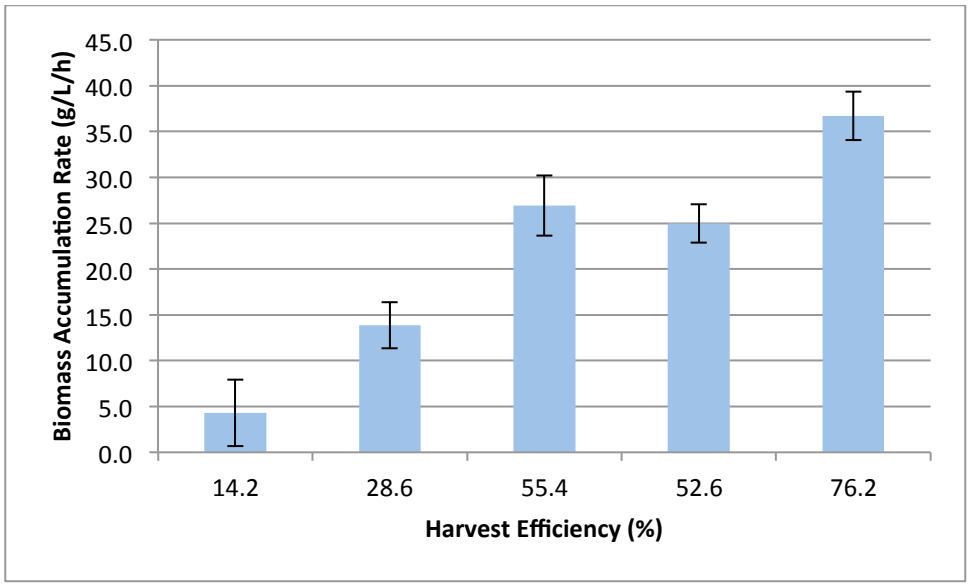

Figure 4.10: The rate of algal biomass accumulation floated to the surface as a result of the combined harvest efficiency of EC/DAF

Comparing the energy of the DAF, EC, Centrifuge as a whole on the algae harvesting process

Amps	Biomass harvested (mg/L)	DAF Energy	EC Energy	Centrifuge	Total (kWh/kg)
0	19.9	2.342	0.000	4.651	6.993
0.4	40.0	1.165	0.129	1.449	2.743
1	77.6	0.601	0.159	0.725	1.484
2	73.2	0.637	0.428	0.800	1.865
3	106.7	0.437	0.554	0.545	1.536

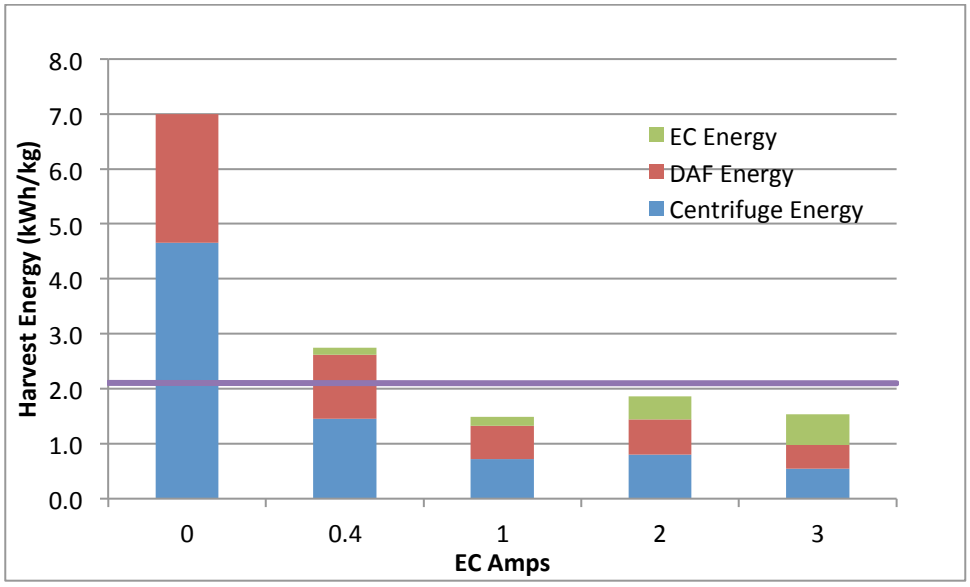

Figure 4.11: A breakdown of the total harvesting energy as a result of applied amperage and harvesting efficiency

Metal analysis conducted on the samples of the continuous testing for Table 4.1

Metals With Digest					
Client Name:	Adam Dassey	**Prep Method:**	EPA 3051	**Analysis Start Time:**	5:00 PM
Address:	LSU AgCenter	**Analysis Method:**	EPA 200.7	**Analysis Start Date:**	3/26/2013

Sample Lab ID	Sample Field ID	Analyte	Dilution Factor	Measured Conc., mg/Kg	Blank-Corrected Sample Conc., mg/Kg	MDL, mg/kg
W2130307-01	A2	Iron	1.0	1.36	1.36	0.05
W2130307-02	A3	Iron	1.0	27.53	27.53	0.05
W2130307-03	B1	Iron	1.0	0.99	0.99	0.05
W2130307-04	B2	Iron	1.0	1.68	1.68	0.05
W2130307-05	B3	Iron	20.0	9.21	184.19	0.05
W2130307-06	C1	Iron	1.0	0.97	0.97	0.05
W2130307-07	C2	Iron	1.0	1.65	1.65	0.05
W2130307-08	C3	Iron	20.0	20.37	407.45	0.05
W2130307-09	D2	Iron	1.0	1.81	1.81	0.05
W2130307-10	D3	Iron	20.0	19.63	392.63	0.05
W2130307-11	E1	Iron	1.0	1.15	1.15	0.05
W2130307-12	E2	Iron	1.0	1.65	1.65	0.05
W2130307-13	E3	Iron	20.0	22.25	445.07	0.05
W2130307-14	F1	Iron	1.0	1.18	1.18	0.05
W2130307-15	F2	Iron	1.0	1.57	1.57	0.05
W2130307-16	F3	Iron	20.0	38.28	765.67	0.05
W2130307-17	H2	Iron	1.0	2.18	2.18	0.05
W2130307-18	H3	Iron	20.0	24.01	480.30	0.05
W2130307-19	I1	Iron	1.0	3.55	3.55	0.05
W2130307-20	I2	Iron	1.0	2.80	2.80	0.05
W2130307-21	I3	Iron	20.0	48.88	977.61	0.05
W2130307-22	J1	Iron	1.0	3.69	3.69	0.05
W2130307-23	J2	Iron	1.0	2.66	2.66	0.05
W2130307-24	J3	Iron	20.0	39.41	788.27	0.05

Raw data of the supernatant growth after 3 amp continuous run

Diluted Influent						
Day 0	**A1**	**A2**	**A3**	**AVG**	**Std Dev**	**95% C.I.**
Initial (g)	0.1275	0.1274	0.1265	0.1271	0.001	0.001
Final (g)	0.1307	0.1302	0.1291	0.13	0.001	0.001
TSS (mg/L)	106.7	93.3	86.7	95.6	10.184	11.524
Day 4	**A1**	**A2**	**A3**	**AVG**	**Std Dev**	**95% C.I.**
Initial (g)	0.1264	0.1259	0.1273	0.1265	0.001	0.001
Final (g)	0.1473	0.1491	0.1496	0.1487	0.001	0.001
TSS (mg/L)	696.7	773.3	743.3	737.8	38.634	43.718
Day 5	**A1**	**A2**	**A3**	**AVG**	**Std Dev**	**95% C.I.**
Initial (g)	0.1274	0.1249	0.1265	0.1263	0.001	0.001
Final (g)	0.149	0.1464	0.148	0.1478	0.001	0.001
TSS (mg/L)	720.0	716.7	716.7	717.8	1.925	2.178
Recycled Effluent						
Day 0	**B1**	**B2**	**B3**	**AVG**	**Std Dev**	**95% C.I.**
Initial (g)	0.1291	0.1274	0.1265	0.1277	0.001	0.001
Final (g)	0.1312	0.1292	0.1281	0.1295	0.002	0.002
TSS (mg/L)	70	60	53.3	61.1	8.389	9.493
Day 4	**B1**	**B2**	**B3**	**AVG**	**Std Dev**	**95% C.I.**
Initial (g)	0.1274	0.125	0.1253	0.1259	0.001	0.001
Final (g)	0.1542	0.1511	0.1517	0.1523	0.002	0.002
TSS (mg/L)	893.3	870.0	880.0	881.1	11.706	13.247
Day 5	**B1**	**B2**	**B3**	**AVG**	**Std Dev**	**95% C.I.**
Initial (g)	0.1268	0.1235	0.1262	0.1255	0.002	0.002
Final (g)	0.1512	0.1479	0.15	0.1497	0.002	0.002
TSS (mg/L)	813.3	813.3	793.3	806.7	11.547	13.066

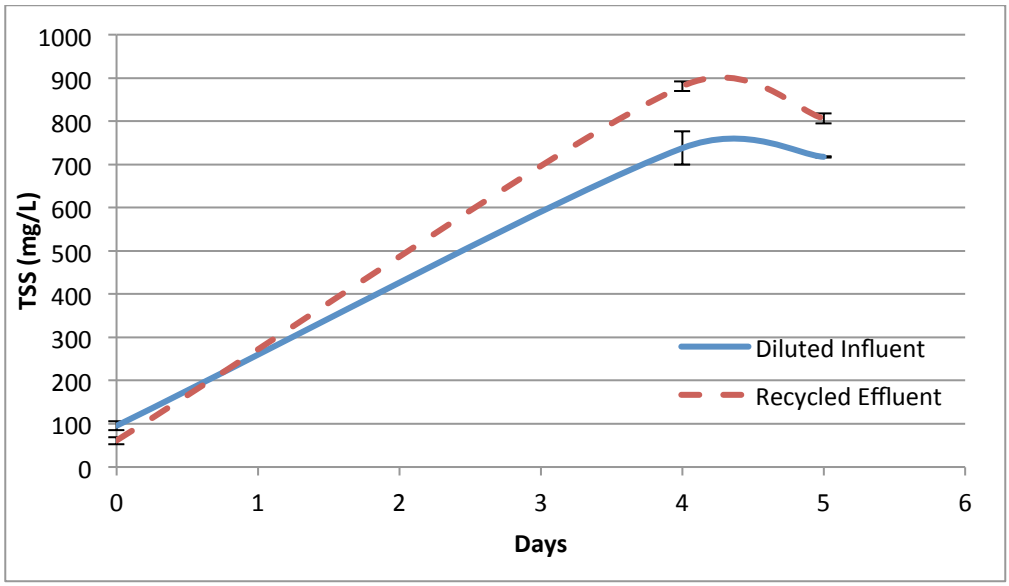

Figure 4.8: Comparing the growth of the *Nannochloris* influent and the effluent after 3 amps of electrocoagulation was applied resulting in an excess of 1.5 mg/L of iron in suspension

Appendix E: Life Cycle Analysis: Harvesting and Final Comparison Data

Table 5.7: A comparison of potential harvesting techniques and costs for algal biomass

Growth Rate ($g/m^2/d$)	Harvest Method	Eff. (%)	Initial Co	Final C	Energy (kWh/kg algae)	kwh/m^3	m^3/day	kWh/ day
25	Flocculation/pH → Settling → Belt Press	90	0.5	200	0.458	0.22957	609.25	139.9
28	Not listed*	100	0.5	200	0.879	0.44060	548.33	241.6
25	Settle → Centrifugation	65	0.5	50	0.235	0.11868	843.58	100.1
12	Flocculation → DAF → Centrifugation	70	0.1	200	1.44	0.14407	783.33	112.9
12	Flocculation → DAF → Belt Press	70	0.1	200	1.086	0.10865	783.33	85.1
25	Centrifugation	100	1	200	0.338	0.33969	548.33	186.3
31.4	Settle → Centrifuge*	65	0.8	120	0.292	0.23516	843.58	198.4
15	Electrocoagulation → DAF → Centrifugation	55	0.14	200	0.944	0.13225	996.96	131.9
15	Electrocoagulation → DAF → Centrifugation	76	0.14	200	1.133	0.15873	721.49	114.5

Need to harvest 15 $g/m^2/day$: 4047 m^2 pond : 60705 g/day harvest
The pond reaches harvest density after 3 days : 182115 g/ 1645 m^3

The combined energy parameters for the LCA

(Kwh/day)	Mixing	CO2	Pumping	Nit.	Phos.	Harvesting	Extraction	Total
High Cost	164.5	74.06	1.214	94.43	37.1	242	121.17	734.4
Low Cost	9.87	1.76	0.166	35.95	1.05	85	39.94	173.7
My Cost	37.21	3.84	0.6	58.68	23.67	114	268.06	506.0
	Mixing	CO2	Nutrients	Harvesting	Extraction	Total	Biodiesel	
	164.5	74.0	131.53	242	121.17	733.26	126	
	9.87	1.76	37	85	39.94	173.57		
	37.21	3.84	82.35	114	268.06	505.46		

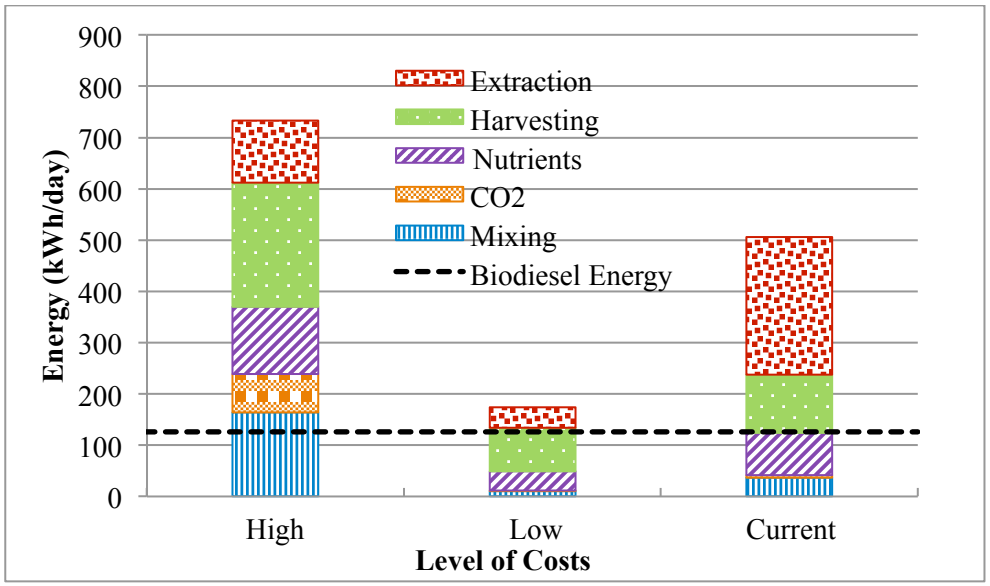

Figure 5.1: Comparison of high, low, and current energy estimates for algal biodiesel production and the available energy from that biodiesel

Raw data for energy parameters for LCA including energy credits from nutrient removal

Mixing	CO2	Harvesting	Extraction	Total	Biodiesel + Nutrients
164.5	74.06	242	121.17	601.73	333
9.87	1.76	85	39.94	136.57	
37.21	3.84	114	268.06	423.11	

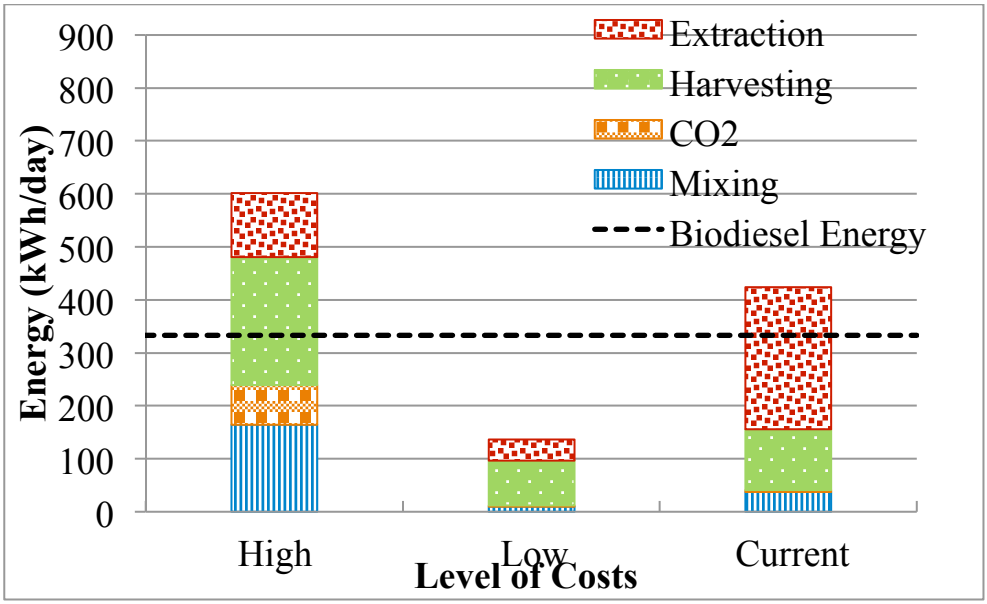

Figure 5.2: Comparison of high, low, and current energy estimates for algal biodiesel production and the available energy from that biodiesel plus supplemental value for wastewater treatment

Raw data of energy parameters for LCA including energy credit from nutrients removal and biogas

Mixing	CO2	Harvesting	Extraction	Total	Biodiesel + Nutrients + Biogas
164.5	74.06	242	121.17	601.73	493
9.87	1.76	85	39.94	136.57	
37.21	3.84	114	268.06	423.11	

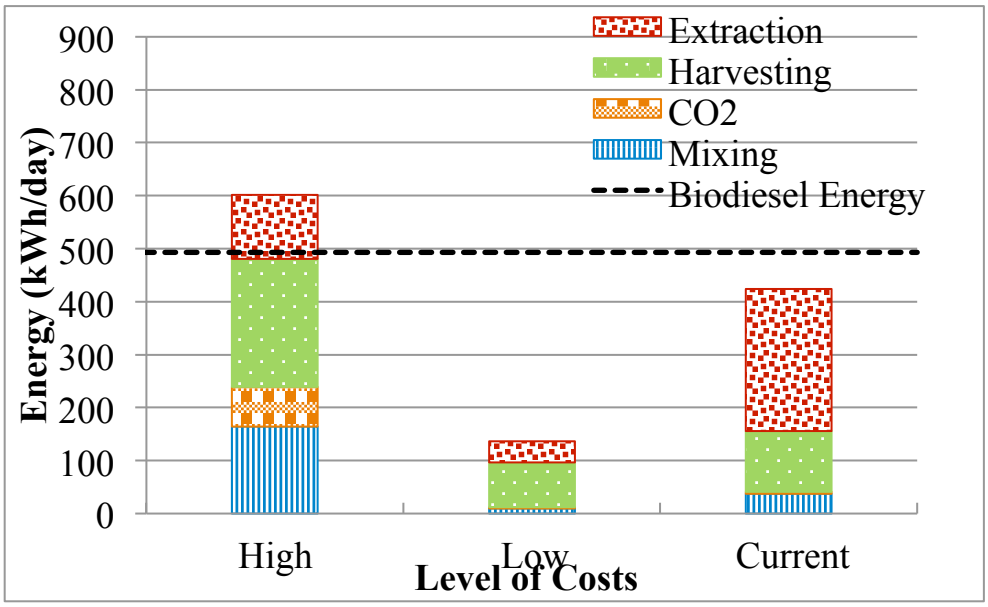

Figure 5.3: Comparison of high, low, and current energy estimates for algal biodiesel production and the available energy from that biodiesel plus supplemental value for wastewater treatment and anaerobic digestion

Appendix F: Photographs of System

Figure F1: Airlift used for culture circulation in the 1700 L tank

Figure F2: Centrifuge used in Chapter 2 testing and final algal paste

Figure F3: Complete multistage harvesting system

Figure F4: Complete multistage harvesting system with focus on the mixed reactors in series

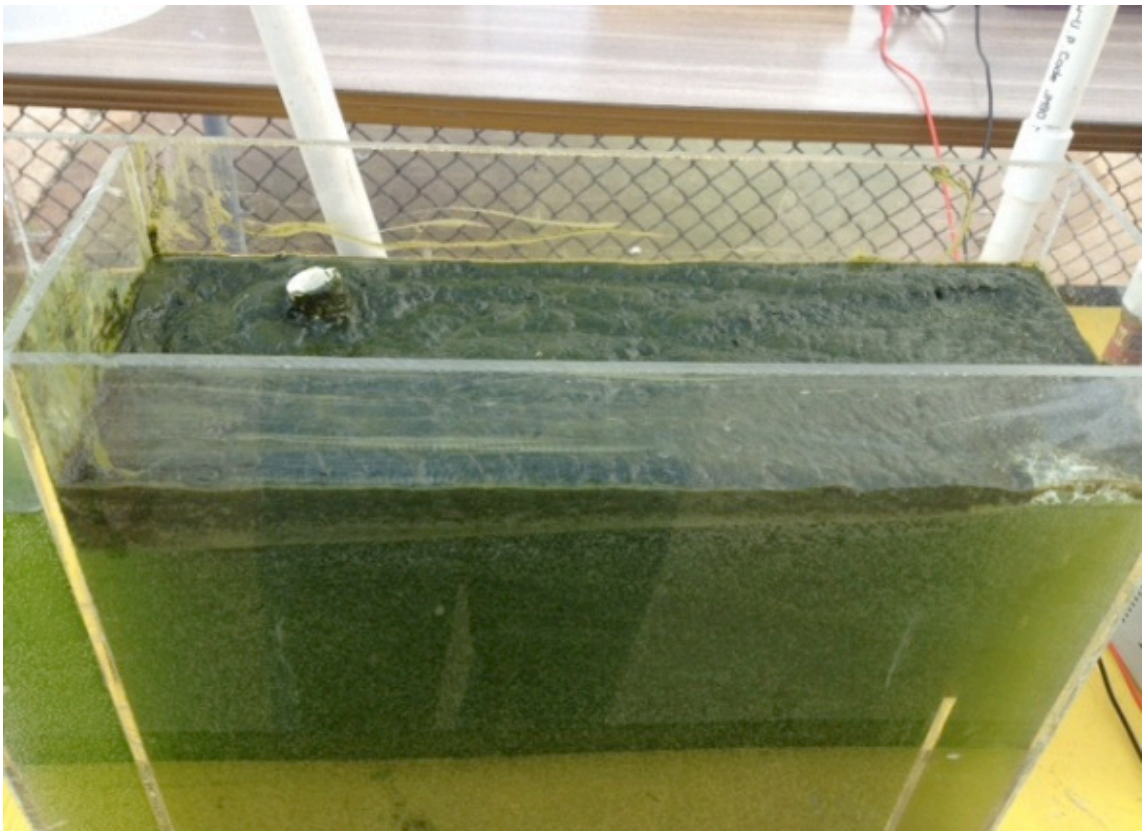

Figure F5: Accumulated algal biomass floated to the surface of the flotation tank (55% efficiency)

Figure F6: Accumulated algal biomass floated to the surface of the flotation tank (28% efficiency)

Figure F7: Complete multistage harvesting setup after initial startup

Figure F8: Complete multistage harvesting setup showing maximum harvesting efficiency

Vita

Adam James Dassey was born in New Orleans, Louisiana to Kim and Peter Dassey. There he attended Brother Martin High School before entering the Biological and Agricultural Engineering program at Louisiana State University, Baton Rouge in 2003. After completing his Bachelor's degree in the fall of 2007, he entered the Master's program in Biological and Agricultural Engineering at Louisiana State University. He completed his Masters in the summer of 2010 while duel enrolled in the Doctorate of Philosophy program in Engineering Sciences. His collegiate career came to an end upon completing his doctorate in the summer of 2013.